Characterization of Modified

Polyimide Adhesives

by

Richard H. Bott

Dissertation submitted to the Faculty of the

Virginia Polytechnic Institute and State University in

partial fulfillment of the requirements for the degree of

DOCTOR OF PHILOSOPHY

in

Chemistry

APPROVED:

L. T. Taylor
Co-Chairman

T. C. Ward
Co-Chairman

J E. McGrath

J. P. Wightman

J. G. Dillard

April, 1988

Blacksburg, Virginia

CHARACTERIZATION OF MODIFIED POLYIMIDE ADHESIVES

by

Richard H. Bott

Committee Co-Chairmen: Dr. Larry T. Taylor
Dr. Thomas C. Ward
Department of Chemistry

(ABSTRACT)

An addition polyisoimide prepolymer was modified through the incorporation of metal particles. The response of this metal/polymer composite to mechanical vibrations and the passage of electric current was measured. Model aluminum conductor bar joints containing this material were assembled and exposed to elevated temperatures for extended periods of time while the electrical properties of the composites were monitored. In the most favorable systems, no thermal degradation of the electrical properties was observed. Dynamic mechanical behavior of the metal/polymer composites indicated good adhesion between particles and the matrix and also a broadening of the glass transition region as well as a post Tg dispersion in the temperature spectrum. The adhesive properties of these metal/polymer composites to aluminum were studied and found to be influenced by the loading level of the metal in the composite.

Chemical reactions occurring during the cure of a neat resin sample of the polyisoimide prepolymer were monitored using infrared spectrometry and differential scanning calorimetry. Both the

crosslinking and isomerization reactions were found to be apparently first order with the isomerization having a lower activation energy than the crosslinking. Linear, high molecular weight, thermoplastic polyimides and poly(imide-siloxane) homo- and copolymers prepared by bulk and solution thermal imidization were investigated as structural adhesives for titanium. The solution thermal imidization procedure was found to result in favorable adhesive characteristics while the presence of siloxane segments in the polymer backbone improved the resistance of stressed specimens to moisture. Aluminum-sec-butoxixde used as a primer was also found to improve the moisture durability of bonds prepared with these materials.

Acknowledgment

I must first thank my advisors; Professors Taylor, Ward and McGrath for their patience and support throughout my stay at Virginia Polytechnic Institute. The opportunities these gentlemen made available to me were among the most rewarding aspects of my work. I also extend my sincere appreciation to Professors Wightman and Dillard for serving on my advisory committee and for many helpful discussions.

I must also thank my fellow graduate students for plenty of inspiration and advice. I want to thank Dr. Jim Rancourt for many stimulating discussions. I also need to thank Dr. John Summers, and for providing precious polymer samples.

It has been my very real pleasure to have worked and been associated with these fine individuals. The knowledge I have acquired from the faculty and students at VPI & SU extends far beyond chemistry.

I must also thank the support groups: specifically the PMIL secretaries, , and especially for typing this manuscript. Without their help and the help of the physics shop, electronics shop and glass shop much of this work would not have been possible.

I also wish to thank the VPI & SU Center for Adhesion Science for encouraging the diversification of graduate studies in the area of adhesion.

I also sincerely appreciate the financial support of ALCOA, the Virginia Center for Innovative Technology, NASA Langley Research Center and the Adhesive and Sealant Council.

Finally, my heartfelt thanks go to my family and especially my parents for their unending support during this endeavor. Prosit.

To the people who made this achievement possible:

My Family

My Teachers

My Friends

Table of Contents

List of Figures

List of Tables

List of Schemes

1.0 Introduction

The need for "high performance" engineering materials in the aerospace, defense and electronics industries has justified enormous research efforts in several areas including advanced composites, polymers, ceramics and metals. Since the 1960's research in the areas of polymers and composites has focused on materials able to withstand not only harsh chemical environments and severe mechanical, electrical and electromagnetic stresses but materials that would also remain useful for varying lengths of time at temperatures as high as 760°C (1). These requirements have also necessitated an interdisciplinary research effort aimed at the rational design and evaluation of materials for many of these "high performance" applications. In particular, polymer chemistry and surface science encompass many of the important criteria with respect to the goals of these advanced materials. In addition, mechanics and rheology also play crucial roles in the design and ultimate applicability of these materials. In conducting a goal oriented research effort in this area, one must recognize these factors in order subsequently to design suitable materials which yield as many favorable characteristics as possible.

Polymers and composites are usually recognized as areas with remarkable potential for innovation. The advantages of structures based on such technology have been recognized and include strength to weight ratio, stability, vibration damping and many others. One of the keys to the utilization of these materials is the ability to design both chemical and physical structures of the materials to achieve certain

properties (2). Polymer modification, thru chemical and physical means, can then expand the utility and effectiveness of polymeric materials.

Modification of the chemistry of these systems often focuses on improvement in processability by conventional means. In this respect the use of unsaturated end groups, particularly acetylenic groups, has received considerable attention recently (1-3). In addition, bulky monomer structures, highly flexible monomer structures, block copolymerization and poly(amic acid) processing have also been investigated and will be discussed further in the historical section. The major advantages derived from acetylenic end groups compared to other types of crosslinking comes from the ability for crosslinking either during or after processing and consequently the possibility of using lower molecular weight starting materials which are more easily processable.

The improved processability that has been demonstrated (4,5) in addition curing polyisoimide systems allows utilization of the already excellent thermal and mechanical properties available in these systems (6-8). In addition, the range of properties available in these materials may be extended significantly by the combination of these materials with other heterogeneous fillers such as metal particles. Such combinations which can be termed polymer/metal composites have a unique combination of properties which extend the utility of polymeric materials. Some interesting effects on the physical properties of the matrix are observed in these systems. For example, in most systems the heat distortion temperature and stiffness increase; while, the thermal expansion coefficient, tensile modulus and impact strength decrease (9).

Another interesting effect is in the area of electrical conductivity. At a critical volume loading of metal filler the electrical conductivity of the composite increases dramatically (10).

Another approach to property modification in the realm of high performance polymers relies on the chemical incorporation of a second component into the polymer backbone. This component is chosen such that its properties compliment those of the first component. When carefully designed, these segmented copolymers can significantly extend the utility of the hybrid material with respect to its two individual constituents. This approach has been exploited in this work in the case of poly(imide-siloxane) segmented copolymers.

There are multiple motives for investigating the imide-siloxane systems. First, incorporation of the bis(aminopropyl) tetramethyl disiloxane has been shown by St. Clair (11,12) to result in thermoplastic copolymers when combined with an aromatic diamine and dianhydride. Also, thermally stable siloxanes can impart a number of desirable properties to the material including impact resistance, weatherability, moisture absorption and surface modification (13-14).

The present study will describe two modifications of polymeric systems. In both cases highly aromatic polyimides are the basic polymers to which the modifications have been applied. Initially, an applied system was investigated which utilized a metal powder to modify the electrical properties of a polyisoimide prepolymer to enhance electrical stability at aluminum conductor interfaces. The basic chemistry and physical properties of this system have also been studied. The second area of modification studied dealt with thermoplastic

polyimides. Chemical modification, specifically the influence of poly(dimethyl siloxane) on the adhesive properties of a condensation polyimide were investigated.

2.0 Historical

This chapter will endeavor to provide some perspective for the original work which is to follow. The literature dealing with any individual aspect of this work is too extensive to be exhaustively reviewed here. An overview of the more recent developments in these areas will be presented. First, some synthetic background in the area of high temperature polymers will be presented. These polymers include acetylene terminated polyisoimides, polyimides, polysulfones, polyquinoxalines and finally thermoplastic poly(imide siloxanes). Next metal filled systems will be described and finally, adhesive testing will be presented.

2.1 Materials

The increasing need for high service temperature adhesives and structural matrix resins has led to the development of many new polymeric systems in recent years. One of the most interesting and potentially useful of these new polymers are the polyimides. Polyimides are noted for their excellent thermal and mechanical properties but their utility has been severely limited due to problems with fabrication and processing of these polymers (14,6-8). Nevertheless, the careful design of polyimides can lead to enhanced processability. In this respect, several approaches have been investigated and found to be useful. One design method which has improved the processability of linear aromatic polyimides is the introduction of meta-substituted aromatic diamines for para substituted analogs (15,16). This procedure, while improving the processability, also has the possible detrimental effect of lowering the glass transition temperature. Another method

which has been successfully utilized in improving polyimide processing and solubility characteristics was the incorporation of bulky side groups through phenylated diamine monomers (17). Although these materials maintain a high glass transition temperature their resistance to solvents may be sacrificed. Processability can also be improved by diluting the rigid imide functionality in the polymer chain through the use of block copolymerization with a flexible segment such as a siloxane (11,18-19). These approaches all rely on enhancing the thermoplasticity of the polyimides through incorporation of flexabilizing linkages.

Finally, processability and fabrication aspects of the polyimides have been improved through the use of low molecular weight imide oligomers terminated with acetylenic groups (20,21). The material (Thermid MC-600) shown in Figure 1 is an example of a commercially available product (National Starch and Chemical Co.). These materials have improved solubility and processing characteristics while maintaining both a high glass transition temperature and good solvent resistance due to their highly crosslinked nature following thermal cure of the acetylene groups. This approach also has problems in terms of processing parameters. Preliminary reactions of the terminal acetylene groups during thermal cure lead to a restriction of flow and wetting properties before good contact with a substrate is achieved (3). In addition, since the glass transition temperature of these imide oligomers is quite high (~200°C) the crosslinking reaction proceeds very rapidly resulting in an infusible, rigid network. The gel time for Thermid MC-600 has been estimated at less than three minutes at 250°C (22). This short gel time severely restricts the uses of the material

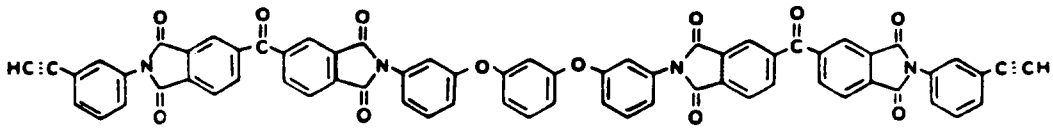

MC-600

Figure 1: Structure of Thermid MC-600 Acetylene Terminated Polyimide Oligomer.

in applications such as matrix resins and adhesives where good flow is necessary prior to the onset of gelation.

In order to circumvent this problem of rapid gelation an isomeric imide structure, termed isoimide, has been introduced into these oligomers (4,22). Materials with this functionality (i.e., Thermid IP-600) (Figure 2) exhibit improved solubility as well as longer gel times and lower glass transition temperatures (~160°C vs ~200°C for the corresponding imide oligomer). Initially, it was thought that the presence of the isoimide structure, as an unfavorable side reaction product in polyimides, led to premature thermal decomposition of polyimides through loss of CO_2 from the imino-lactone heterocyclic ring (23). However, later work (24) showed that the isoimide functionality thermally isomerized to the imide functionality (Scheme 1) prior to any significant degradation of the polymer backbone.

Since the utility of these materials is improved by the incorporation of these reactive functionalities without severely decreasing other favorable properties such as thermooxidative stability and solvent resistance, the chemistry of the isoimide isomerization and acetylene crosslinking reactions is of considerable interest. Previous work has also shown that these materials, when loaded with metal powders, provide a convenient and effective method of optimizing the electrical conductance and thermal stability of aluminum conductor joints (25).

2.1.1 Acetylene Terminated High Performance Polymers

These high performance polymers such as polyimides, polyquinoxalines and polysulfones are not new but the problems

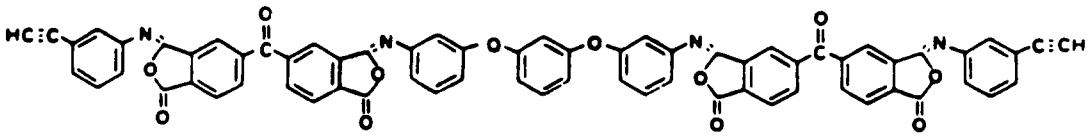

IP-600

Figure 2: Structure of Thermid IP-600 Acetylene Terminated Polyisoimide Oligomers.

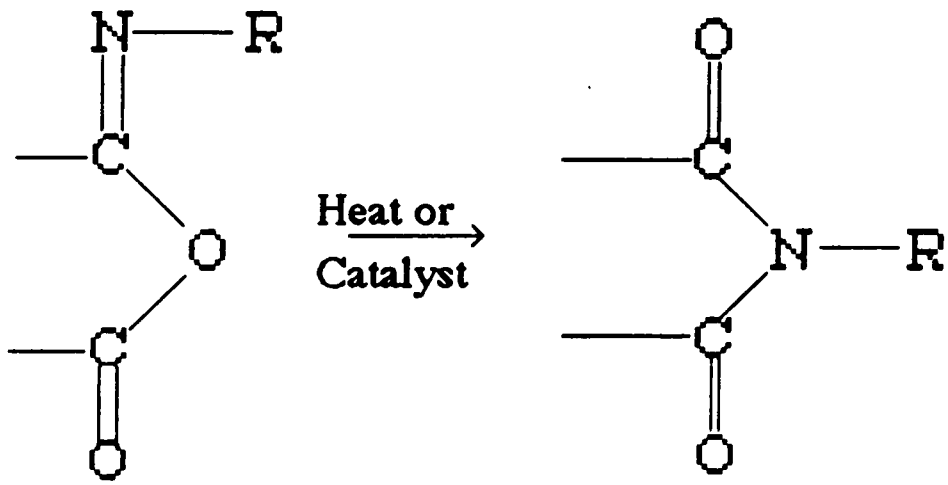

Scheme 1: Thermal or Catalytic Isomerization Reaction of Isoimide Functionality.

associated with their fabrication and processing are just now beginning to be solved. For example, the insoluble, infusible nature of many of these polymers along with their very high softening temperatures (>150°C) makes fabrication of these materials a very difficult task. One solution to these problems is to modify the backbone chemically to help avoid some of the major processing problems while still maintaining as many of the advantages associated with the basic chemical structure as possible.

In this respect the use of unsaturated end groups, particularly acetylenic groups, has received considerable attention recently (3). The major advantages which come from incorporating acetylenic end groups include the wide applicability to existing polymer systems, the variety of ways the group can be introduced into the structure (3), and most importantly, a potential for crosslinking of the terminal acetylene unit under controlled conditions. Although the acetylenic group may be used to terminate a wide variety of polymeric structures, the primary interest is in the area of high performance polymers.

For this reason this portion of the review will focus on the acetylene terminated oligomers of three classes of high performance oligomers; polyimides, polysulfones, and polyquinoxalines. In addition, some attention will also be given to the thermally induced crosslinking reactions which are most commonly used in these cases.

2.1.1.1 Acetylene Terminated Polyimides

The excellent thermal stability and strength characteristics of polyimides make them attractive candidates for high performance adhesive and composite applications. However, the most common condensation

polyimides have a variety of problems associated with them which preclude their widespread use as structural materials. For example, the water given off in the final stages of the condensation polyimide cure leads to severe void formation in composite materials and adhesive bonds. One way to avoid this problem is to use an acetylene terminated oligomer (Scheme 2) (26) which can be dehydrated totally before the lay up of the composite or the final fabrication steps take place.

The synthesis of these materials can be modified to give oligomers of various molecular weights. The amount of monofunctional reagent, which in this case refers to a structure containing only one primary amine group, determines how long the average oligomeric chains will be. The synthesis of the acetylene terminated oligomer is as follows; a dianhydride is the excess reagent which is reacted at room temperature in a polar solvent with a deficient amount of diamine. The resulting anhydride capped amic acid is further reacted with an acetylene containing monoamine resulting in an acetylene terminated amic acid. This amic acid is subsequently cyclodehydrated in what amounts to a combination of thermal and chemical steps where the amic acid is introduced into a solution of acetic anhydride and pyridine at about 150°C. The acetylene terminated imide oligomer can then be isolated.

2.1.1.2 Polyisoimide Prepolymers

The preparation of polyisoimide prepolymers is based on the incorporation of the isoimide functionality through chemical rather than thermal cyclization reactions. This iminolactone or isoimide structure was first reported in 1893 by Hoogewerff et al (27). The first relatively modern characterization of this structure was not reported

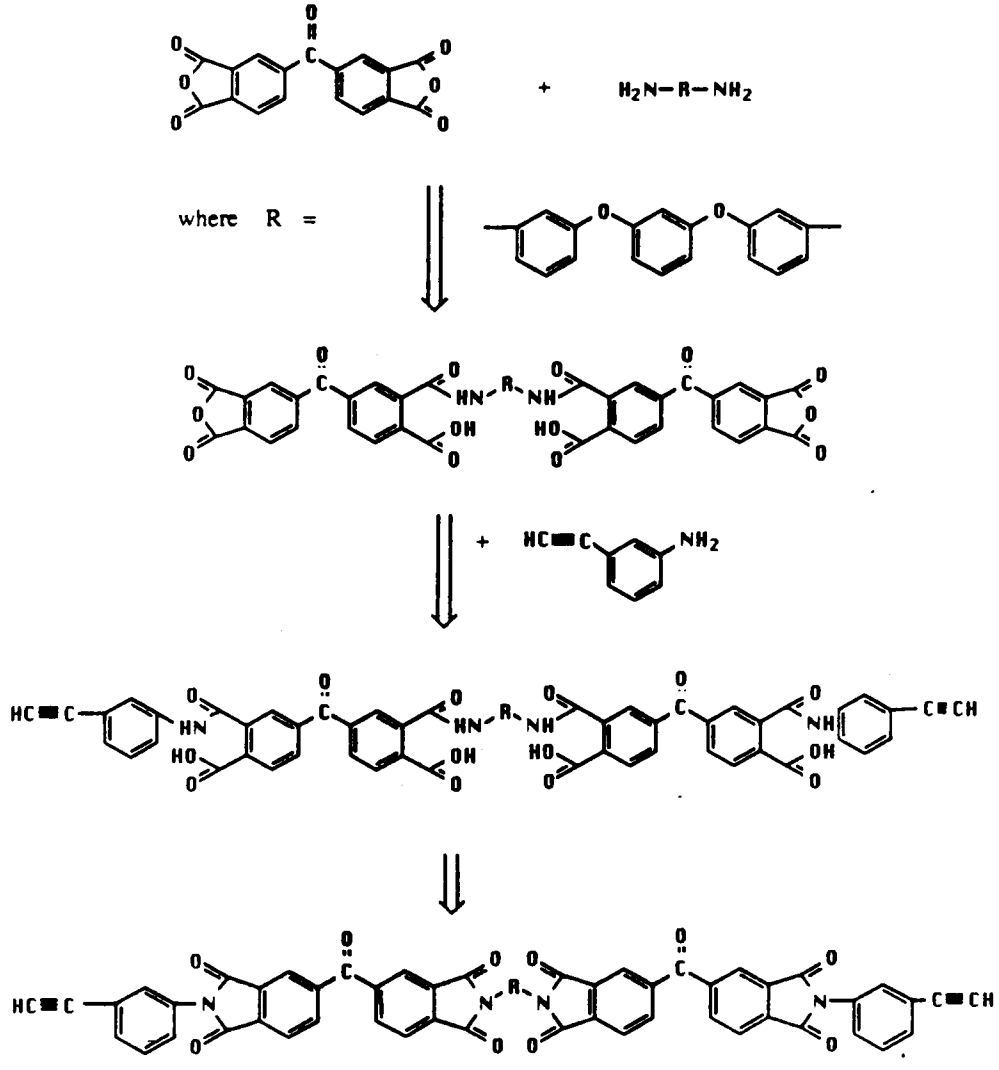

Scheme 2: Synthesis of Acetylene Terminated Polyimide Oligomers.

until 1961 (28-30). These more recent reports discuss the synthesis of monomeric isoimides and isomaleimides prepared by cyclization of the amic acids with various dehydrating agents. The choice of dehydrating agent was crucial in the overall yield of isoimide compared to imide. A limited number of cyclizing agents studied were efficient dehydrating agents in terms of maximizing isoimide functionality (29,31-35).

The extension of this chemistry to polymeric imide systems was reported by Landis in 1983 (5). It was also reported that only two cyclizing agents, trifluoroacetic anhydride and dicyclohexyl carbodiimide (DCC), are effective in generating a high level of isoimide structure in the Thermid prepolymer system mentioned above. Additionally, it was reported that only the DCC was practically useful due to problems with purification of the polymer prepared with trifluoroacetic anhydride. These problems were thought to have resulted from the previously reported reaction (28) of the trifluoracetic acid with the isoimide functionality after the dehydration had occurred. Nevertheless, DCC use was shown to lead to no such problems since the dehydration of the poly(amic acid) results in isoimide and dicyclohexyl urea in this case. The urea is not further reactive in the solution since it precipitates from the THF solution and can thereby be easily removed by filtration. This is a rather sophisticated approach to the design of these polymers. Next, a few more general approaches to other high temperature acetylene terminated polymers will be presented.

2.1.1.3 Acetylene Terminated Polysulfones

The use of polysulfones as engineering resins is rapidly expanding. These materials will find even more use now that solutions

are being found for some of the problems associated with earlier polymers. Unlike polyimides, the problems do not deal with the processability of the polysulfones but rather with their softening temperature and also low chemical resistance in terms of environmental stress crazing and cracking. The solution to these problems is however, the same. The use of acetylene terminated sulfone oligomers provides a route by which both the chemical resistance and softening temperature of the system can be increased. In this case the acetylene group is added to the starting material, hydroxyl-terminated sulfone, (36) through the multistep sequence depicted schematically below (37) (Scheme 3).

This synthesis involves the reaction of the terminal hydroxyl group with 4-bromobenzoyl chloride. The bromine is then displaced by trimethylsilyl-acetylene in the presence of a palladium catalyst. All that is further required is the cleaving of the trimethyl silyl group with a weak base, in this case potassium carbonate, leaving the acetylene terminated sulfone oligomer.

2.1.1.4 Acetylene Terminated Polyquinoxalines

Polyquinoxalines and polyphenylquinoxaline in particular have received much attention recently due to their thermooxidative stability as well as their excellent moisture resistance. Many of the applications for which these materials have been suggested as candidates require a melt processable system. This requirement led to the development of a thermosetting quinoxaline oligomer and again one of the most favorable ways of achieving this goal was through the use of acetylene terminated quinoxaline oligomers (38-39). Acetylene terminated polyphenylquinoxaline oligomers are prepared through the

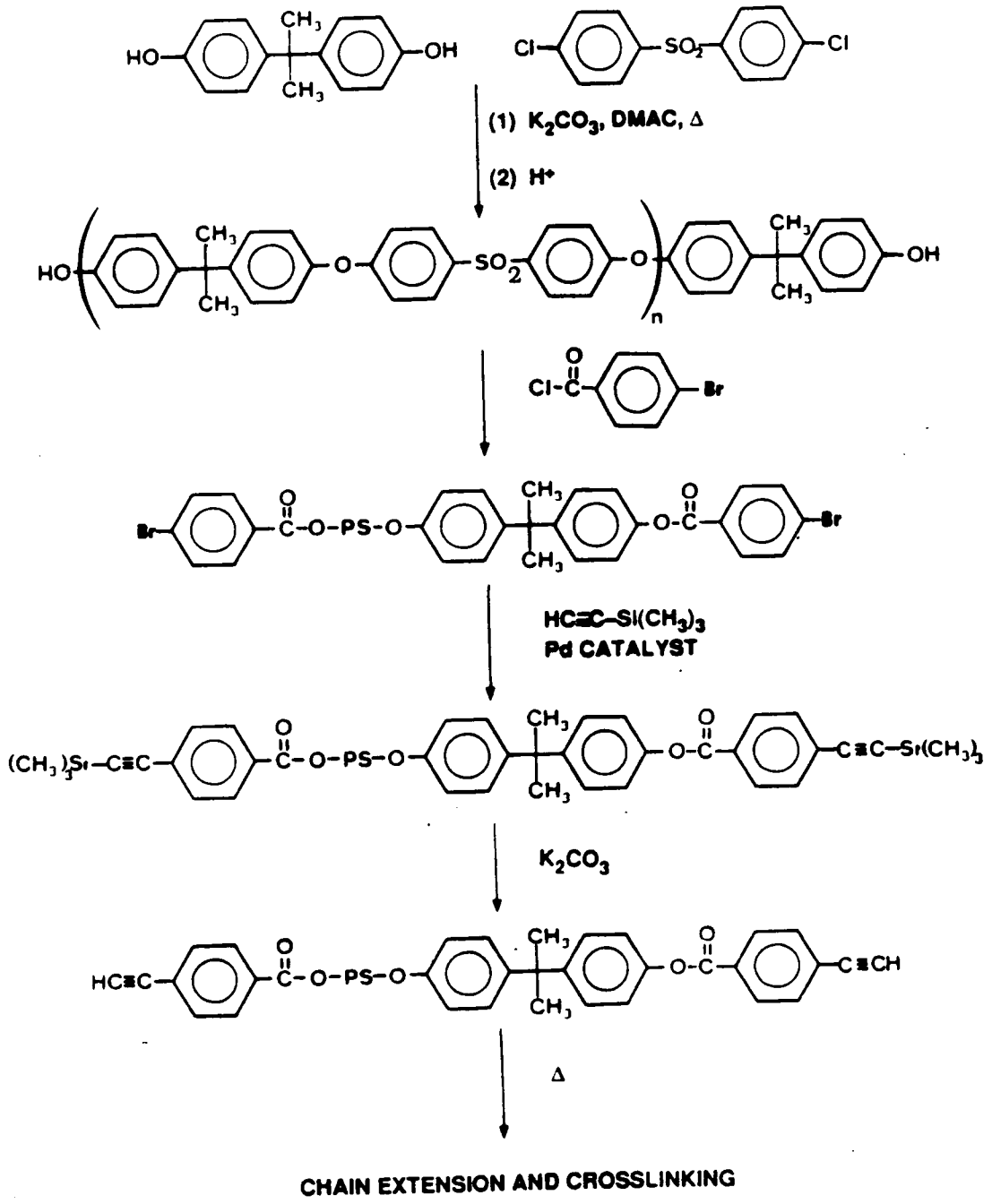

Scheme 3: Synthesis of Acetylene Terminated Sulfone Oilgomers.

condensation of a bis-phenyldiketone with an excess of a tetraaminobiphenyl. This process is then completed by the capping of the excess amino functionalities with an ethynl-phenoxy benzil as shown below (Scheme 4).

2.1.3 Thermally Induced Crosslinking Reactions

The characterization of the thermally induced crosslinking reactions of acetylene terminated polyimides was first studied by Landis (26) using differential thermal analysis. They proposed but did not verify a crosslinking reaction based on the trimerization of acetylene groups to a substituted aromatic structure. Since then, however, further work by Hergenrother (40) and Lind (41) has shown that complete trimerization was not actually the case although all of the acetylene groups did react during the thermal cure process.

The evidence for these statements was found in the DSC data for the oligomer. This support was also applicable to acetylene terminated oligomers other than polyimides. Hergenrother (40) has reported, for acetylene terminated polyimide oligomers, that the exotherm of reaction is -38 ± 0.7 kcal/mole but the exotherm for the trimerization of substituted acetylene has been estimated to be -142 kcal/mole (42). The great discrepancy between these two numbers provided evidence for a crosslinking reaction other than trimerization to substituted aromatic rings. Lind (41) has used these data along with spectroscopic techniques such as ^{1}H and ^{13}C NMR as well as FT-IR to get a more complete understanding of the cure of these networks. Their objective was to determine independent cure state parameters based on the time and temperature schedule to which the material had been subjected. In this

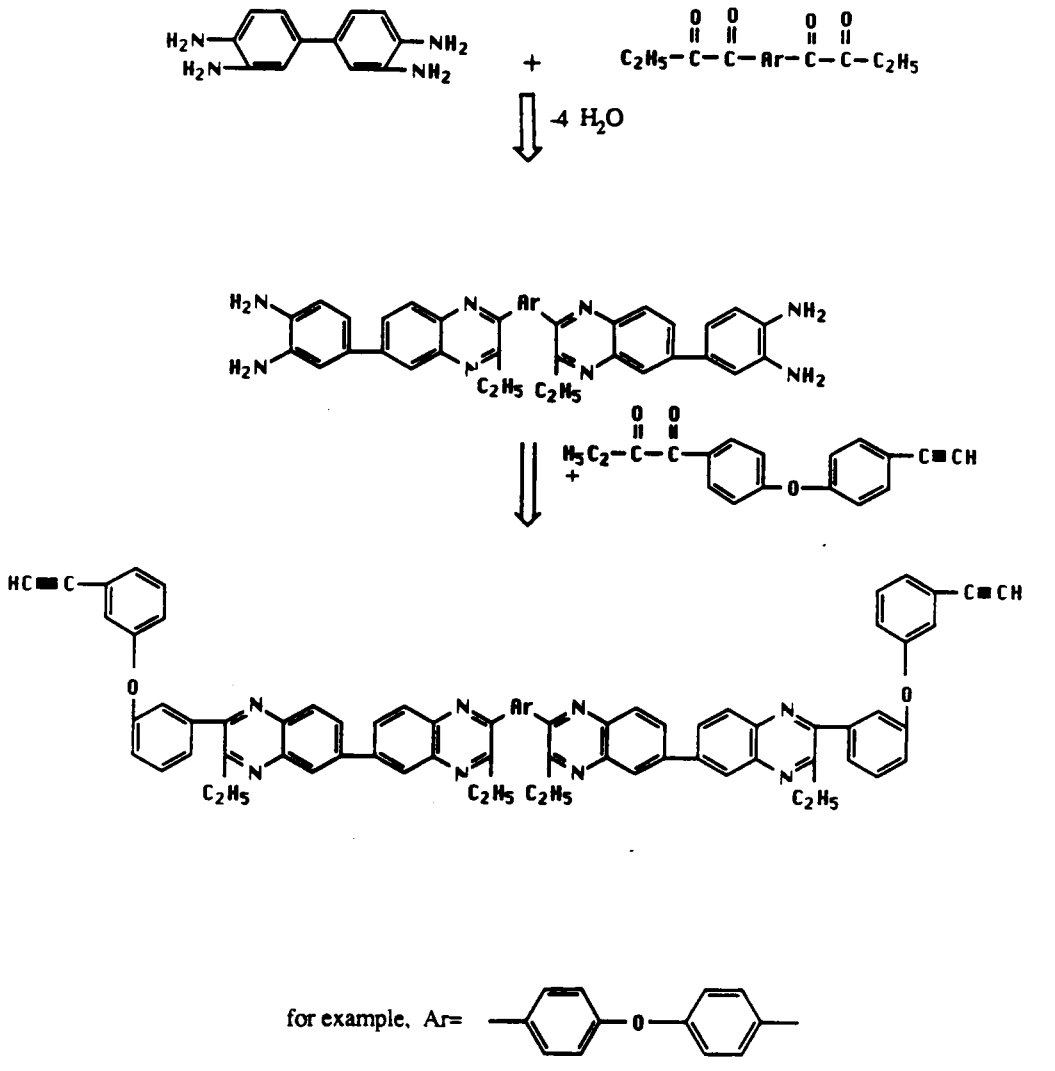

Scheme 4: Synthesis of Acetylene Terminated Polyquinoxaline Oligomers.

respect, they found that the relative area beneath the acetylene carbon peak in the solid state ^{13}C NMR as well as the relative area beneath the acetylene IR bands are valid as independent cure state parameters. These authors also provide spectroscopic evidence which disproved the theory of trimerization of acetylene groups to aromatic structures. That is, the number of aromatic carbon atoms stays the same throughout the course of the crosslinking reaction since the relative area beneath the aromatic carbon peaks was constant as a function of cure time and temperature. The resolution of these spectra was, however, too low to separate the aliphatic and olefinic resonances well enough to allow speculation as to the structures actually formed during the crosslinking reactions.

Kuo and Lee (43) have studied the effects of cure environment on the networks formed through the thermal crosslinking of acetylene terminated sulfones. Their results suggested that the presence of oxygen during the cure was very important to the mechanical properties of the cured resin. They studied various cure temperatures both in air and nitrogen and found that the cure atmosphere affected various mechanical properties including tensile strength, elongation at break, modulus and even the density of the cured resin. In all cases and at all cure temperatures the air cured systems had more favorable properties. The difference between the property values for air and nitrogen cure also becomes greater at higher cure temperatures. No precise explanation for the chemical differences in the final network which gave rise to these property differences was offered.

Another method of modifying pre- and post-cure properties of these acetylene terminated systems is the use of reactive diluents (44-47). These reactive diluents are essentially of the same functionality as the polymer backbone but they contain only one pendant acetylene group. This group can then thermally polymerize into the network resulting in a network with rather different physical properties than a network made up only of diacetylenic oligomer. Also, by varying the length of the monofunctional unit as well as its concentration, the glass transition temperature of the network can be varied. The effect of the reactive diluent on the network structure is complex. The relationship is neither that of a plasticizer nor that due simply to decreased molecular weight between crosslinks but rather a combination of these factors with others such as increased free volume which together dictate the final properties of the network.

This review has attempted to provide a brief look at the ways a few high performance polymers can be modified through acetylene incorporation. Many of the techniques presented here are already in use but no doubt as more and better structural materials are developed these techniques will be supplemented with many others. One such area of current interest is the utilization of other unsaturated crosslinking systems such as bis maleimides etc. (48-49).

2.1.3 Poly(Imide Siloxanes)

The first reported chemical incorporation of siloxane species into imide functional polymers appeared in 1966 (50). This report dealt with the reaction of aromatic and aliphatic amine terminated dimethyl siloxane dimers and pyromellitic dianhydride. This reaction produces

polyimides containing the dimethyl siloxane dimer as the only amine component. Essentially, the result was to replace completely the aromatic or aliphatic diamines traditionally utilized for the preparation of polyimides by the dimethyl siloxane unit.

More recently, lesser fractions of the amine terminated siloxane dimers have been incorporated along with aromatic or aliphatic diamines to modify both linear (14,51-56) and addition type (57-60) polyimides. The results of these studies indicated that the incorporation of siloxanes, as a fraction of the total amine content was an effective way of improving the processability and toughness of linear and addition polyimides, respectively.

In the case of siloxane dimer incorporation into linear polyimides, it has been shown that low levels of dimer incorporation improve solubility compared to unmodified polyimides (11). At higher levels of siloxane dimer incorporation solubility in low boiling solvents such as THF has been observed. However, incorporation of siloxane dimer at levels high enough to provide this solubility also results in a loss of thermal stability. In addition to the drop in use temperature resulting from the lowered thermooxidative stability, the mechanical utility of these materials was also limited by a precipitious drop (>100°C) of the glass transition temperature at high levels of siloxane dimer incorporation (60). The lowering of thermooxidative stability has been proposed to be due to the high fraction of aliphatic character present in copolymers containing large fractions of the aminopropyl siloxane dimer. Also, since this is such a short segment of very low T_g no phase separation was observed (61) resulting in a

drastically lower glass transition temperature, another limitation on the upper use temperature. Despite these temperature limitations these materials containing the bisaminopropyl dimethyl siloxane dimer have improved processing characteristics compared to unmodified polyimides. High quality moldings and high strength adhesive test coupons have been fabricated from these materials (62).

The overall concentration of siloxane dimer in the copolymer has also been shown to be crucial with regard to the bulk mechanical properties of these copolymers (63). Essentially, these observations suggest that when the siloxane is the major component (>50% w/w) the materials are elastomeric whereas at low levels of siloxane dimer incorporation the mechanical properties approach those of the unmodified polyimide. Another study supporting these observations (64) concerning the mechanical properties versus siloxane content utilized a quite different synthetic approach for the introduction of the siloxane species. In that study the monomeric siloxane segments were contained within the dianhydride component which was then reacted with aromatic diamines. Another less than favorable consequence of dimeric siloxane incorporation was the lack of siloxane surface enrichment (61).

These limitations have not significantly hindered the research in this area especially by commercial concerns (65-67). The advantages of dimer incorporation as opposed to higher molecular weight siloxane appear to be practical: solubility in lower boiling solvents (68), ease of synthesis and improved moldability (58).

Several publications have appeared (69-71), which detail the preparation and properties of copolymers prepared from higher molecular

weight siloxanes in polyimide backbone systems. Also, previous work at VPI & SU has addressed higher molecular weight siloxane segments in polyimides (13,14) and other structural polymers (61,72-79). Some of the advantageous properties achieved in these materials were: 1) enhanced thermal stability due to a lower fraction of aliphatic units, 2) microphase separation resulting in better mechanical properties as well as a higher glass transition temperature, and 3) less sensitivity to moisture (80). Another interesting phenomenon associated with siloxane incorporation has been that of surface enrichment of the siloxane phase (13,14,72-79). It has been observed in these and other copolymers (81) and blends (82) that enrichment of the surface in the low surface energy, highly mobile, siloxane component takes place. The properties discussed here for polyimides modified by siloxane incorporation have also been studied for a number of other copolymer systems containing siloxane as one component (83-96).

With all of the varied interests in these copolymer systems, one may justifiably wonder where the applications lie? Much of the academic and government work cited above was based on evaluation of these materials as structural adhesives, matrix resins and high performance coatings for the aerospace and defense industries (97-98). In the private sector these types of materials are being developed for electronics (99-100) and also as potential gas separation membranes (101).

2.1.4 Metal Filled Polymers

Synthetic polymers filled with various materials such as glass, metals, and ceramics have been and will continue to be a rapidly

growing, high volume area of polymer utilization. Within this broad class of polymer matrix composites, metal filled polymers occupy a rather unique niche. Although many fillers have been able to provide modifications of physical and mechanical properties (102-103), metal fillers have been generally very efficient in modifying other properties such as electrical and thermal conductivity (104). This section presents an overview of the aspects of filled polymers, specifically metal filled polymers, pertinent to the experimental results and discussion in later chapters.

In practice, for large scale operations, most fillers have been introduced in a so-called compounding step (105). This compounding involves bulk mixing of the polymer with the filler. This bulk mixing generally has been achieved either by roll mixing (i.e. Banbury) or through extrusion. One problem with these methods, however, was the mechanical degradation of the filler during processing. Other, less harsh methods such as tumbling a mixture of powders have also been used to produce high quality composite materials (106).

The influence of metallic fillers on the properties of the composites may manifest itself in several ways. First, as mentioned above, mechanical properties may be modified (103). Specifically, the impact resistance and tensile modulus usually decrease (9). The dynamic mechanical behavior is quite complex and related to the quality of adhesion between matrix and filler (107). Paipetis (107) observed in an epoxy/aluminum system that if interfacial adhesion was good, as measured by surface analysis of fracture specimens, then an increase in tensile storage modulus (E′) was observed as well as a large increase in the

loss factor near the glass transition. Their discussion also stated that if less favorable adhesion was achieved the effect of the incorporation of filler was much less pronounced. The authors also presented theoretical considerations based on agglomeration of particles and the relation between dynamic shear moduli and volume fractions of fillers. This theory predicted that the stress/strain fields in the neighborhood of the individual particles dictated the dynamic moduli. The parameters which influenced this response were quite similar to those which will be presented later with regard to electrical and thermal properties. These parameters were: 1) the size and aspect ratio of the fillers, 2) the distribution (i.e. uniform or segregated) of particles within the matrix and 3) the residual stress due to polymer shrinkage during crosslinking and thermal coefficient of expansion mismatch (108-110). It was also proposed that only in the case of good adhesion between matrix and filler particle can an efficient transfer of the stress between the matrix and filler occur. This proposition seems almost intuitive in light of the present state of the art with regard to fiber reinforced composites but has not been as well understood in the case of metal particles in a polymer matrix. Small inclusions or voids around poorly bonded particles were proposed to have caused anomalous dynamic mechanical behavior (107).

The physical properties, glass transition temperature, thermal conductivity, electrical conductivity and adhesive properties, have all been affected by the presence of metal fillers in polymer matrices. Generally the presence of fillers in polymer matrices slightly increases the glass transition temperature (9) but cases of lowered glass

transition temperatures have been reported (111). The usual explanation for the increase in glass transition temperature in the presence of fillers relies on favorable adhesion between matrix and filler. If good adhesion was present, then the polymer segments, whose concerted motions are responsible for the glass transition, would be more conformationally and energetically restrained in the glassy state. These segments would not only have to exceed the thermal energy barriers to motion imposed by inter- and intra-molecular considerations but also an added energy barrier; that imposed by the interaction of the polymer with the heterophase filler. If particles were present, then additional energy must be provided to free the bonding of the polymer to the particles as well. The presence of the filler particles also constrains the polymer segments physically causing a shift of the relaxation time spectrum and a subsequent broadening of the tan δ damping spectrum. This explanation also accounts for the observation that the glass transition temperature only increases with filler loading up to a certain point. After the maximum number of interactions of particle with polymer is achieved, further introduction of filler does not affect the T_g.

Thermal conductivity of metal filled polymers has also been studied (112). Theoretical considerations predicted and experimental results supported the proposal that this property is governed not only by the overall loading of filler in the polymer matrix but by the size, shape and distribution or orientation of particles in the matrix. Essentially, the connectivity of the particles within the matrix plays a very important role in determining this and other properties. Many of the theoretical considerations which have been applied to this analysis

come from percolation theory. In addition, the work described above (114) considered the percolation threshold as the starting point in the analysis. Extending from this basis, equations were presented which allow for contributions due to both the filler and the matrix. Although these two contributions were quite different if low aspect ratio particles were used; both the filler and the matrix contribute to the overall property when dilute dispersions of large aspect ratio particles were studied.

The effect of metallic fillers on the electrical properties of metal/polymer composites has also been studied (10,106,113-117). Theoretical treatments are available which describe the electron transport processes within these systems (118). The connectivity among particles determined the level at which the electrical conductivity changed dramatically. Typically, at low loading levels of metallic fillers there is no connectivity between particles and the resistive nature of the polymer matrix predominates. At the loading level where a connected macroscopic network is formed among the filler particles the electrical conductivity of the composite increases several orders of magnitude. The shape, orientation and distribution (119) of the particles determine when this threshold is reached. Generally, based on a random distribution of spherical particles, the percolation threshold in 3 dimensions is approximately 30% by volume filler. Aharoni (120) reports that this level is around 20% by volume for iron particles in a poly(amide-imide) matrix. It has also been shown (119) that for very high aspect ratio fillers, fibers with an length/diameter ratio of 10^2, volume loadings required for conductivity may be as low as 5%. It was

noted also, that the current carrying potential of these low loading materials was reduced.

Many potential applications exist for electrically conductive composites. One of the most common is that of EMI (Electro Magnetic Interference) shielding (115-117). Much work in this area as well as theoretical arguments have pointed out that the shielding effectiveness at radio frequencies, of a packaging material, is directly related to the electric conductivity of the material.

Finally, metal fillers have been used to modify adhesive properties of polymers. One such report (121) dealt with the American Cyanimid Company FM-34 polyimide adhesive system. In this case the tensile shear strength at 250°C was found to have been greatly improved on addition of aluminum fillers to the neat polymer system. Not only was the fraction of strength retained at elevated temperatures improved by the incorporation of metal particle fillers but also the resistance to aging at elevated temperatures was also enhanced (122). Some work has shown that up to 65% by weight metal filler could be incorporated into an adhesive system to improve the properties at elevated temperatures (123). The mechanism of this improvement depended on the temperature of the test. At room temperature the enhancement was presumably due to the reinforcing effect of the filler within the matrix while at higher temperatures the mechanism was thought to involve a reduction in thermal stress due to better matching of thermal expansion coefficients between adhesive and substrate (124). It was also possible that the increased stiffness produced in the adhesive due to the presence of the filler resulted in a more effective load transference

between the two adherends. In terms of failure mechanisms the fillers improved fracture properties if good bonding was be achieved between the filler and the matrix. This observation has been explained in terms of a mesophase concept (125). If good adhesion exists, the energy required to fracture a filled composite was greater than the unfilled system due to the tortortous path that the crack must follow to circumvent the particles embedded in the matrix. The failure cracks may also have been split at particle interphases causing eventual arresting of the cracks. Also, a significant fraction of the strain energy stored in the crack tip may have been reflected thereby causing crack deceleration and eventually arresting crack growth completely.

2.2 Adhesive Testing

The ever growing widespread utilization of adhesives for joining structural members requires evaluation of many new materials under conditions appropriate to their potential end use. In addition, since the goal of testing should be to predict performance one must recognize the limitations of the test procedure employed to draw conclusions from the results (126). The advantages of adhesive bonding over mechanical fasteners have been shown to be quite significant and include uniformity of stress distribution and resistance to corrosion (127). Despite these advantages durability (127-129) in adhesively bonded systems has been a major problem. Some applications may require resistance to harsh chemical environments such as solvents, deicers, or reactive gases. Most structural adhesive systems are exposed to a much simpler but no less hostile environment, that of everyday humidity and temperature and their variations. Moisture in the atmosphere may affect adhesives in

several detrimental ways. Water may be absorbed by the adhesive causing plasticization and loss of modulus (130). Water can also interfere with the crucial physical and chemical bonds which must exist in the interphase for adhesion to occur (131). Additionally, it has been proposed (132) that water may change the oxide morphology of aluminum adherends causing failure. Testing and analysis of adhesive specimens exposed to conditions of high humidity and temperature as well as the design of adhesive/adherend systems which perform well under these conditions are of critical importance if greater utilization of structural adhesives is to be realized.

It must also be noted however, that the improvements in resistance to environmental attack would be most valuable if accomplished without sacrificing favorable ultimate strength properties of the system. In effect, the goal of much current research is to combine the best of two worlds; maintain high ultimate properties achieved with some adhesive systems while providing resistance to environmental degradation through modifications of the adherend surface treatment prior to bonding (121). The use of metal alkoxides as primers for titanium has been explored and has been shown to enhance the resistance of adhesive bonds to hot/wet environments (127,133-135). The mechanism of this improvement in durability due to the use of aluminum alkoxide primers has not been completely understood.

2.2.1 Lap Shear Testing

One of the most common tests encountered in evaluation of new polymers for adhesives is the single lap shear test. Ideally, this test would measure the strength of a polymeric adhesive in a pure shear mode.

In reality the test measures a combination of both shear and cleavage properties as shown in Figure 3 (136). The reason for this combination of failure modes results from the inhomogeneous stresses within the bond as shown in Figure 4 (136). Both of these effects are due to the geometry of this particular joint. Many modifications of this geometry have been developed in order to minimize these problems but since many actual applications mimic the design of the single lap shear test the test seems appropriate for the evaluation of new adhesives (135). Further justification for the use of this test results from its widespread use by researchers in all areas of adhesion science. Finally, an overwhelming advantage of this test in the area of new materials evaluation is based on the relatively small amounts of adhesive polymer required to fabricate enough adhesive specimens to get significant averages for the performance of the material (138).

2.2.2 Durability Testing

The true utility of an adhesive system can be determined by the resistance of that system to common adverse environments. Much effort has been addressed at evaluating and predicting the durability of adhesive systems (127-129). Accelerated testing is appropriate since attempting to evaluate structures over their entire expected lifetime would be futile. Since humidity and temperature can be varied over a large range accelerated testing can be achieved by using high humidity and elevated temperatures.

Availability of data for comparison and applicability of sample geometry provide the motivation for the type of testing chosen. Also,

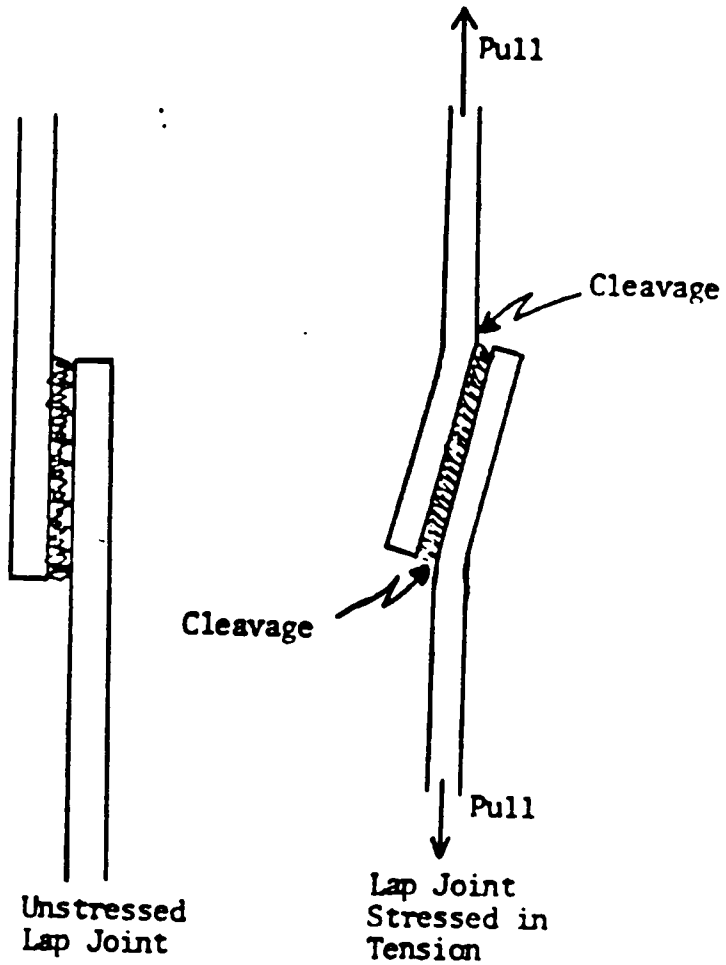

Figure 3: Generation of Cleavage Forces in a Lap Joint Undergoing Tension.

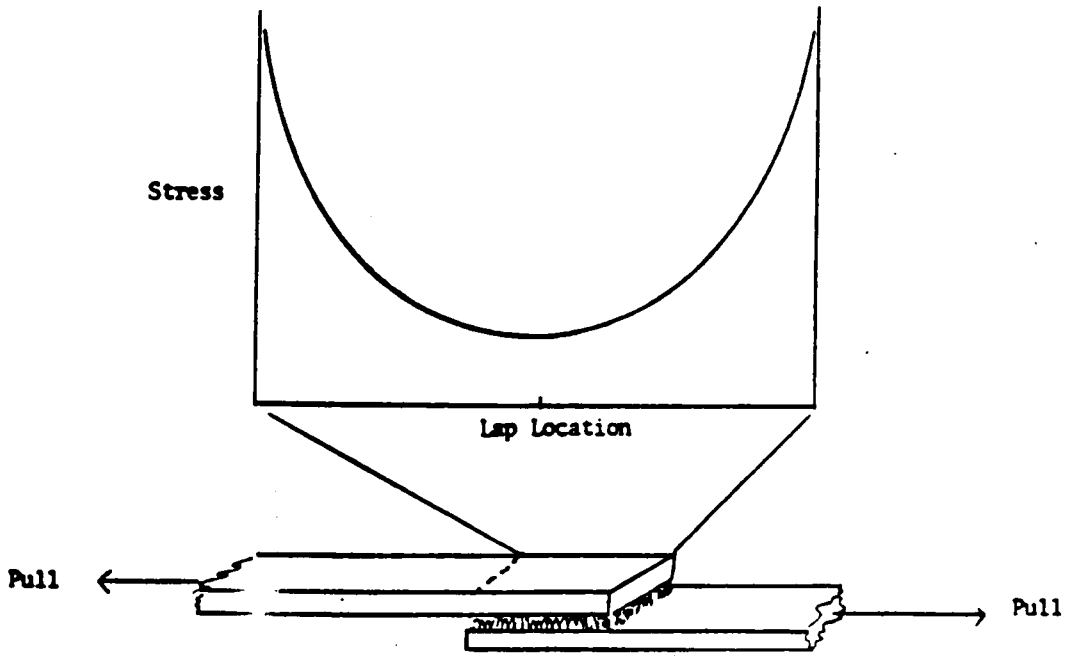

Figure 4: Stress Concentration in a Lap Joint Undergoing Tensile Shear Stress.

the correlation between the geometry which is used for testing and the geometry likely to be encountered in actual practice is important.

The justifications mentioned above for the single lap shear geometry also apply to stress durability testing. Several durability tests based on this geometry have been examined (139). Other geometries which are also quite prevalent in durability testing include the wedge (127) and blister tests (139). These tests generally measure either the time to failure or resistance to crack propagation of an adhesive specimen in the stressed state when exposed to conditions of high temperature and humidity.

This background information has shown several chemical and physical modifications of polymer systems. In the work that is to follow, several of these strategies of modification will be explored and characterized with respect to specific crosslinked and thermoplastic linear polyimide homo- and copolymers. Specifically, the electrical, mechanical and adhesive properties of metal/polymer composites will be studied as well as adhesive properties of polyimides modified by siloxane segment incorporation.

3.0 Experimental

3.1 Materials

3.1.1 Solvents

In all cases exposure to atmospheric moisture was minimized and the bottles were purged with dry nitrogen after each use. Rubber septa were placed on the bottles and the solvents dispensed using syringe techniques to minimize exposure to atmospheric moisture.

3.1.1.1 N,N Dimethyl Acetamide

(DMAC: Aldrich) was obtained in high purity HPLC grade and used without further purification. Care was taken to prevent contamination especially by water. To each 500 ml bottle, after opening, was added type 4A molecular sieves.

3.1.1.2 N methyl-2-pyrrolidinone

(NMP: Fisher) was dried by stirring over ground calcium hydride for at least 12 hours. The solvent was then distilled from this mixture under reduced pressure to avoid thermal degredation.

3.1.1.3 N-cycohexylpyrrolidinone

(CHP: GAF) was dried by stirring over ground calcium hydride for at least 12 hours followed by distillation under reduced pressure.

3.1.1.4 Tetrahydrofuran

(THF: Aldrich) was obtained in uninhibited, HPLC grade and used as received.

3.1.2 Monomers

3.1.2.1 3,3′-diaminodiphenylsulfone

(DDS: Mitsui Toatsu) was obtained as a fine white to yellow powder. DDS was purified by recrystallization from deoxygenated

methanol by adding 10% (w/w) of solid DDS to methanol through which nitrogen had been purged for 20-30 minutes. DDS was dissolved by heating the solution to boiling. This solution was then filtered through a preheated coarse sintered glass funnel. The methanol/DDS solution was then cooled to 0°C in an ice bath at which time white crystals formed. The crystals were collected by vacuum filtration and dried in a vacuum oven at 110°C. The material was then stored in a desiccator until used.

3.1.2.2 3,3′ 4,4′-benzophenonetetracarboxylicacid dianhydride

(BTDA: Allco Chemical) was obtained in high purity and was simply dried in vacuum at 110°C. The material was then stored in a desiccator until used.

3.1.3 Polymers

3.1.3.1 Commercial Polymers

The commercial polymers used in some of these studies were obtained from several sources. Addition polyisoimides and polyimides were obtained from National Starch and Chemical Company and used as received. Thermoplastic polyimides (Upjohn PI 2080, Ultem 6000, Kerimid 601, XU 218) were obtained from colleagues and used as received in all cases.

3.1.3.2 Novel Polymers

In the adhesive/durability aspects of this work the polyimides and poly(imide-siloxanes) used were generally obtained through the courtesy of Professor J. E. McGrath's research group; specifically John Summers, Cynthia Arnold, and Barbara McGrath. A detailed study of the synthetic

approaches to these materials is available elsewhere (14) so only an abbreviated summary will be provided here.

3.1.3.2.1 Poly(Amic Acids)

Polyimides and poly(imide siloxanes) were prepared by two different methods; bulk and solution thermal imidization. In both cases high purity monomers and solvents were required to achieve high molecular weight according to the stoichiometry and difunctionality requirements of step growth polymerizations. In addition, moisture was minimized within the system to prevent possible hydrolysis of the poly(amic acid) intermediate. This moisture minimization was accomplished through careful drying of glassware by exposure of the reactor system to a Bunsen burner flame while dry nitrogen purged the system. Drying tubes were also attached to minimize moisture intrusion into the system during stirring. In both cases the preparation of the precursor poly(amic acid siloxanes) was identical. In this preparation thermally treated 3,3′-4,4′ benzophenonetetracarboxylicacid dianhydride (BTDA) was added to NMP in a reactor system diagramed in Figure 5. 3,3′ diaminodiphenylsulfone (DDS) was added to the stirring anhydride solution. The resulting poly(amic acid) solution was stirred under nitrogen for 6-16 hours to insure complete reaction.

After formation of the poly(amic acid) precursor the solutions were stored in a freezer at 0-5°C until used.

3.1.3.2.2 Bulk Thermal Imidization

In the case of bulk thermally imidized polymers, these poly(amic acid) solutions were then simply cast on glass plates at 0.25-0.45 mm (10-18 mils) thickness and heated in a forced air inert atmosphere oven

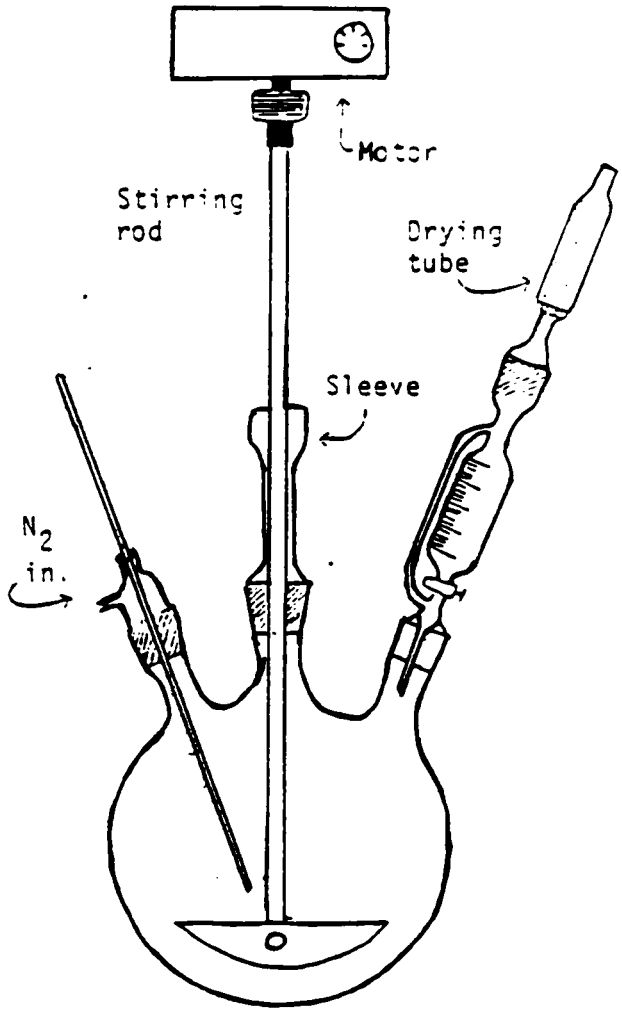

Figure 5: Reactor Used for Synthesis of Poly(amic acids).

at 80°C for 0.5 hour, 100°C for 1 hour, 200°C for 1 hour and 300°C for 1 hour in a dynamic dry air atmosphere at a flow rate of from 8-15 liters/minute. After the final hour at 300°C the air flow was stopped and the resulting films were then allowed to cool slowly to room temperature.

3.1.3.2.3 Solution Thermal Imidization

The second imidization process involved the use of a cosolvent system to eliminate water from the reaction mixture and to keep the reacting species solublized during the entire course of the reaction. The reactor used in this system is shown in Figure 6. The poly(amic acid) solution was added to an equal volume of a 60/40 v/v mixture of N-methyl pyrrolidinone (NMP) and N-cyclohexyl pyrrolidinone (CHP) which was maintained at 160°C. The addition of the poly(amic acid) was controlled such that the temperature of the reacting solution was kept above 150°C. In addition, a fast flow of nitrogen was passed through the reaction vessel to help minimize H_2O in the system. After all of the poly(amic acid) solution was added to the reactor, the addition funnel was removed. Water, in addition to some NMP, was collected in the Dean-Stark trap. This reaction was then allowed to proceed for 16-20 hours at 160±10°C, after which the system was allowed to cool slowly to room temperature. In this case isolation of the polymer was accomplished by precipitation of the reaction solution into a 10X volume excess of methanol containing 0.5-1.0% (v/v) acetic acid to assist in coagulation. This coagulation was done in a waring blender. The resulting solid was filtered under vacuum, dried at 140°C in vacuum and then the redissolved in NMP or DMAC and reprecipitated as above. The

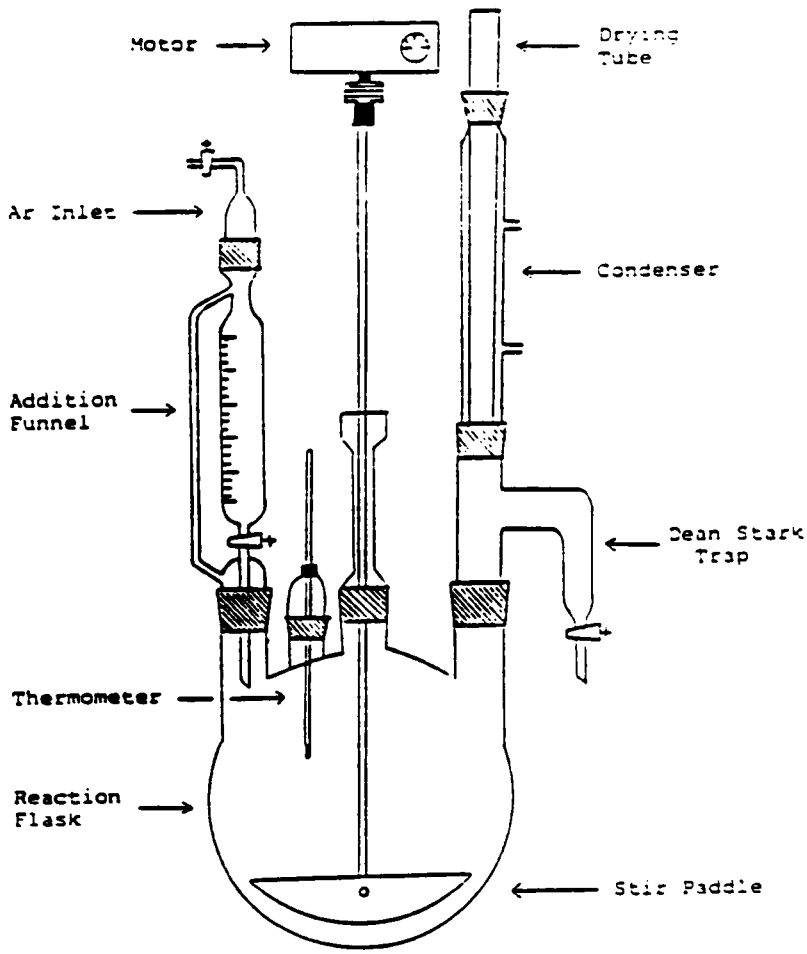

Figure 6: Reactor Used for Solution Imidization of Polyimides.

utilization of these polymers for the adhesive preparations described later required modification of the bulk thermal imidization mentioned above. These modifications will be discussed in the section on sample preparation. The method outlined above for the case of bulk thermal imidization was used to prepare samples for thermal analysis evaluations.

3.1.4 Metal Powders

3.1.4.1 Aluminum Nickel 1 to 1 Alloy Powder

This 1:1 atomic alloy powder was obtained in 3 particle sizes from Alcoa Corporation. The designations of the as received powder were fine (-270 mesh; 20-70 μm), medium (-270 + 140 mesh; 20-200 μm) and coarse (+ 140 mesh; 200-300 μm). No cleaning or other pretreatment was carried out prior to use of these powders.

3.1.5 Aluminum Bus Conductor Bars

These bars were supplied by Alcoa Corporation and were comprised of 1350 HT aluminum. This designation represents a minimum aluminum concentration of 99.50% with no major alloying elements (140). These bars were used as received except for cleaning and abrasion which will be described below.

3.1.6 Mechanical Fasteners

Anodized aluminum nuts and bolts were provided by Alcoa . Alcoa also provided stainless steel belleville spring washers and stainless steel nuts and bolts.

3.1.7 Surfactants

3.1.7.1 Electrical Joint Compound

(EJC #2: ALCOA) was used as received.

3.1.7.2 Alkaterge E

Alkaterge E was provided by Angus Chemical Company, 211 Sanders Road, Northbrook, Illinois and used as received.

3.1.8 Lap Shear Coupons

3.1.8.1 Aluminum 6061 T6

Aluminum alloy sheet was provided by Alcoa. The sheets were then fabricated into 5 inch by 1 inch coupons by shearing the metal with a foot operated brake.

3.1.8.2 Titanium

Titanium 6% aluminum, 4% vanadium coupons were obtained from personnel at NASA-Langley Research Center. Detailed pretreatment descriptions will be discussed later in an appropriate section. Since these coupons had already been used once for bonding some gross pretreatment was required. Specifically, the joining sections between the coupons were mechanically ground off to produce a uniform 5 inch by 1 inch coupon. Additionally, excess polymer from the first bonding was mechanically brushed from the surfaces.

3.1.9 Pasa Jell 107

Acid etch surface pretreatment was obtained from H.S. Bancroft Corporation, and was used as received. This surface etch solution was brightly colored. After many coupons had been treated (100-120) the color was dulled and the solution replaced.

3.1.10 Scrim Cloth

A-1100 surface treatment, E glass woven cloth was obtained from NASA. This cloth was spread in a brass frame (Figure 7) and heated at 110°C in vacuum immediately prior to coating.

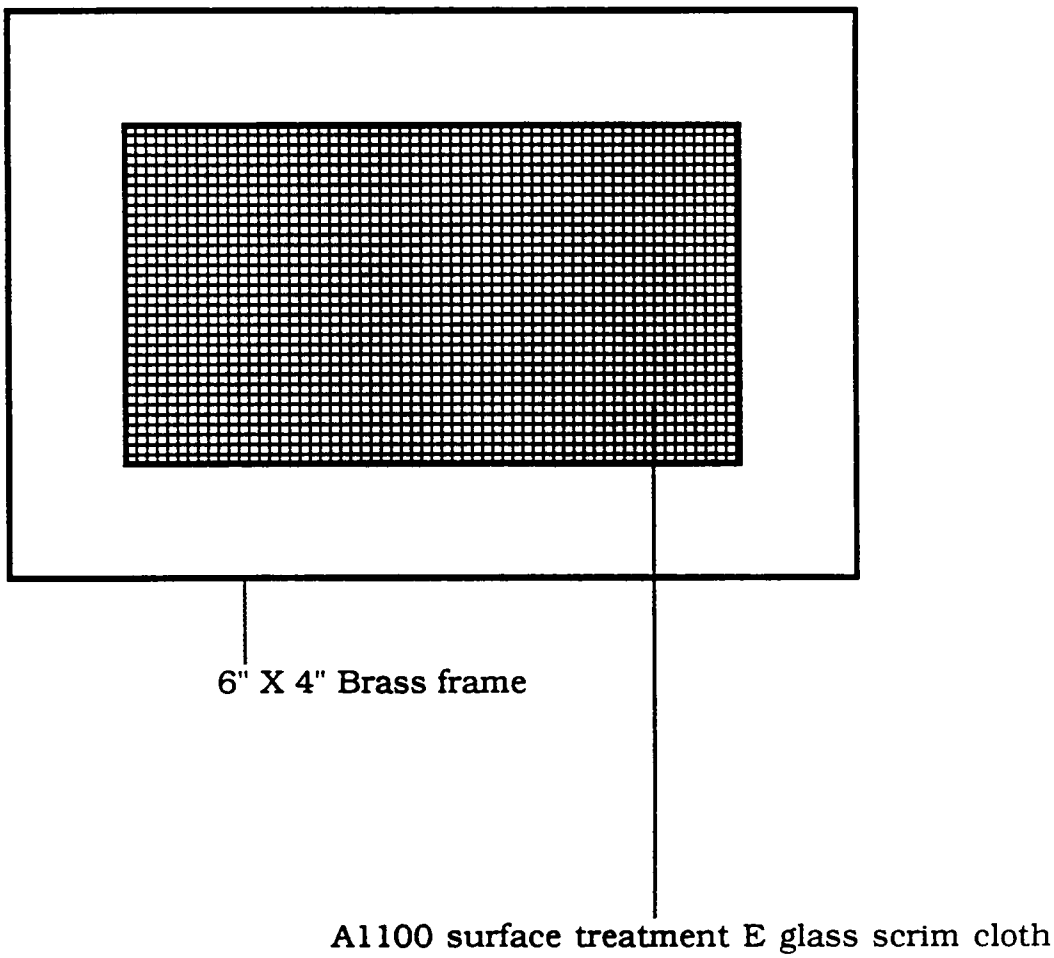

Figure 7: Brass Frame Used to Hold Scrim Cloth During Coating.

3.2 Techniques

3.2.1 Sample Preparation

3.2.1.1 Electrical Joint Fabrication

All aluminum bars were pretreated by sanding with a belt sander to remove the mill finish and to provide a roughened surface for better electrical contact. Several different methods were used for applying the polymer/grit mixture to the aluminum bars prior to bonding. These included application of a mixture of the two powders with no carrier, application of a suspension consisting of the polymer powder and grit in either EJC #2 or Alkaterge E surfactant and application of a slurry of the polymer solution in THF or DMAC and grit. Formulations not containing carrier were prepared by measuring polymer powder and grit into a vial in a 1:1 (w/w) ratio followed by vigorous shaking for several minutes. This mixture was then applied to one aluminum bar. The other bar was then carefully attached and the bolt tightened until the Belleville spring washers were fully compressed. These joints were then treated thermally as indicated in Chapter 4. Formulations containing a carrier paste or solvent were prepared via two procedures. With Alkaterge E or EJC #2 a paste was prepared with the polymer powder/grit mixture. The paste was applied to each bar with a spatula. The bars were then bolted together as previously described and thermally treated. With DMAC or THF, the solid polymer powder was dissolved at a loading of 25-35% (w/w) solids. The powder was then added to this solution and dispersed by mechanical stirring. This slurry was then applied to the substrates with a spatula after which the bars were bolted together. Joints were then allowed to stand for 24 hours to

allow for evaporation of the solvent and for hardening of the polymer matrix.

3.2.1.2 Metal Polymer Composites

(MPC) samples were prepared from intimate mixtures of polyisoimide prepolymer and metal powder in various ratios. Mixing was accomplished by grinding the two components together in a mortar/pestle until homogeneity was achieved. These powder mixtures were then compressed to densify and heated to 220°C under less than 0.8 MPa (150 psi) pressure to achieve curing of the polyisoimide.

3.2.1.3 Infrared Samples

Polyisoimide samples for infrared cure experiments were prepared by casting a thin film of solution (THF 5% w/w) onto a KBr plate. The solvent was removed by heating the crystal in a vacuum oven at 60°C. Care was taken to obtain thin films from which all the solvent could be removed under these conditions. The vacuum was adjusted to prevent bubbling of the polymer film.

3.2.1.4 Adhesive Specimens

Two substrates were used in the lap shear tests. Aluminum 6061 T6 was used in the metal polymer composite study and titanium (6-4) was used in the poly(imide siloxane) study.

3.2.1.4.1 Pretreatment of Substrates

3.2.1.4.1.1 Aluminum Coupons

In the case of the aluminum substrates the pretreatment consisted exclusively of mechanical abrasion of the surface to be bonded. This abrasion was accomplished with 80X superkote sandpaper. The specimens were sanded by hand until a uniform degree of roughness was achieved and

no native finish was observed. The abrasion was conducted perpendicular to the long axis of the coupons.

3.2.1.4.1.2 Titanium Surface Treatment

A crucial step in the bonding of titanium adherends involved preparation of the surfaces. Since this study involved the evaluation of different modified adhesives, a consistent surface treatment was desired. Pasa Jell 107 acid etch was chosen for several reasons. First, Pasa Jell 107 has been shown, by the wedge test, to provide a relatively good surface treatment in terms of bond durability (141). Second, it was readily available and easy to use. It has usually been recognized that after environmental attack the locus of failure occurs near the interfacial region of the bond (142). Since durability testing was planned, a pretreatment stable under hot/wet conditions was required. Titanium (6%Al, 4%V) coupons (127 mm x 25.4 mm) were grit blasted to remove the native oxide surface. The coupons were then wiped with methanol to remove any loose abrasive. At this point the coupons were vertically dipped in Pasa Jell 107 for 1 minute, etched for 10 minutes, then dipped and etched again for the same time periods. The coupons were then cleaned of excess etch by rinsing in hot tap water and mechanically cleaned with an acid brush. The coupons were then placed in an ultrasonic cleaning bath, in tap water, for 5 minutes and allowed to dry for 5 minutes. Next, the coupons were placed in an ultrasonic cleaning bath in distilled water for 10 minutes and hung to dry for 10 minutes. Finally, the coupons were heated in a forced air oven at 70°C for 10 minutes and coated with primer within 30 minutes of this final step (See also Appendix 1).

3.2.1.4.2 Bonding Procedures

Different bonding procedures were used for the metal polymer composite systems than for the poly(imide-siloxane) systems.

3.2.1.4.2.1 Metal Polymer Composite Bonding

Samples were prepared for adhesive and electrical testing from the metal polymer composites as follows. First, the aluminum coupons, pretreated as above, were arranged in the bonding jig shown in Figure 8 to allow for one-half square inch overlap. Next, the metal polymer composite precursor was placed in the overlap area. This precursor consisted of the mixed alloy/isoimide powders which had been cold pressed at room temperature 34-68 MPa (5,000-10,000 psi) pressure to achieve densification. The bonding jig was then assembled and placed between the press platens, Figure 9. The platens were then heated to 220°C and the pressure increased to 0.7 MPa (100 psi). These temperature and pressure conditions were maintained for 1 hour to achieve a reproducible state of cure in the addition polymer. Cool down was accomplished slowly under pressure.

3.2.1.4.2.2 Poly(imide siloxane) Bonding

Pretreated and primed titanium coupons were arranged in a bonding jig, Figure 8, which had been shimmed to provide zero bond thickness and 12 mm x 25 mm overlap area. Next, the adhesive scrim or film was sandwiched between these adherends and the jig was placed in a Carver lab press, Figure 9. Contact pressure was applied while the platens were heated to 280°C (approx. 20-25 minutes). After the glass transition temperature had been exceeded (~280°C), 2.0-2.1 MPa (250-300 psi) pressure was applied. The platens were then further heated to 320-

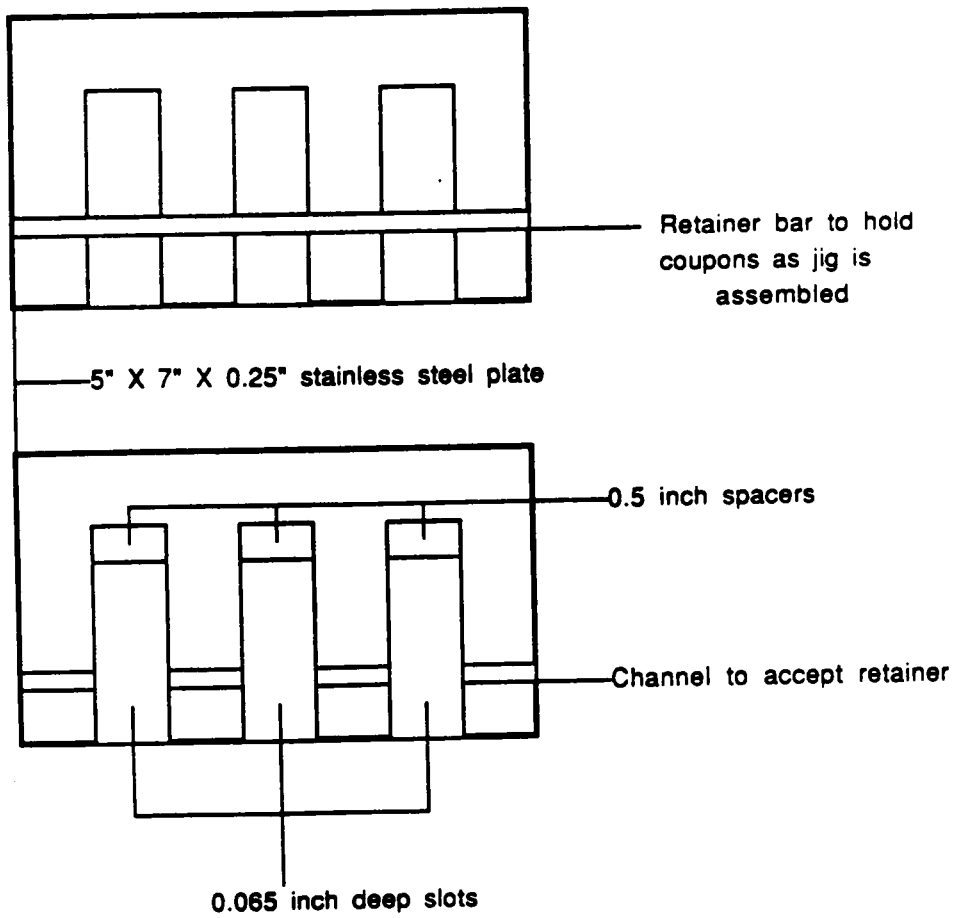

Figure 8: Bonding Jig Used to Prepare Single Lap Shear Samples.

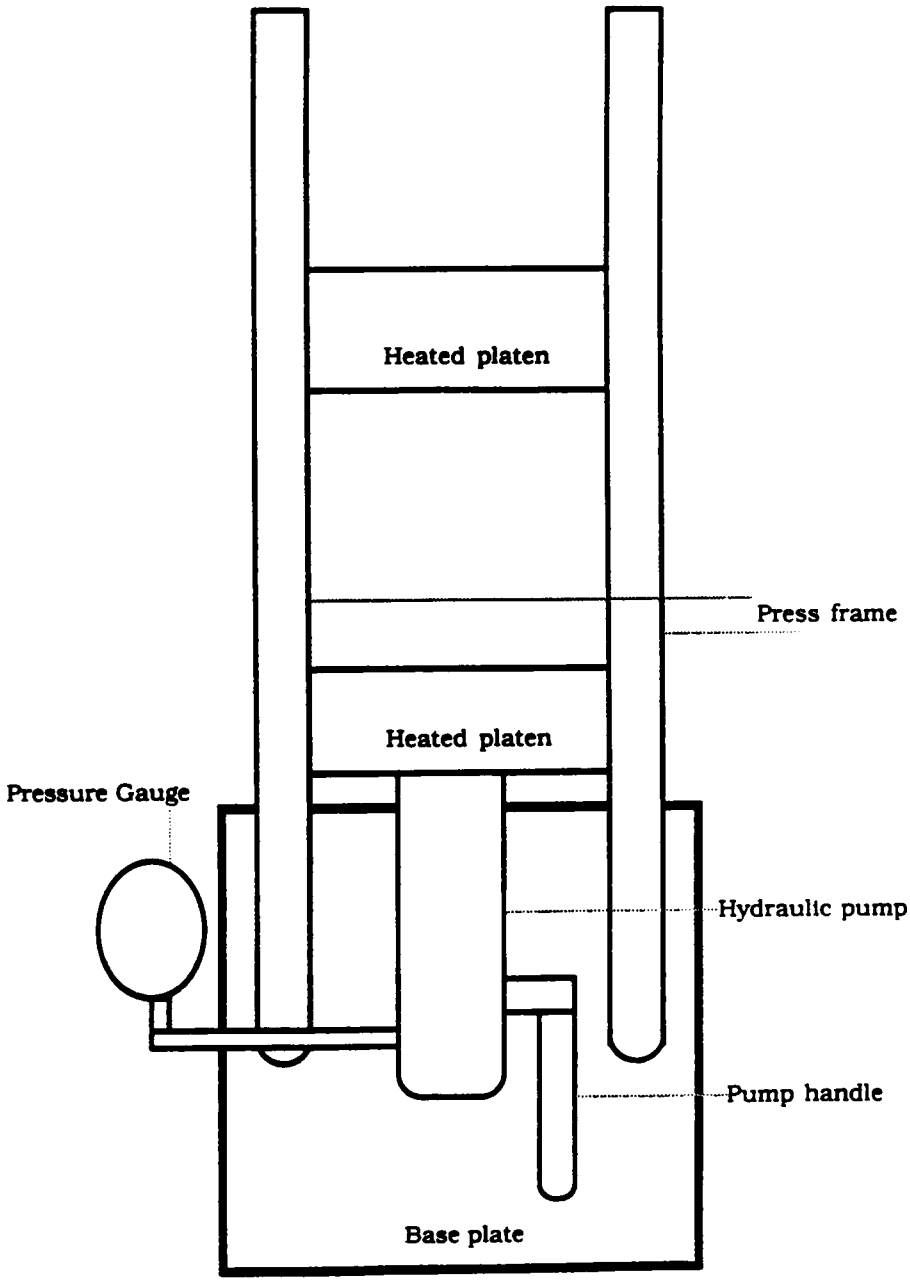

Figure 9: Press Used to Prepare Adhesive and Composite Samples.

330°C for 30 minutes to complete the bonding cycle. Cool down was accomplished slowly by stopping power to the platens. The cool down cycle was carried out under pressure. Generally, the samples were removed from the press after the temperature dropped below 50°C (4-5 hours). Bonding temperature was monitored throughout the cycle by thermocouples inserted in a slot within the bonding jig.

3.2.2 Instrumental

3.2.2.1 Thermal Analysis

All of the thermal analysis data presented here were obtained on Perkin Elmer (P-E) Instrumentation. A Perkin Elmer System-4 microprocessor controller was used to generate heating profiles for the P-E DSC-4, Differential Scanning Calorimeter; TMS-2, Thermomechanical Analyzer and the TGS-2, Thermogravimetric Analyzer. The data were collected by means of the P-E TADS Thermal Analysis Data Station computer with appropriate software. In the case of the TMA, data were collected using a P-E 2 pen chart recorder.

3.2.2.1.1 Differential Scanning Calorimetry (DSC)

DSC was performed with a Perkin Elmer DSC-4. The heating rate used for routine analysis was 10°K/min. The atmosphere for the DSC experiments was dynamic nitrogen which was purged through the system at a rate of 20 cc/min. Baseline optimization procedures were performed periodically. Data presented here reflect automatic subtraction of reproducible baseline curvature through the scanning autozero feature of this instrument (SAZ). This feature, SAZ, relies on the point by point subtraction, during the experimental scan, of an identical scan run without the presence of sample. The DSC was also calibrated for energy

and temperature periodically using indium metal as a standard (T_m = 156.6°C, ΔH_m = 6.80 cal/g).

3.2.2.1.2 Thermogravimetry (TG)

TG was performed on a Perkin-Elmer TGS-2 Thermogravimetric Analyzer. For routine experiments the heating rate was 10° K/min. and the atmosphere was dynamic air at a purge rate of 50 cc/min. The balance was calibrated for mass using a 100 mg class M calibration weight. Temperature calibration was accomplished using the calibrate mode of the System 4 controller. Additionally, this temperature calibration was verified using the loss of water of hydration from copper sulfate pentahydrate. In the case of the metal polymer composite samples the standard platinum sample pans could not be used. The presence of the aluminum in the aluminum nickel alloy filler caused irreversible contamination of the platinum pans. To avoid this contamination problem glass liners were fabricated for use within the platinum pans. These liners protected the platinum and apparently did not influence the degradation of the polymer.

3.2.2.1.3 Thermomechanical Analysis (TMA)

TMA was performed on a Perkin Elmer TMS-2 Thermomechanical Analyzer. The experiments were done in the penetration configuration with an applied load of 20 grams. Samples were run in film form in a nitrogen atmosphere and were heated at 5° K/min. Additionally, first derivative curves were generated simultaneously during the experiment using the FDC-1 first derivative computer.

3.2.2.1.4 Dynamic Mechanical Thermal Analysis (DMTA)

DMTA was performed on a Polymer Laboratories Dynamic Mechanical Spectrometer. The samples were run in the single cantilever mode using a 16 mm frame and 14 mm spreader clamp. In this configuration the free unclamped length of the sample is 1 mm. The widths of the samples varied from 12-15 mm and the thicknesses from 0.20-0.50 mm. The strain factor used was X4 and the frequency was 1 Hz. The temperature range covered was from 0-300°C. In all cases the heating rate was 5 K/min.

3.2.2.2 Surface Analysis

Various surface analytical techniques were used to examine the chemistry and topology of substrates both prior to and after adhesive bonding. The experimental parameters outlined below are intended to give a general description of the procedures used for each of the techniques. In some cases variations from these parameters was required in order to accommodate certain samples.

3.2.2.2.1 X-Ray Photoelectron Spectroscopy (XPS)

XPS was performed on a Perkin Elmer PHI 5300 ESCA (Electron Spectroscopy for Chemical Analysis) system. The incident source was magnesium K^{α} radiation (Mg K^{α} 1253.6 ev) at 250 watts. Generally, a 5 minute survey scan was used to determine the elemental composition of the surface. This survey was followed by a multiplex procedure lasting 30-40 min. These multiplex data are then used to determine the atomic concentration of the elements of interest. These concentrations were calculated by the computer using the self-contained elemental sensitivity factors.

3.2.2.2.2 Optical Microscopy (OM)

OM was carried out on a Bausch & Lomb Optical Stereo Microscope. Magnification available was from 10-70X. This instrument was used in conjunction with an external high intensity light source.

3.2.2.2.3 Scanning Electron Microscopy (SEM)

SEM was accomplished using a Philips EM-420T electron microscope. Samples in these experiments were generally 3 mm X 7-10 mm in area and were 0.5-1.5 mm in thickness. At the higher range of sample thickness 1.3-1.5 mm the limits of the lens systems in this microscope were reached and consequently the microscope could be focused only at relatively low magnifications < 10,000 X. Non-conductive samples were sputter coated with approximately 20 nm of gold to reduce the effect of charging by the electron beam. SEM was also conducted with an International Scientific Instruments (ISI) XS-40 SEM. Backscatter electron detection was used. The filament bias was adjusted such that the emission current was 80 μA over the background current. Non-conductive samples were sputter coated with 20 nm of gold prior to analysis to reduce charging by the electron beam.

3.2.2.2.4 Fourier Transform Infrared Microscopy (FT-IR-M)

FT-IR-M was accomplished using a Spectra-Tech IR PLAN infrared microscope in conjunction with a Nicolet 6000 Infrared Spectrometer. Spectra were collected in the reflectance mode from titanium (6-4) substrates. In most cases the background used was a pretreated titanium surface with no further coating. Spectra represent the average of 512 scans for both the background and sample files. Except as noted the microscopy conditions were 150X magnification utilizing a 10X eyepiece

in conjunction with a 15X cassagrain objective/condenser. Under these conditions the sampling area is approximately 600 μm X 600 μm. Except as noted no further aperturing of the sample was needed. Under these conditions the energy through put to the detector was approximately 3.5 volts/scan which was sufficient to allow data acquisition with a detector gain of 1.

3.2.2.2.5 Indicator Dye Testing

Residual surface acidity of basicity was measured using indicator dyes (143). Bromothymol blue solution was used as received (LaMotte Chemical Products). For the following dyes 0.01 g of dye was dissolved in 25.0 mL of deionized water: thymol blue, orange I (both Pfaltz and Bauer, Inc.), and bromophenol blue (Arthur H. Thomas Company). In the case of bromocresol purple 0.1 g of dye was dissolved in 9.25 mL of 0.02 N sodium hydroxide solution and diluted to 250 mL with deionized water. The dye, 2-5 drops, was applied to the pretreated surfaces and allowed to dry.

3.2.2.3 Adhesive Testing

Two types of adhesive testing, room temperature and stress durability, were performed. Both tests utilized the single lap shear test geometry (Figure 3, for example). Bonds fabricated as above were then aged at least 5 days, to minimize physical aging effects, and subjected to the test procedures outlined below.

3.2.2.3.1 Lap Shear Testing

Tensile shear testing was carried out generally according to ASTM D-1002-72. An Instron Model 1123 testing machine was used equipped with self tightening grips and a 5000 lb. load cell. Electronic load

calibration was used and the data were collected by computer at a rate of 9.1 pts/sec. Bonds were arranged in the grips with 2 inches of their length held in each grip. The crosshead speed for these experiments was 0.05 in/min. All data presented later represent the maximum load achieved multiplied by a factor of 2 to normalize the stress to a 1 square inch area. In this experiment the errors were generally less than 10% between duplicate bonds either prepared at the same time or on different days with the same batches of material.

3.2.2.3.2 Stress Durability Testing

Durability testing was performed generally according to ASTM D-2919 utilizing the same single lap shear geometry described above. The fixture used for this experiment is shown in Figure 10. This fixture has the advantage of being portable which allows it to be used in a variety of environments. In this case the specimens were placed in the fixture and loaded to 7.6 MPa (1200 psi). Depending on the sample, this load represented 30-50% of ultimate bond strength. This load value was chosen since it allowed for failure of the samples within a reasonable time period (2-30 days) with adequate reproducibility (0.5-1.0 days). The load was applied by means of the external spring which had been compressed to this known load by means of a hydraulic stud tensioning device. The fixture, with the loaded specimen in place, was then placed into a large incubator/water bath, which had been modified to accept many of these fixtures at one time. The conditions of the exposure within the water bath were 80°C and 100% relative humidity. The atmosphere was kept saturated by means of 2-4 inches of excess water present in the bottom of the water bath. Time to failure of the lap

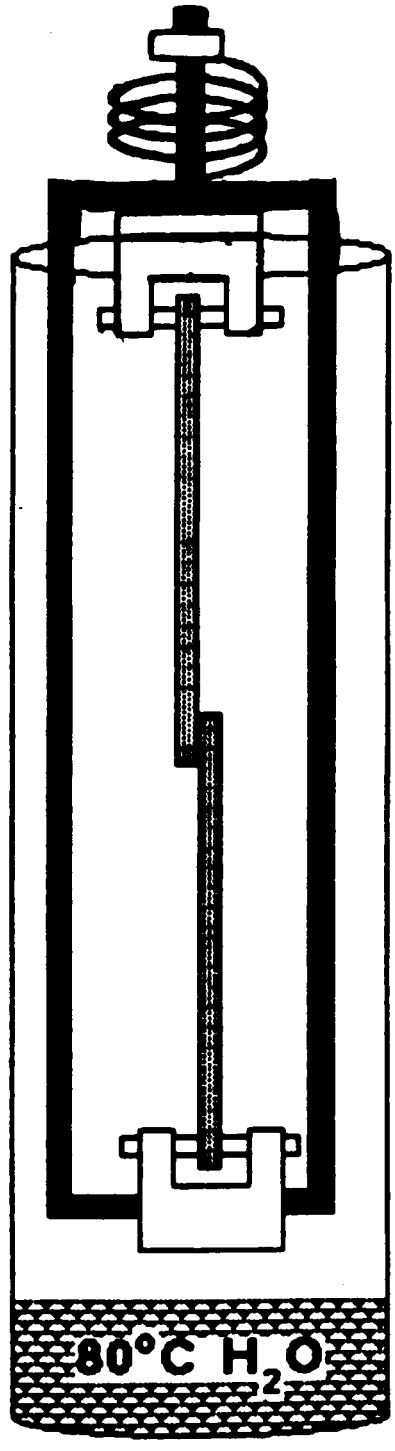

Figure 10: Stress Durability Test Fixture.

shear specimens under these conditions was measured. This time measurement was accomplished through a switched timer arranged at the top of the tensioning stud such that when the bond is intact the switch is held closed by means of a laboratory clamp holding the switch to the top of the stud. However, when the specimen breaks the position of the tensioning stud changes thereby dislodging the timer switch which then opens, stopping the timer.

3.2.2.4 Fourier Transform Infrared Spectrometry (FT-IR)

FT-IR was performed on a Nicolet 6000 Infrared Spectrometer. Transmission spectra were obtained at a minimum of 4 an^{-1} resolution and were the average of at least 10 scans. FT-IR cure experiments were conducted using a Barnes Model C019-020 heated cell. One modification was made in that the temperature of the crystal and sample was monitored independently of the cell heater. This was accomplished by drilling a small hole in the side of the KBr crystal and inserting a narrow gauge thermocouple into this hole. The actual sample temperature, 5-10 degrees less than the heater set temperature, could thus be measured. Also, in the heated cell experiments spectra were collected as a function of time at a given temperature by means of the gas chromatography system software. Generally, the spectral data were collected as 10 co-added interferograms and stored to a particular file. After the completion of the experiment other MACRO programs were used to Fourier process the interferograms in each file and also to integrate the peaks of interest in each of the spectra.

3.2.2.5 Electrical Testing

Electrical testing was performed on aluminum/metal polymer composite (Al/MPC) aluminum conductor bar specimens using equipment shown schematically in Figure 11. Additionally, the lap shear joints were tested using the same electrical configuration but applied to the different sample geometry. Generally, 1-3 amps of current were passed across the interface of interest by means of a Hewlett-Packard 8264A DC power supply. The voltage drop across the interface was measured using a Keithly 177 Microvolt DMM multimeter.

3.2.2.6 Gel Permeation Chromatography

GPC of some addition polyisoimides was carried out on a Waters system using THF as the solvent. The columns were Ultrastyragel with pore sizes of 500Å, 1000Å, 10,000Å, and 100,000Å. The flow rate was 1 mL/min and column temperature was 30°C. Detection was accomplished with a Waters 401 differential retractometer.

3.2.2.7 ^{13}C Nuclear Magnetic Resonance Spectroscopy (^{13}C NMR)

High resolution ^{13}C nuclear magnetic resonance (NMR) was carried at a frequency of 50.33 MHz at room temperature using a WP200-SX spectrometer. The samples (10% w/v) were in d_6-DMSO. Typically, 1000 free induction decays were accumulated with a recycle delay of 4.0 sec and Fourier Transformed. The spectra were referenced through DMSO (σ = 39.5 ppm).

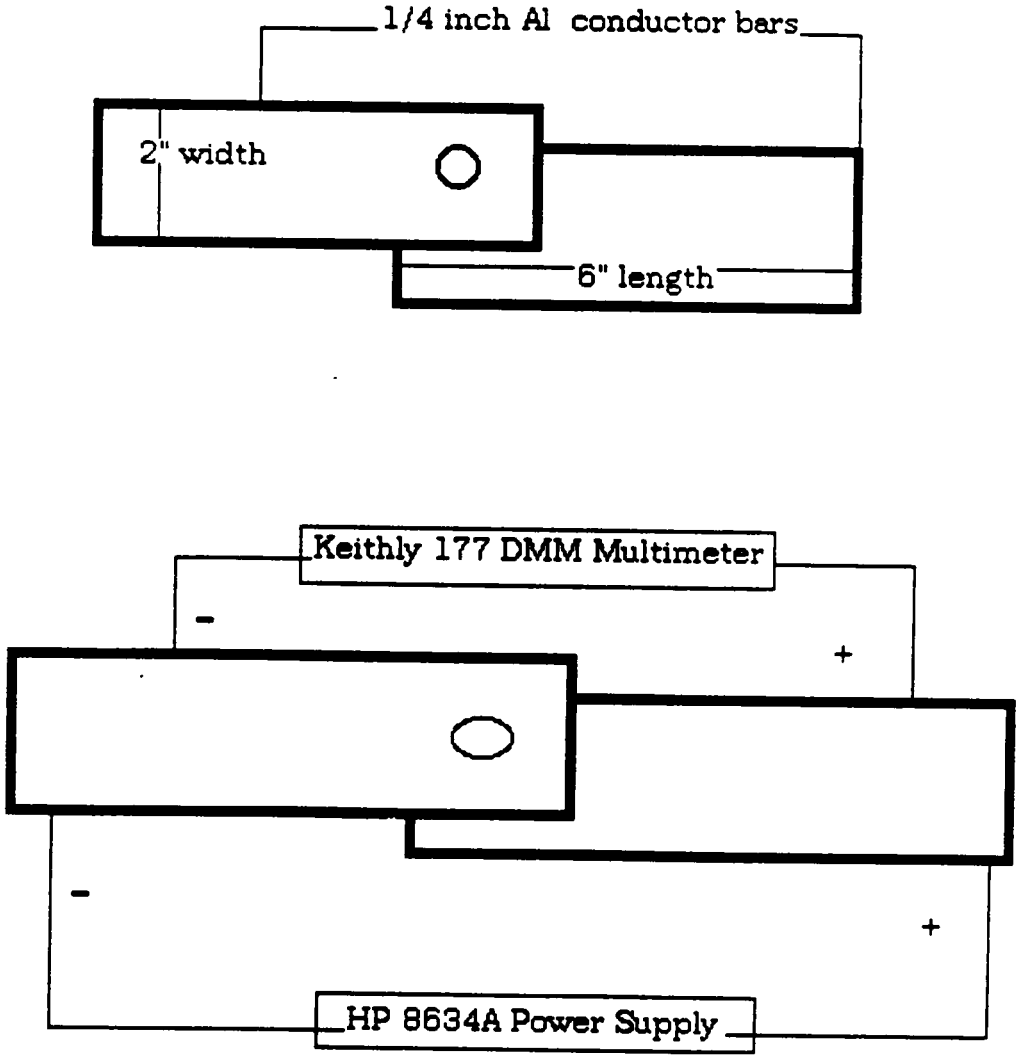

Figure 11: Electrical Conductivity Test Configuration.

4.0 Isothermal Ageing of Conductive Bonds Between Aluminum

4.1 Introduction

The use of a metal filled polyimide matrix to maximize both the electrical conductance and thermal stability of aluminum bus bar connections is of considerable interest. After an initial study be E. A. Madigan at VPI & SU (25) employing condensation polyimides, research has been concentrated in the areas of addition or thermoplastic, soluble polyimides. These materials were predicted to provide better adhesive strength and ease of processing than the thermoset condensation polyimides used in previous work (25). This study with addition polyimides also builds on the previously investigated effects of metal (grit) loading, grit mesh size, and surface preparation of the aluminum bars prior to bonding.

During this study promising polyimides were screened while investigating the effects of (1) thermal aging, (2) presence of additives such as EJC#2 and Alkaterge E, and (3) experimental parameters such as bolt pressure and current level on the measured electrical resistance. Solvent-casting the polymer slurried with Ni/Al grit powder rather than using EJC#2 or Alkaterge E as a carrier for the powders has also been explored. In addition work has been done to determine whether or not the grit particle size or loading level has any effect on the thermal stability of the polymer when grit and polymer are mixed as powders.

4.2 Results and Discussion

4.2.1 Effect of Addition Polyisoimide Molecular Weight

Two different addition polyisoimides were studied to determine

what, if any, effect the molecular weight of the prepolymer has on the measured resistance. Joints were prepared by applying a polymer/grit slurry in THF to one of the Al substrates. An uncoated bar was then bolted in place to the treated bar and the assembly allowed to stand at room temperature for 24 hours to allow the solvent to evaporate (Figure 11, for example). The following general measurement procedure was then employed. The room temperature resistance with bolt was first measured. The bolt was then removed and the room temperature resistance without bolt measured. The joint was next wrapped with heating tapes and the elevated temperature resistance without bolt obtained. Finally, the bolt was replaced and the heating tapes once again attached and the elevated temperature resistance with bolt measured.

Thermid IP-600 has a molecular weight of 1099; while Thermid IP-630 has a molecular weight of 17,877 according to the manufacturer. Comparison of the electrical performance of these two prepolymers is shown in Table 1. It is interesting that the higher molecular weight material shows a greater increase in resistance on removal of the bolt than the lower molecular weight polymer at room temperature. This would suggest that the lower molecular weight material maintains better contact with the aluminum bars. This effect could be due to (1) easier removal of solvent from the lower molecular weight slurry or (2) a thinner overall matrix between the bars due to the lower viscosity of the Thermid IP-600 slurry. Elevated temperature data would support the trapped solvent explanation since the resistance of the joint without the bolt and with the higher molecular weight polymer rises dramatically on heating to 100°C. On a more positive note if the joints remain

Table 1

Electrical Conductor Joints:
Comparison of Addition Polyisoimide Molecular Weight[a,b]

	Room Temperature (μΩ)		100°C (μΩ)	
	Bolt	No Bolt[c]	Bolt	No Bolt[c]
Thermid IP-600	13.3±1.0	14.5±1.5	12.4±1.5 (100 hrs.)	19.5±2.5 (613 hrs.)
Thermid IP-630	15.5±2.0	46.3±20.0	-----	900±500 (24 hrs.)

[a]Formulation: 50% polymer, 50%-270 mesh Al/Ni Grit, THF carrier.

[b]*Data represent the average of at least 2 individually measured joints.

[c]Bolt removed prior to resistance measurement.

bolted together with the lower molecular weight addition polyimide, resistance is essentially invariant even after maintaining the joint at 100°C for 100 hours. The volatility of the solvent used to form the slurry also plays a part in the behavior of the Thermid polyimide systems studied. As will be discussed below the higher boiling solvent DMAC leads to higher elevated temperature resistances due to continued evaporation of the solvent at the measurement temperature. This continued evaporation leads to loss of contact and increased resistance. The low boiling THF is removed more thoroughly at lower temperatures. One problem with THF seems to be most apparent with the higher molecular weight Thermid IP-630. This material seems to trap the THF so that when heated the solvent evaporation causes void creation in the matrix and subsequent increased resistance.

4.2.2 Comparison of Polyimide Matrices

A number of commercially available soluble polyimides were screened in this study. The resistance data are given in Table 2. Joints were prepared by application of the polymer/grit slurry (THF) to one of the aluminum substrates. After bolting and fastening with Belleville springs, the joints were allowed to stand 24 hours at room temperature to allow the polymer matrix to harden. No further curing of the polymer was carried-out. There seems to be little significant difference in resistance between the three soluble polymers with bolts in place. The XU218 material is very comparable in resistance behavior to both Thermid IP addition polyisoimides. However, the UpJohn 2080 and Ultem 6000 materials which are not soluble in THF but are soluble in DMAC showed somewhat different behavior. The UJ2080 joints increased in

Table 2

Electrical Conductor Joints:[a,b]
Comparison of Polyimide Matrix

Polyimide	Room Temperature (μΩ)		100°C (μΩ)	
	Bolt	No Bolt	Bolt	No Bolt
XU218	13.4±4.0	16.0±4.0	---	18.7±3.5 (24 hrs.)
UpJohn 2080[c]	15.1±1.0	67.6°40.0	---	250[d] (24 hrs.)
Ultem 6000[c]	1900±1500	---	5500[d]	---
Thermid IP-600	13.3±1.0	14.5±1.5	12.4±1.5 (24 hrs.)	19.5±2.5 (613 hrs.)
Thermid IP-630	15.5±2.0	46.3±20.0	---	900±500 (24 hrs.)

[a]Formulation: 50% polyimide, 50% -270 mesh Al/Ni Grit, THF carrier unless noted

[b]Data represent the average of 3 individually measured joints.

[c]DMAC carrier employed.

[d]One joint measured.

resistance upon removal of the bolt and increased even more dramatically when measured at 100°C; on the other hand, the Ultem starts with a very high resistance at room temperature that increases further when monitored at 100°C even though the joints are bolted together. The increase in resistance on going to the higher temperature in the DMAC system is believed to be due to the loss of solvent as the temperature is increased which causes loss of Al-Al contact even though the bolt may still be in place as in the case for the Ultem 6000 joints. The reason this effect is more apparent in the case of the DMAC solvent is that DMAC is a much higher boiling solvent than THF (166°C vs 67°C). The DMAC is still evaporating at 100°C while all of the THF is gone by that temperature allowing the polymer matrix to fill any voids created by its evaporation.

The reason for the high initial resistance of the Ultem 6000 joints is almost certainly due to the thickness of the matrix layer. Besides being the most viscous polymer tested it was also slowest to dissolve so that after 24 hours of stirring a 30% (w/w) solution still contained many undissolved particles which were extremely difficult to remove. It is believed that these undissolved particles are responsible for keeping the aluminum bars apart resulting in poor contact and high resistance. This high temperature instability of the carrier is also responsible for higher resistances noted with the non-solvents such as EJC#2 which were also tested as potential carriers for the polyimide-grit mixture.

4.2.3 Comparison of Polyimide Carrier

Several carriers were tested for application of the polyimide/grit

powders to the aluminum bar. The carriers and associated joint resistances are given in Table 3. The formulation applied as an EJC #2 paste and cured at 250°C gives the lowest room temperature resistance but this resistance increases dramatically when measured at 250°C. This increase in resistance at elevated temperature is probably due to thermal degradation or evaporation of the grease-like component of EJC #2. Such phenomenon would cause the aluminum sustrates to be spread apart resulting in a loss of contact through the formation of voids leading ultimately to a higher measured resistance.

The formulation in which no carrier was used was probably too viscous in its molten state to spread adequately through the joint and therefore resulted in a thicker polymer layer and a fairly high resistance value. The increase in resistance for this joint experienced at 250°C can be explained by the absence of the bolt. During thermal cure the joint was bolted together, however, for measurement purposes the bolt was removed. No doubt the polymer softened slightly wherein the compression which was locked in after the initial heating cycle was allowed to relax slightly and some contact was lost.

The joint containing the Alkaterge E surfactant formulation which was cured at 250°C did not increase in resistance significantly on reheating to 250°C but its value was still not as favorable as the formulation applied with tetrahydrofuran as the carrier which was not cured at elevated temperature. The joint formulation containing THF maintained essentially constant resistance on going from room

Table 3

Electrical Conductor Joints:
Comparison of Polyimide Carrier[a,b]

Carrier	Cure Treatment	Room Temperature (μΩ)		250°C (μΩ)	
		Bolt	No Bolt	Bolt	No Bolt
None	250°-30 min.	--	21.2±3.0	--	29.6[c]±1.0
EJC#2	250°-15 min.	--	8.0±1.5	--	51.0±3.0
Alkaterge E	250°-15 min.	--	20.5±3.0	--	25.0±4.0
THF	None	13.4±1.0	14.5±1.0	12.3±1.0[d]	17.3±1.0

[a]Formulation: 50% Thermid IP-600 polymer, 50% -270 mesh Al/Ni Grit.

[b]Unless otherwise noted all measurements represent an average of three joints.

[c]Value for single joint. Other joints broke apart before measurement.

[d]Measured at 100°C.

temperature to 100°C. This joint also maintained favorable room temperature resistance after removal of the bolt indicating that the uncured polymer is rigid enough to maintain electrical contact without requiring external mechanical pressure. The next section provides a more detailed study of the effect of bolt pressure on the measure resistance.

4.2.4 Effect of Bolt Pressure

A series of joints was prepared with and without bolts and Belleville springs in place during the resistance measurement to determine the effect of the presence of the bolt and springs on the measured resistance. The joints for this study were prepared by application of the grit containing polymer solution to one of the aluminum substrates. The coated and uncoated substrates were then bolted and joined using Belleville spring washers to maintain pressure. The joints were then allowed to stand 24 hours prior to testing to allow for the evaporation of the solvent and subsequent hardening of the polymer matrix. The results obtained, presented in Table 4, indicate that the pressure created by the bolt and springs leads to a decrease in joint resistance. Data with Thermid IP-630 best illustrate this effect. The explanation which is suggested is that the IP-630 slurry is very viscous and probably contains more trapped solvent than the IP-600 slurry. The higher viscosity would account for a thicker matrix; while, the presence of solvent would suggest a softer material overall. If this is the case then removal of the bolts allows this softer material to expand thereby decreasing contact and increasing resistance. The current leakage through the bolt is not thought to be a major effect

Table 4

Electrical Conductor Joints:
Effect of Bolt Pressure at Room Temperature [a,b,c]

	Resistance		
Joint Configuration	Joint 1	Joint 2	Joint 3
with Bolt			
IP-600	13.6±1.0	14.0±1.0	12.6±1.0
IP-630	14.8±1.0	18.3±1.0	13.8±1.0
without Bolt			
IP-600	15.7±1.0	12.7±1.0	---
IP-630	34.8±1.0	73.5±1.0	---

[a]All joints fastened during cure with Belleville springs and bolts.

[b]Formulation: 50% Thermid IP-630 (IP-600), 50% -270 mesh al/Ni Grit. THF carrier.

[c]Cure Cycle: Joints were allowed to stand 24 hours with bolts and springs in place to allow solvent evaporation. No further heating except during testing at 100°C.

since the bolts are heavily anodized. Also supporting the thickness effect is the increased scatter in the data after removal of the bolt. If the decreased resistance was due to current carried by the bolt it would be expected to affect each joint to approximately the same extent. This is not the case since removal of the bolts results in wider scatter of the measurements. The extremely high and scattered resistance data at 100°C, shown in Table 5, are also thought to be due to the presence of trapped solvent. At elevated temperatures the creation of voids due to solvent evaporation would be expected to decrease the contact and consequently increase resistance. This is supported by the 100°C data for the IP-600 material with bolt which show approximately the same or slightly decreased resistance due to better contact when the polymer softened with the bolt in place.

4.2.5 Effect of Isothermal Aging on Resistance

Several joints were subjected to elevated temperatures for extended periods of time to determine the effect of isothermal aging on the electrical resistance of the joints. The joints were prepared by application of the polymer solution-grit slurry to one substrate and then bolting the second substrate in place with Belleville spring washers. The assembly was allowed to stand 24 hours to allow solvent evaporation prior to testing. It should also be noted that the current was passed through the bar assembly continuously during the entire aging experiment. Also of interest is the fact that the bolts and springs were removed during the aging experiment. In this case, the only external pressure applied was due to the heating tapes and the C clamps which were used to hold insulation in place over the tapes. The results

Table 5

Electrical Conductor Joints:[a,b,c]
Effect of Bolt Pressure at 100°C

Joint Configuration	Resistance Joint 1	Joint 2	Joint 3
with Bolt			
IP-600	13.8±1.0 (10 hrs.)	12.5±1.0 (10 hrs.)	10.8±1.0 (10 hrs.)
IP-630	---	---	---
without Bolt			
IP-600	21.7±1.0 (613 hrs.)	16.6±1.0 (613 hrs.)	---
IP-630	600±30 (24 hrs.)	2000±30 (24 hrs.)	275±15 (24 hrs.)

[a]All joints fastened during cure with Belleville springs and bolts.

[b]Formulation: 50% Thermid IP-630 (IP-600), 50% -270 mesh al/Ni Grit. THF carrier.

[c]Cure Cycle: Joints were allowed to stand 24 hours with bolts and springs in place to allow solvent evaporation. No further heating except during testing at 100°C.

are tabulated in Table 6. These results indicate that no significant deterioration of the electrical resistance of the joints occur after over 600 hours at temperatures around 100°C. This means that the contact which was achieved initially during the 24 hour period allowed for solvent evaporation by application of pressure from the Belleville springs is maintained even after the assembly has been heated for extended periods. This suggests that even though the addition polyimide is uncured it acts as a rigid adhesive which prevents the expansion of the joint at elevated temperatures. Any expansion would be expected to decrease the Al-Al contact and thereby increase the electrical resistance of the joint. It is thought that the volatile solvent (THF) is almost completely gone after the 24 hour room temperature cure cycle and as such does not contribute to the formation of voids during the heating of the joints. It therefore is somewhat surprising that although the polymer used in this study (Thermid IP-600) has a molecular weight of only 1099 (according to the manufacturer) it forms a rigid matrix upon evaporation of the solvent.

A second set of data shown in Table 7 was obtained on joints containing the same formulation but with the bolts in place and heated to a higher temperature (250°C). Since the data at 250°C, even after 161 hours, are still within the uncertainty of the measured resistance at 100°C the additional curing of the polymer, which occurs above 160°C, has no effect on the resistance of the joint. These data also further support the conclusions reached earlier regarding the bolt carrying current since the resistances are the same with and without the bolt in place. A third set of elevated temperature data shown in Table 8

Table 6

Electrical Conductor Joints:
Resistance vs. Time at 106°C [a,b,c]

Time (hour)	Temperature (°C)	Resistance (μΩ)
0	ambient	14.5
1	66	11.3
3.5	72	12.6
5.25	73	13.0
99	104	13.6
100	106	14.0
120	106	13.0
126	106	13.3
144	106	13.6
147	106	13.0
613	95	16.6

[a]Formulation: 50% Thermid IP-600, 50% -270 mesh Al/Ni Grit, THF carrier.

[b]Cure cycle: Room temperature, 24 hours with bolt and spring resistance measurement conducted without bolt.

[c]All values have an uncertainty of ±2.0μΩ.

Table 7

Electrical Conductor Joints:
Resistance versus Time at 250°C [a,b,c]

Time (hour)	Temperature (°C)	Resistance (μΩ)
0	Ambient	11.0
0.16	50	11.3
0.33	100	13.3
0.46	165	13.3
0.63	165	15.7
0.90	189	16.3
1.5	212	16.7
17	244	17.3
20	244	16.7
39.5	244	16.7
135	244	17.0
139	258	17.7
161	251	18.0

[a]Formulation: 50% Thermid IP-600, 50% -270 mesh Al/Ni Grit, THF carrier.

[b]Cure cycle: Room temperature, 24 hours with bolt and spring resistance measurement conducted with bolt.

[c]All values have an uncertainty of ±2.0μΩ.

Table 8

Electrical Conductor Joints: [a,b]
Resistance versus Time at 260°C

Time (hour)	Temperature (°C)	Resistance (μΩ)
0	Ambient	6.9
0.25	42	7.0
0.36	47	7.0
0.45	54	7.3
0.55	66	8.3
0.65	69	7.3
0.75	107	6.0
0.85	112	7.6
0.95	130	7.6
1.05	139	8.3
1.15	148	8.7
1.25	157	8.7
1.35	167	8.7
1.45	172	9.7
1.55	175	9.3
1.65	178	9.7
1.75	181	9.7
1.85	190	9.7
1.95	196	10.0
2.05	201	9.7
2.15	209	10.0
2.25	211	10.0
2.35	217	10.0
2.45	225	10.0
2.55	230	10.7
2.65	234	10.3
2.75	240	10.7
2.85	245	11.0
2.95	250	11.0
12.0	255	11.3
16.0	241	11.1
18.0	245	11.3
22.0	250	11.7
37.0	253	11.3
44.0	247	11.3
60.0	246	11.3
66.0	261	11.7
85.0	266	11.3
87.0	266	11.0
108.0[c]	263	11.3
110.0[c]	Ambient	181.0
110.0[c]	Ambient	154.7
110.0[c]	Ambient	140.7

[a]Formulation: EJC#2 (with HF). No polymer present.

[b]All values have an uncertainty of ±2.0μΩ.

[c]Individual joint resistances after removal of the bolts; insulated c-clamps were used to maintain constant joint thickness.

wherein only the EJC#2-HF containing formulation (i.e. no polymer) was used showed a dramatic effect on whether the bolt was in place. In this case when the bars were heated initially the bolts were kept in place. The resistance data remained constant at ~10-12μΩ even after remaining at ~250°C for over 100 hours. This was very unexpected considering the thermal instability of the EJC#2 compound. The joint was then cooled-down and the bolts were removed but only after C clamps which were insulated with Teflon were applied to hold the bars together at approximately the same pressure as the bolts. The room temperature resistance was then measured and found to be an order of magnitude greater than that measured with the bolts in place. It was noticed when the bolts were removed that the yellowish color of the anodized bolts was missing in places where the bolts contacted the bars. This would suggest that contact between each of the bars and the "de-anodized" bolt accounted for the low measured resistance with the bolts in place. It should be noted that only one joint containing EJC#2 was maintained at 250°C for the duration of the experiment due to problems with two of the voltage sources for the heating tapes. These two joints only achieved temperatures in the 140-160°C range. However, after the bolts were removed it was found that this temperature range was great enough to cause degradation of the joint compound.

Also tested was a joint containing a thermoplastic polyimide, UJ2080, which was not soluble in THF and was therefore cast as a DMAC solution. This higher boiling solvent remains in the polymer to a much greater extent than the volatile THF. A thermogravimetric analysis of this formulation indicates that even after standing at room temperature

for 24 hours the formulation contains ~60% (w/w) DMAC. However, with the bolts in place the resistance of the joints is relatively low (~15 μΩ). After 200 hours at 200°C the values are unchanged as seen in Table 9. These data can be understood in light of the "bolt-created" pressure during solvent evaporation. In other words, if pressure is maintained on the joint during solvent evaporation, the polymer which is softer at elevated temperature can be deformed to maintain electrical contact. Another set of data was obtained for the same formulation but with the bolts removed after a 24 hour room temperature cure. Insulated C-clamps were used to maintain contact since the constant pressure provided by the bolts and spring washers was eliminated. These data in Table 10 show that solvent evaporation even at temperatures around 100°C causes a loss of contact due to void formation and subsequent increased resistance. It should be noted that although the resistances increased by a factor of 2 when the bolts were removed, heating the joint caused the resistance to increase to 130μΩ. This indicates that the more rapid evaporation of the solvent which is to be expected as the measurement temperature nears the DMAC boiling point may be responsible for a large increase in resistance at elevated temperatures in joints where no external pressure is applied (no bolts). On the basis of the resistance increase on removal of the bolts one can conclude that the UJ2080 in DMAC system is a less efficient adhesive after the room temperature cure than the Thermid IP600 in THF. The latter system which is rigid enough after the room temperature cure to function as an adhesive maintains low resistance after bolt removal. Regardless of the electrical data, the UJ2080 system qualitatively proved to be a poorer adhesive. For

Table 9

Electrical Conductor Joints:[a,b,c]
Resistance versus Time at 235°C

Time (hour)	Temperature (°C)	Resistance (μΩ)
0	Ambient	7.7
1.5	35	8.3
3.0	78	7.7
4.0	300	17.4
144.0	209	14.0
168.0	226	15.0
212.0	235	14.8
215.0[d]	Ambient	14.1

[a]Formulation: 50% UpJohn 2080, 50% -270 mesh Al/Ni Grit, DMAC carrier.

[b]All values have an uncertainty of ±2.0μΩ

[c]Cure cycle: Room temperature, 24 hours with bolt and spring.
Resistance measurement conducted with bolt in place.

[d]After cooling and removal of bolt and spring.

Table 10

Electrical Conductor Joints:
Resistance versus Time at 240°C [a,b]

Time (hour)	Temperature (°C)	Resistance (μΩ)
0	Ambient	7.7[c]
0	Ambient	15.3[d]
0.5	65	21.3
1.0	82	155.8
24.0	102	149.3
25.0	134	148.7
26.0	213	159.0
43.0	224	129.3
45.0	244	130.4
76.0	240	128.9
91.0	238	126.7

[a]Formulation: 50% UpJohn 2080, 50% -270 mesh Al/Ni Grit, DMAC carrier.

[b]All values have an uncertainty of ±2.0μΩ.

[c]Room temperature resistance before bolt removal.

[d]Room temperature resistance after bolt removal.

example, when the bolts were removed from the joints which contained UJ2080 after heating, two of the joints began to come apart under the stress of bolt removal. This would account for the increased resistance observed in these two joints in subsequent room temperature measurements after bolt removal.

4.2.6 Effect of Cure on Measured Resistance

According to the manufacturer the addition polyisoimides used in this study require a temperature in excess of 160°C in order to crosslink the terminal acetylene groups. A comparison of two sets of joints was made to determine whether this thermal treatment was responsible for any lowering in the resistance of the joints. The results are given in Table 11. The first joint was prepared by mixing the polymer and grit powders in a 1:1 ratio then applying this powder mixture to one aluminum bar. The other bar was then attached and the bolts tightened until the Belleville springs were fully compressed. This joint was then heated with the bolts and springs in place at 250°C for 30 minutes. The second joint was prepared by first dissolving 15g of Thermid IP-600 in 50 mL of HPLC grade tetrahydrofuran. Next, 15g of Al/Ni-270 mesh grit was added to the stirring solution. This slurry was then applied to an aluminum bar; then, the other bar was then attached and the bolts tightened to compress the springs. This joint was then allowed to stand overnight to allow the solvent to evaporate. These results indicate that thermal treatment was detrimental to the resistance of the joints. The resistance for solvent cast slurries are lower than for those joints made by applying the powder to the joint and then heating the joint to above the melting/cure temperature of the

Table 11

Electrical Conductor Joints:
Effect of Thermal Treatment [a,b]

Heat Cycle	Room Temperature(μΩ)		Elev. Temperature (μΩ)	
	Bolt	No Bolt	Bolt	No Bolt
250°C for 30 minutes (powder)	---	21.2±2.0	---	26±1.0 (30 hours at 250°C)
None (THF Cast)	16.7±2.0	14.5±1.5	12.3±1.5 (100 hours at 100°C)	11.3±1.0 (100 hours at 250°C)

[a]Formulation: 50% Thermid I.P. 600, 50% -270 mesh Al/Ni Grit. Applied to joint as indicated in parenthesis.

[b]Data points are the average of 2 joints measured separately 3 times.

polymer while under the pressure of the Belleville springs. This effect may be due to the thickness of the polymer layer present between the aluminum bars. The molten polymer is much more viscous than a 50% (w/w) slurry containing Thermid IP-600 and Al/Ni grit. Also the strength of the Belleville springs would be expected to decrease at elevated temperature. Both of these influences, but primarily the influence of viscosity, would lead to a greater matrix thickness for the joint made by the application of powder. It is suggested that the increased thickness of the matrix layer is responsible for the higher resistance observed in the case of the joint prepared by application of the powder mixture.

4.2.7 Comparison of Current Level

The electrical resistance measurements, as described in the experimental section, were made at two current levels. The formulation employed in this study was a paste made by dispersing equal amounts of polyimide and grit in EJC#2 and applying this mixture to the aluminum bars. These bars were then fastened by bolting to 30 foot-pounds with a torque wrench. The assembly was then heat treated for 15 minutes at 250°C to cure the polymer. After cooling to room temperature the resistance measurements were made. Initially, a 1 amp current source was used; in this case the voltage drops measured were tens of microvolts which is near the lower limit of measurable voltage drops with the voltmeter used. Resistance measurements were made also at a 3 amp current level. A comparison of the measured resistances is given in Table 12. There is good agreement between the resistances measured at the two current levels with the differences being less than 10%. These

Table 12

Electrical Conductor Joints:
Comparison of Current Level[a,b]

Current Level	Average Voltage Drop (μΩ)			Resistance (μΩ)		
	Joint 1	Joint 2	Joint 3	Joint 1	Joint 2	Joint 3
1 amp	19.6±1.0	11.3±1.0	13.0±1.0	19.6±1.0	11.3±1.0	13.0±1.0
2 amps	61.6±3.0	37.8±1.0	41.9±1.0	20.5±3.0	12.6±1.0	13.9±1.0

[a]Formulation: 50% Thermid IP-600, 50% -270 mesh Al/Ni, EJC#2 paste carrier. Cured at 250°C for 15 minutes.

[b]Data represent an average of 3 measurements made at room temperature without bolt.

results comparing 1 and 3 amp current levels also agree favorably with previous results obtained by comparing 1 amp resistance data obtained from N. Bond at Alcoa's Messena facility.

4.3 Summary

The data presented here demonstrate that metal containing polyimides are effective in maintaining favorable electrical properties at interfaces between aluminum conductor bars after aging at elevated temperatures. The key parameters in accomplishing this objective have been polymer/slurry viscosity during fabrication and solvent volatility. It has also been shown that the presence of mechanical fasteners (i.e. bolts) in these test fixtures can lead to errors in interpretation of observed electrical characteristics when conventional non-adhesive joint compounds such as EJC#2 are used.

Next, various physical and chemical properties of the neat polyisoimides and metal/polymer composites were studied under more controlled experimental conditions.

5.0 Chemical Characterization of Thermal Cure Reactions of an Acetylene Terminated Polyisoimide Prepolymer

5.1 Introduction

The increasing need for high service temperature adhesives and structural matrix resins has led to the development of many new polymeric systems in recent years. One of the most interesting and potentially useful of these new polymers are the polyimides. Polyimides are noted for their excellent thermal and mechanical properties but their utility has been severely limited due to problems with fabrication and processing of these polymers (6-8). Nevertheless, the careful design of polyimides can lead to enhanced processability. In this respect, several approaches have been investigated and found to be useful. One design method which has improved the processability of linear aromatic polyimides was the introduction of meta-substituted aromatic diamines for para substituted analogs (15,16). This procedure, while improving the processability, also had the possible detrimental effect of lowering the glass transition temperature. Another method which has been successfully utilized in improving polyimide processing and solubility characteristics was the incorporation of bulky side groups through phenylated diamine monomers (17). Although these materials maintained a high glass transition temperature their resistance to solvents may have been sacrificed. Processability has also been improved by diluting the rigid imide functionality in the polymer chain through the use of block copolymerization with a flexible segment such as a siloxane (11,18-19). These approaches all relied on

enhancing the thermoplasticity of the polyimides through incorporation of flexibilizing linkages.

Finally, processability and fabrication aspects of polyimides have been improved through the use of low molecular weight imide oligomers terminated with acetylenic groups (20-21). The material (MC-600) shown in Figure 1 is an example of a commercially available product (National Starch and Chemical Co.). These materials have improved solubility and processing characteristics while maintaining both a high glass transition temperature and good solvent resistance due to their highly crosslinked nature following thermal cure of the acetylene groups. It has been found (3) that preliminary reactions of the terminal acetylene groups during thermal cure led to a detrimental restriction of flow and wetting properties before good contact with a substrate was achieved. In addition, since the glass transition temperature of these imide oligomers was quite high (~200°C) the crosslinking reaction proceeded very rapidly resulting in an infusible, rigid network. Once the glass transition temperature has been exceeded, enough mobility is available in the system for rapid crosslinking of the terminal acetylene groups. In this case, above 200°C (the T_g of the uncured polymer) this crosslinking reaction proceeded very rapidly. The gel time for MC-600 has been estimated at less than three minutes at 250°C (22). This short gel time severely restricts the uses of the material in applications such as matrix resins and adhesives where good flow is necessary prior to the onset of gellation.

In order to circumvent this problem of rapid gelation an isomeric imide structure, termed isoimide, has been introduced into these systems

(4,22). Materials with this functionality (i.e., IP-600) (Figure 2) exhibit improved solubility as well as longer gel times and lower glass transition temperatures (~160°C vs ~200°C for the corresponding imide oligomer). Initially, it was thought that the presence of the isoimide structure, as an unfavorable side reaction product in polyimides, led to premature thermal decomposition of polyimides through loss of CO_2 from the imino-lactone heterocyclic ring (23). However, later work (24) showed that the isoimide functionality thermally isomerized to the imide functionality (Scheme 1) prior to any significant degradation of the polymer backbone.

Since the utility of these materials has been improved by the incorporation of these reactive functionalities without severely decreasing other favorable properties such as thermooxidative stability and solvent resistance the chemistry of the isoimide isomerization and acetylene crosslinking reactions has been of considerable interest. Previous work has shown that these materials, when loaded with metal powders, provide a convenient and effective method of optimizing the electrical conductance and thermal stability of aluminum conductor joints (25). The goal of this work has been to elucidate the relationship between the thermal isomerization and crosslinking reactions occurring in this acetylene terminated polyisoimide oligomer: Thermid IP600. The techniques of Fourier transform infrared spectrometry (FTIR) and differential scanning calorimetry (DSC) have been shown to be useful in determining the cure states of acetylene-terminated resins such as imides and sulfones (5,41,144-145). These

techniques were applied to the cure reactions occurring in the IP600 acetylene-terminated isoimide system.

5.2 Results and Discussion

5.2.1 DSC Energy Data

The incorporation of the isoimide functionality into acetylene-terminated oligomers has been shown to result in enhanced solubility, a lower glass transition temperature and improved processability compared to the analogous imide oligomers (145). Chemical changes occurring in curing systems can be monitored in a variety of ways, two of the most common of which are DSC and FTIR. DSC provides an overall energetic profile of the reactions occurring in a given temperature range; while FTIR provides detailed structural information concerning the relative concentrations of functionalities present in the system. By establishing a reaction energy profile using DSC one can effectively choose the proper temperatures at which to conduct isothermal FTIR experiments. These isothermal FTIR experiments can then be used to establish the nature and kinetics of the chemical changes occurring in the system as a function of time at the given isothermal temperature.

The DSC thermograms of MC-600 and IP-600 are shown in Figure 12. It is apparent from these scans that the isoimide oligomer (IP-600) has not only a lower glass transition temperature but also a larger exotherm of reaction than the corresponding imide oligomer (~ -80 cal/g for IP-600 vs ~ -40 cal/g for MC-600). This observation along with the fact that these oligomers were of the same nominal molecular weight (~1100 g/mole) leads to the conclusion that the isomerization of the isoimide to the imide functionality is sufficiently exothermic to contribute

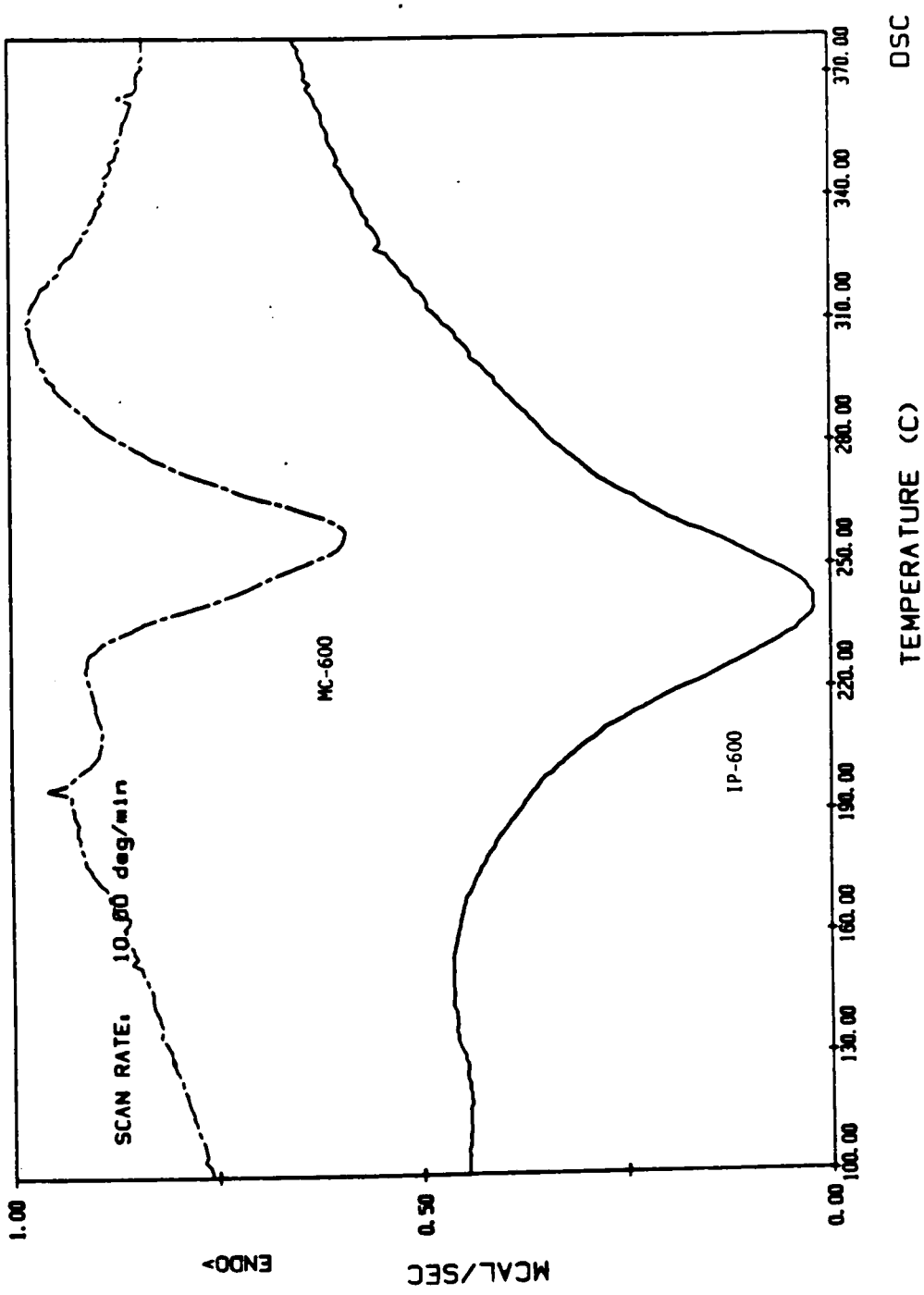

Figure 12: Comparison of DSC Thermograms of Acetylene Terminated Polyimide and Polyisoimide Oligomers.

significantly to the exotherm of the net reaction measured by DSC. Activation energies for these two samples were calculated from the variation of peak reaction temperature with heating rate. The activation energies so calculated along with the equation used in this calculation are shown in Table 13. The non-agreement of activation energies suggest a substantial difference in reaction pathways for these two samples. The method chosen for extracting activation energies is expected to be more accurate than analysis of a single scan for situations where two overlapping peaks occur in the DSC scan (146). The activation energy calculated for the imide oligomer, MC-600, is 19.7 ± 0.7 Kcal/mole which agrees with values obtained for similar model systems such as sulfones (24.2 ± 0.7 Kcal/mole) (147) and phenoxy phenyl acetylene (23.2 ± 1 Kcal/mole) (148). The activation energy for the isoimide oligomer is substantially lower (13.6 ± 0.5 Kcal/mole). This result is consistent with the lower initial reaction temperature of the isoimide oligomer and also suggests that the isomerization reaction may precede the crosslinking reaction to some extent.

5.2.2 FT-IR Kinetic Data

In order to characterize the kinetics of these two processes (i.e., isomerization and crosslinking) in the isoimide oligomer more thoroughly, heated cell FTIR experiments were conducted. The infrared spectrum of uncured IP-600 isoimide oligomer is shown in Figure 13. This spectrum shows characteristic absorbances for the acetylene functionality at 3295 cm^{-1} and 940 cm^{-1} (19) and for the isoimide functionality at 1805 cm^{-1} and 930 cm^{-1} (23-24). A small amount of imide is also evident by the presence of a shoulder at 1725 cm^{-1}. To

Table 13. Calculated Activation Energies From DSC Data at Various Heating rates*

Material	10-5°/min	5-2.5°/min	10-2.5°/min
IP-600	14.1	13.1	13.6
MC-600	20.4	19.1	19.5

Method of Calculation:

$$E_a = \frac{-R}{1.052} \quad \frac{\Delta \ln \phi}{\Delta (1/T_p)}$$

*Kcal/mole

ϕ = Heating Rate (°K/min)

T_p = Peak Reaction Temperature (°K)

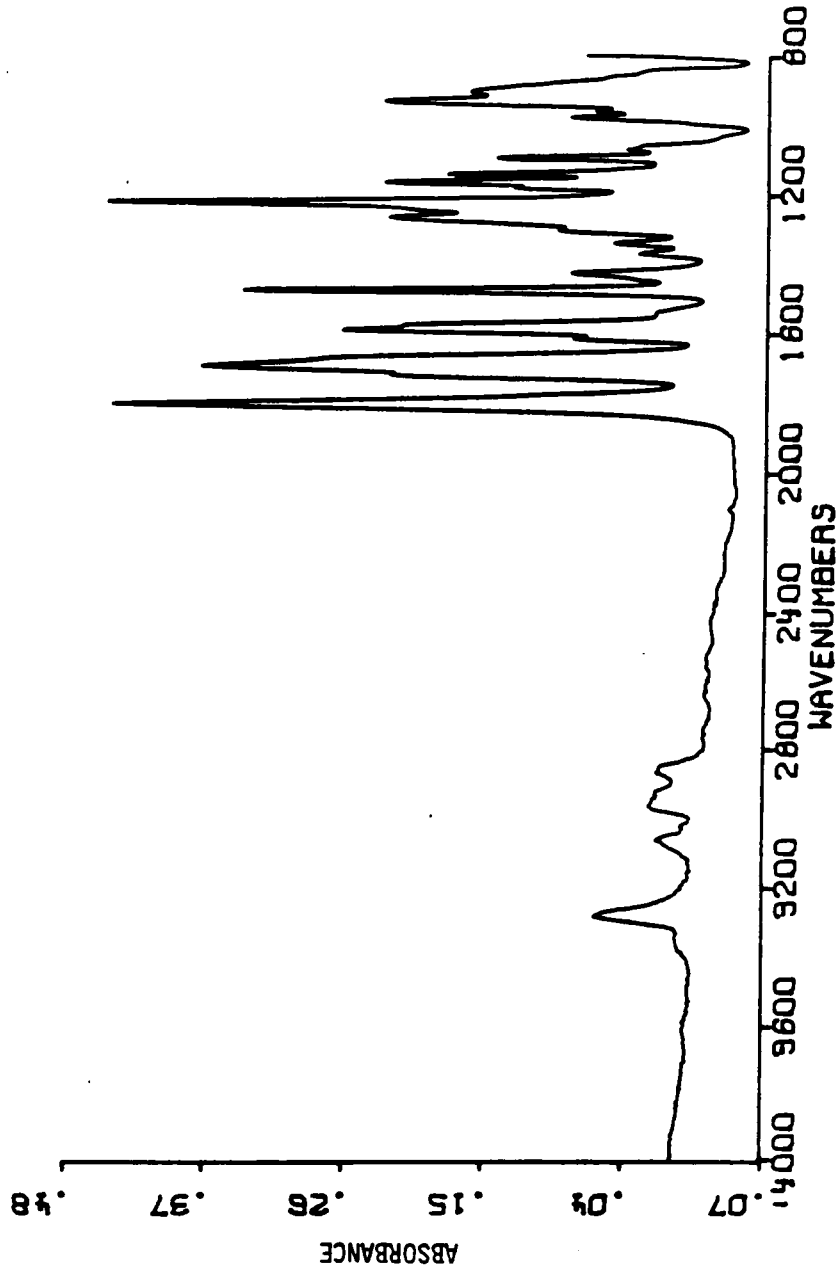

Figure 13: FT-IR Spectrum of Uncured Polyisoimide Oligomer.

minimize the amount of interference due to adjacent bands we chose the 3295 cm^{-1} band for monitoring the concentration of acetylene functionality and the 1805 cm^{-1} band for monitoring the concentration of isoimide functionality. Some interference was still observed in the case of the isoimide band due to a 1775 cm^{-1} band assignable to the imide structure.

5.2.2.1 Example of Infrared Kinetic Analysis at 183°C

A sample was placed in the cell and the cell was heated to a temperature of 183°C. Infrared spectra of the sample were then recorded as a function of time at this temperature. Figure 14 shows the isoimide-imide region of the spectrum as a function of time. It can be seen that the isoimide peak decreases rapidly during the first six minutes of the experiment (the amount of time necessary for the 183°C isothermal temperature to be reached) and then continues to decrease at a steady rate. Figure 15 shows the acetylene region of the spectrum at the same times. Here it appears that the decrease in absorbance is not as rapid as in the case of the isoimide band.

Figures 16 and 17 show the first order kinetic plots for the isomerization and crosslinking reactions, respectively. In the data analysis the area of the isoimide peak was measured between consistent limits chosen to exclude any contribution from the 1775 cm^{-1} imide band. These data were generated by measuring the area of the appropriate peak in a baseline corrected spectrum and ratioing this area to that of a reference peak (1472 cm^{-1} which was invarient during the experiment) in the same spectrum. This concentration indicative number was then ratioed to the concentration ratio observed on the initial scan. Plots

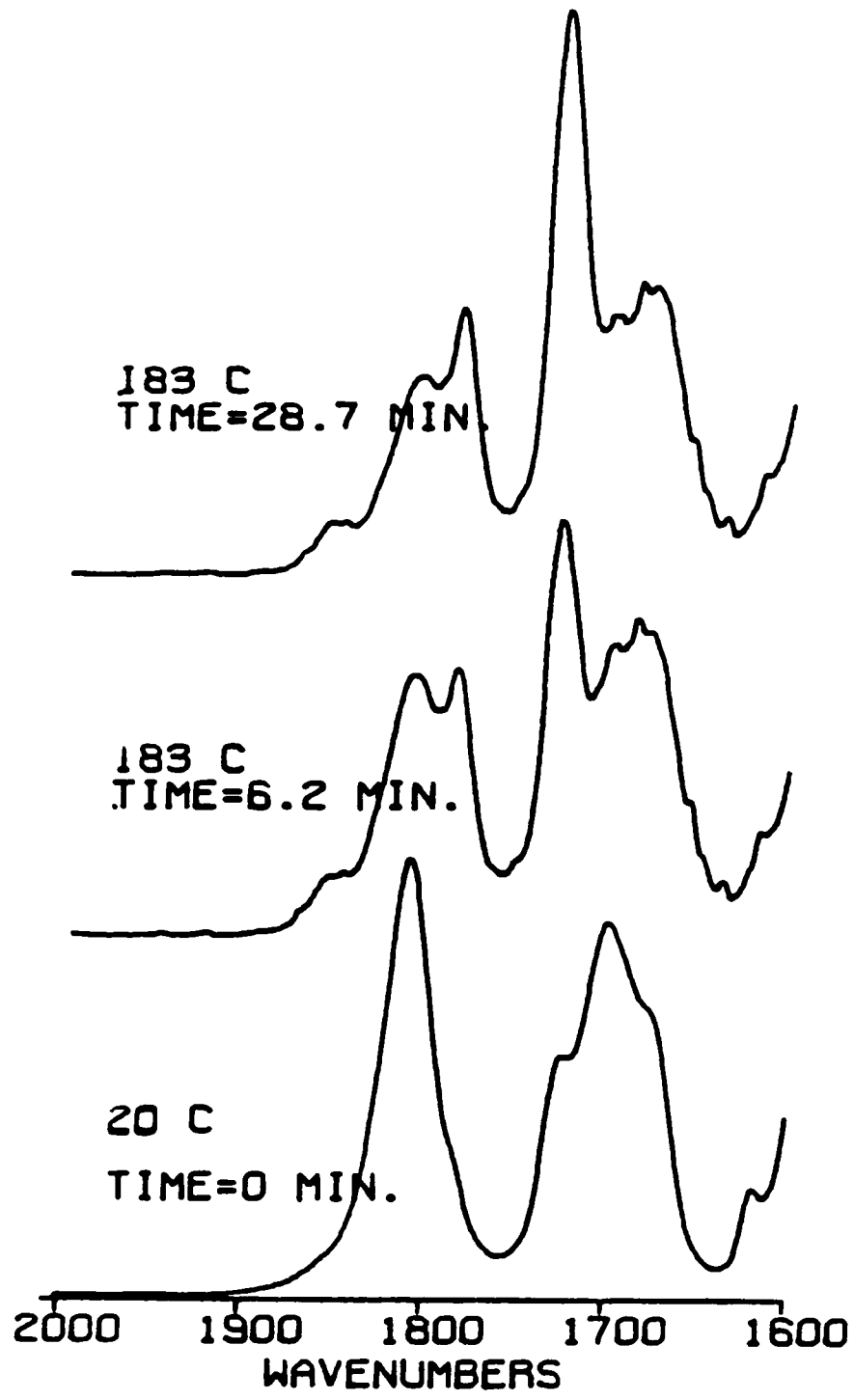

Figure 14: Isoimide-Imide Region of FT-IR Spectrum at 183°C.

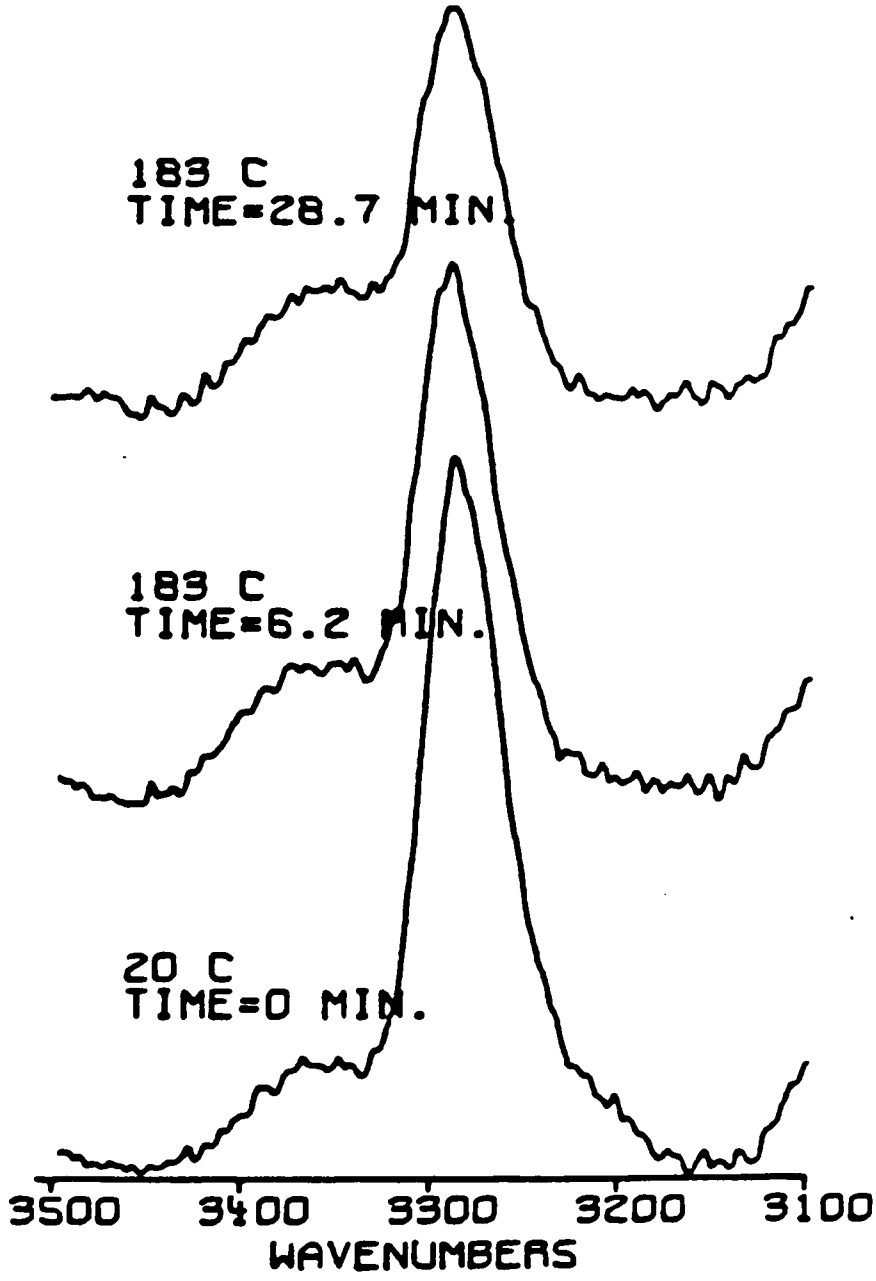

Figure 15: Acetylene Region of FT-IR Spectrum at 183°C.

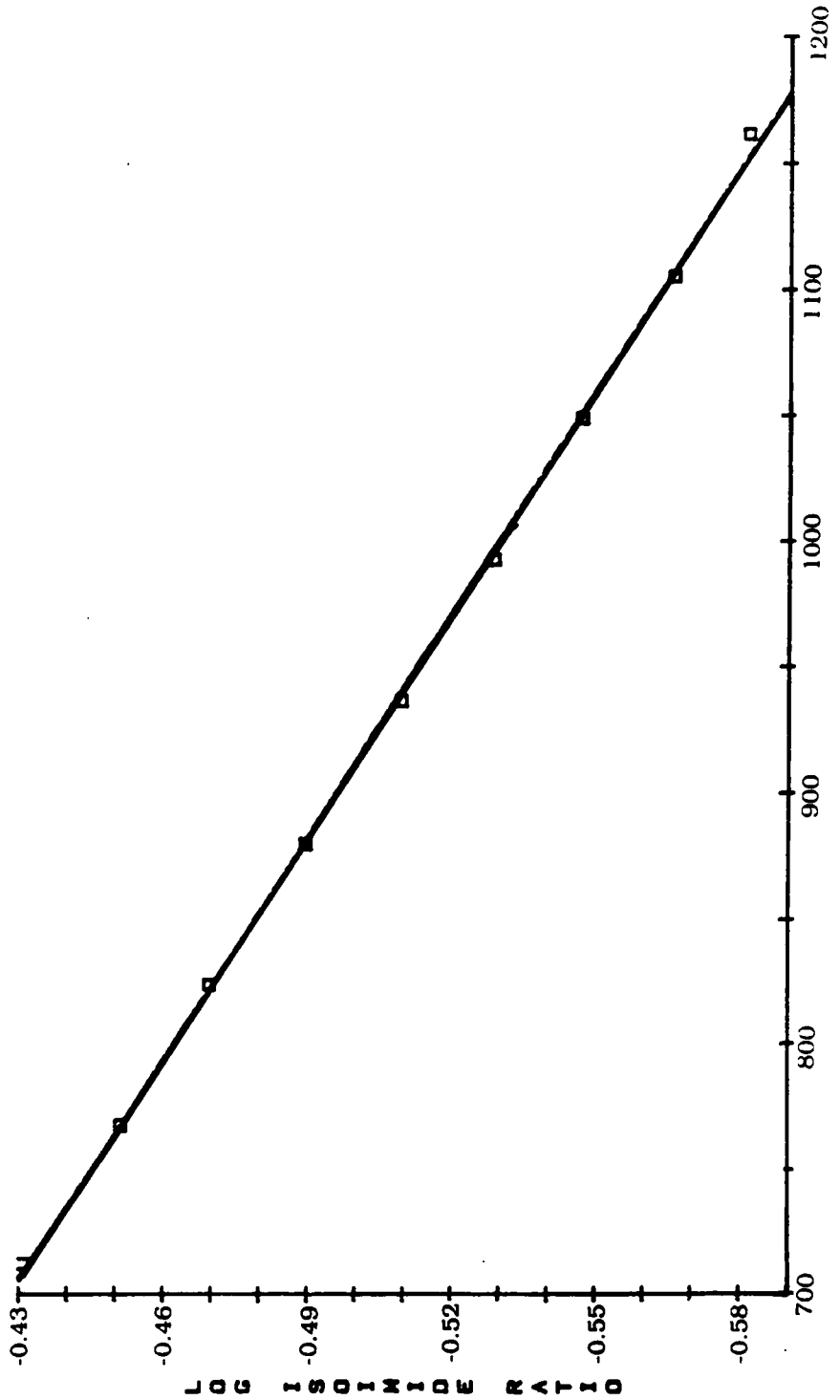

Figure 16: First Order Kinetic Plot for Isomerization at 183°C.

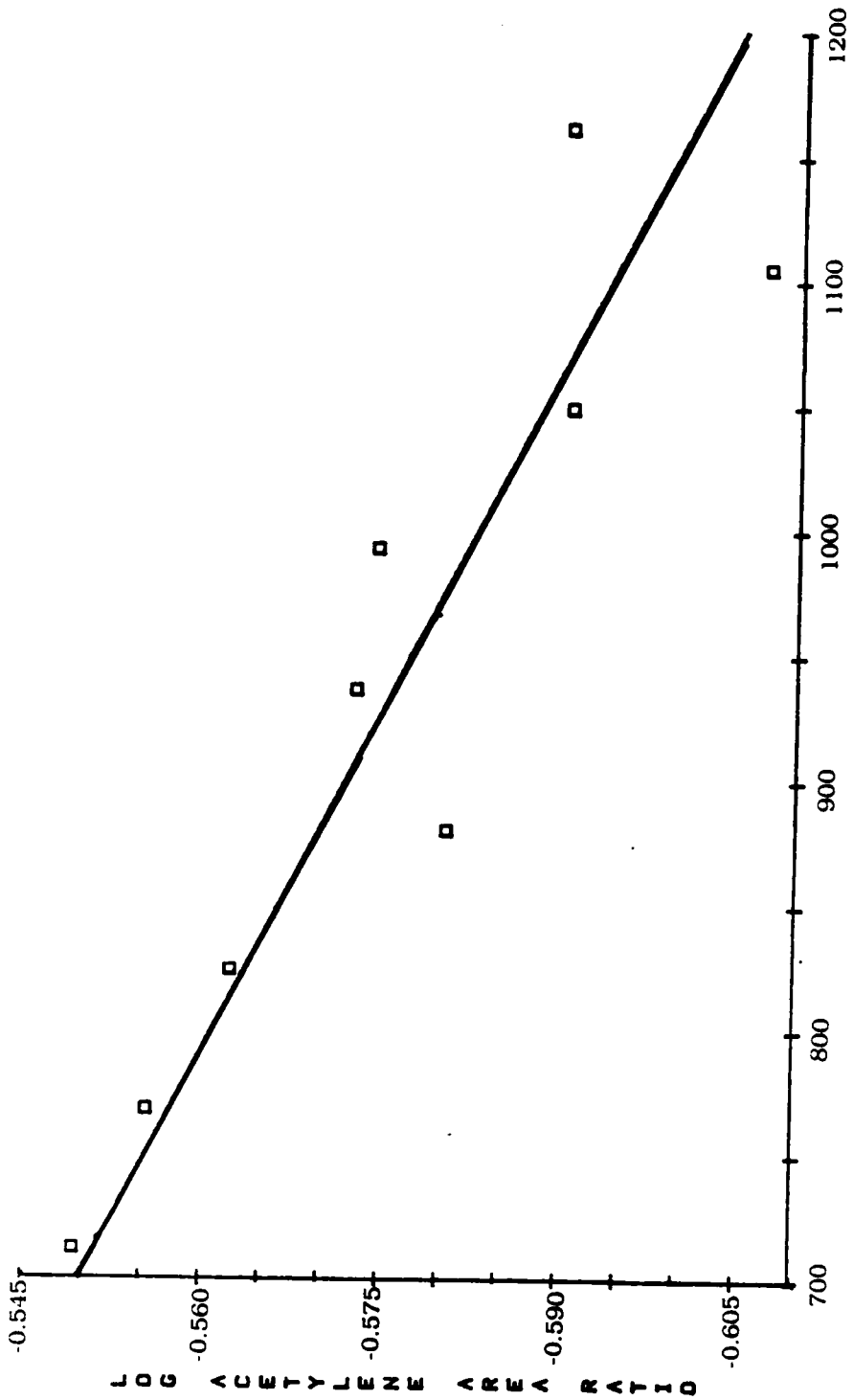

Figure 17: First Order Kinetic Plot for Corsslinking at 183°C.

of the log of the ratio of the concentration of the functionality at time "t" to the concentration of the functionality at t = 0 were then constructed. In order to insure that the trends in the data were not artifacts of this procedure or of the baseline correction routine, we also plotted the data in terms of peak intensity in absorbance units and observed the same trends but with more scatter in the data.

The first order plot for the isomerization reaction shows a good linear fit (correlation coefficient = 0.998); while there is more scatter in the acetylene first order plot. The apparent rate constants calculated from these data are 1.6×10^{-3}/sec for the isomerization of the isoimide to the imide and 2.0×10^{-4}/sec for the loss of the acetylene group. These are apparent rate constants since this first order fit does not take into account changes in mobility which undoubtedly occur during these processes; nor is it established that either of these processes is uniquely first order in nature. We can, however, interpret the trend in the apparent rate constants in terms of the isomerization reaction proceeding more rapidly than the crosslinking reaction of the acetylene group.

A similar kinetic analysis was conducted at 160°C and 200°C. Figures 18 and 19 show the data obtained for the first order crosslinking reaction at 160°C and 200°C, respectively. These data also show reasonable linearity in the time region after temperature stability has been achieved. Analogously for the isoimide isomerization reaction, the data are shown in Figures 20 and 21 for the 160°C and 200°C experiment, respectively. These data show significant scatter in the low temperature experiment possibly due to the reaction being mobility

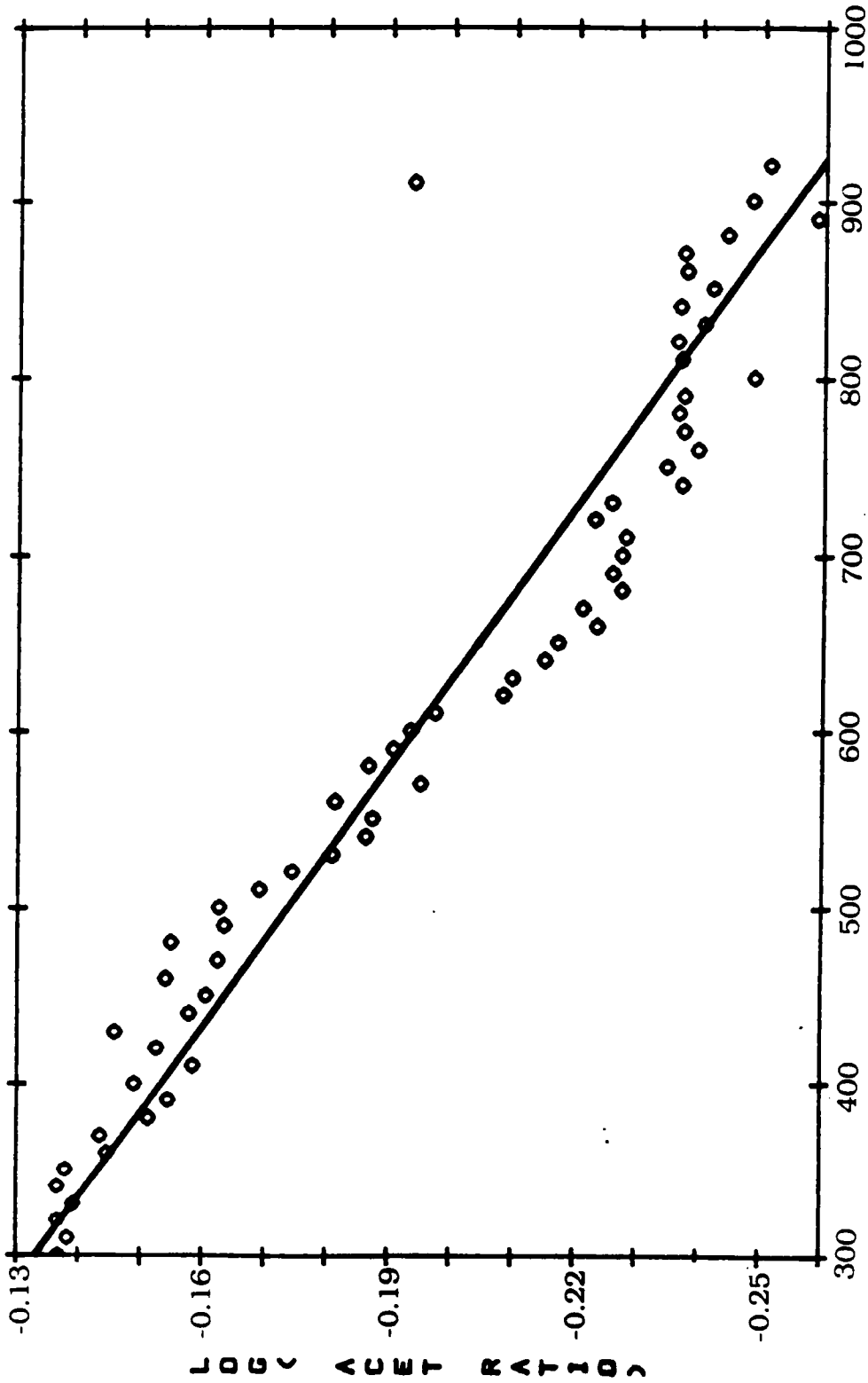

Figure 18: First Order Kinetic Plot for Corsslinking at 160°C.

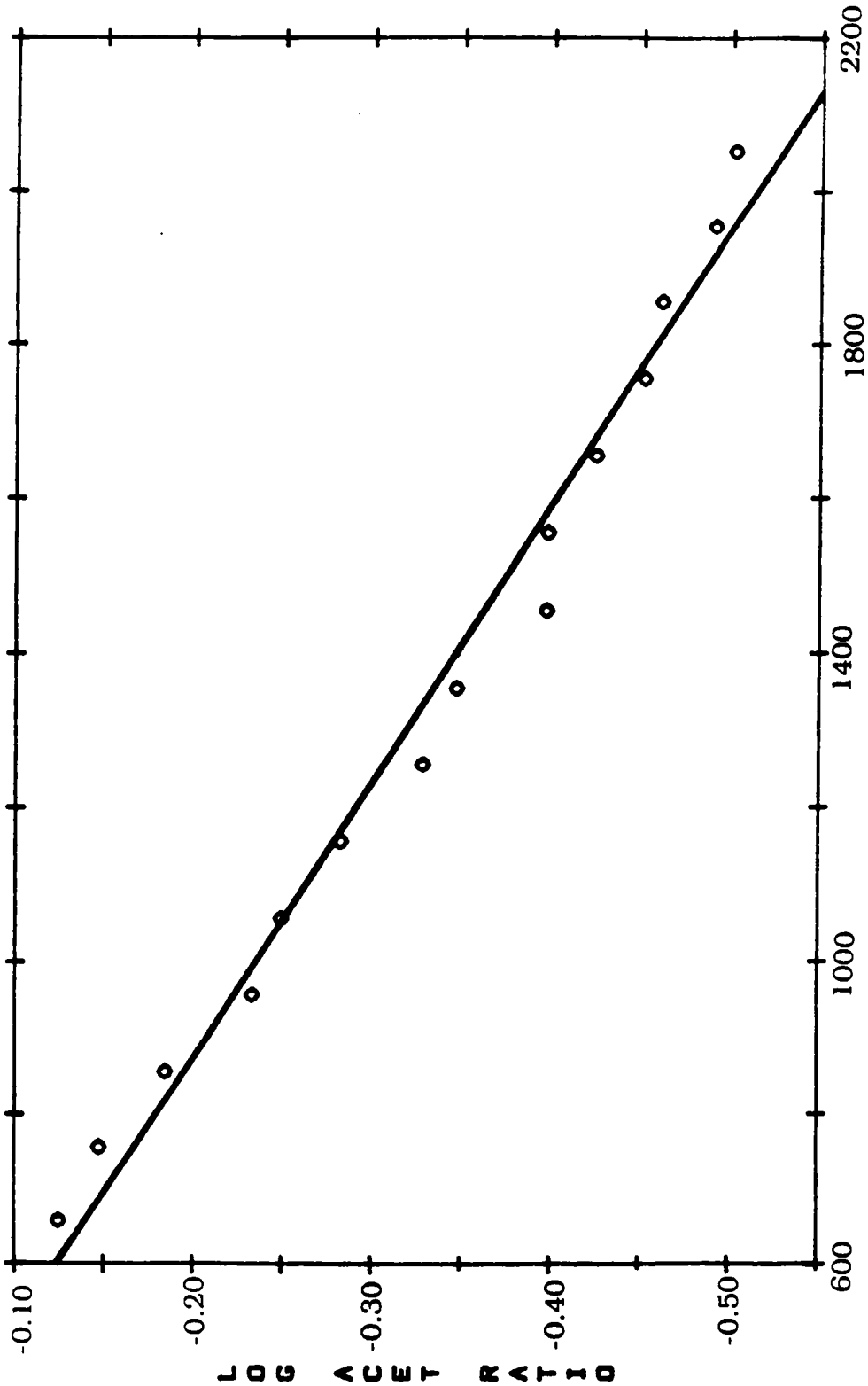

Figure 19: First Order Kinetic Plot for Crosslinking at 200°C.

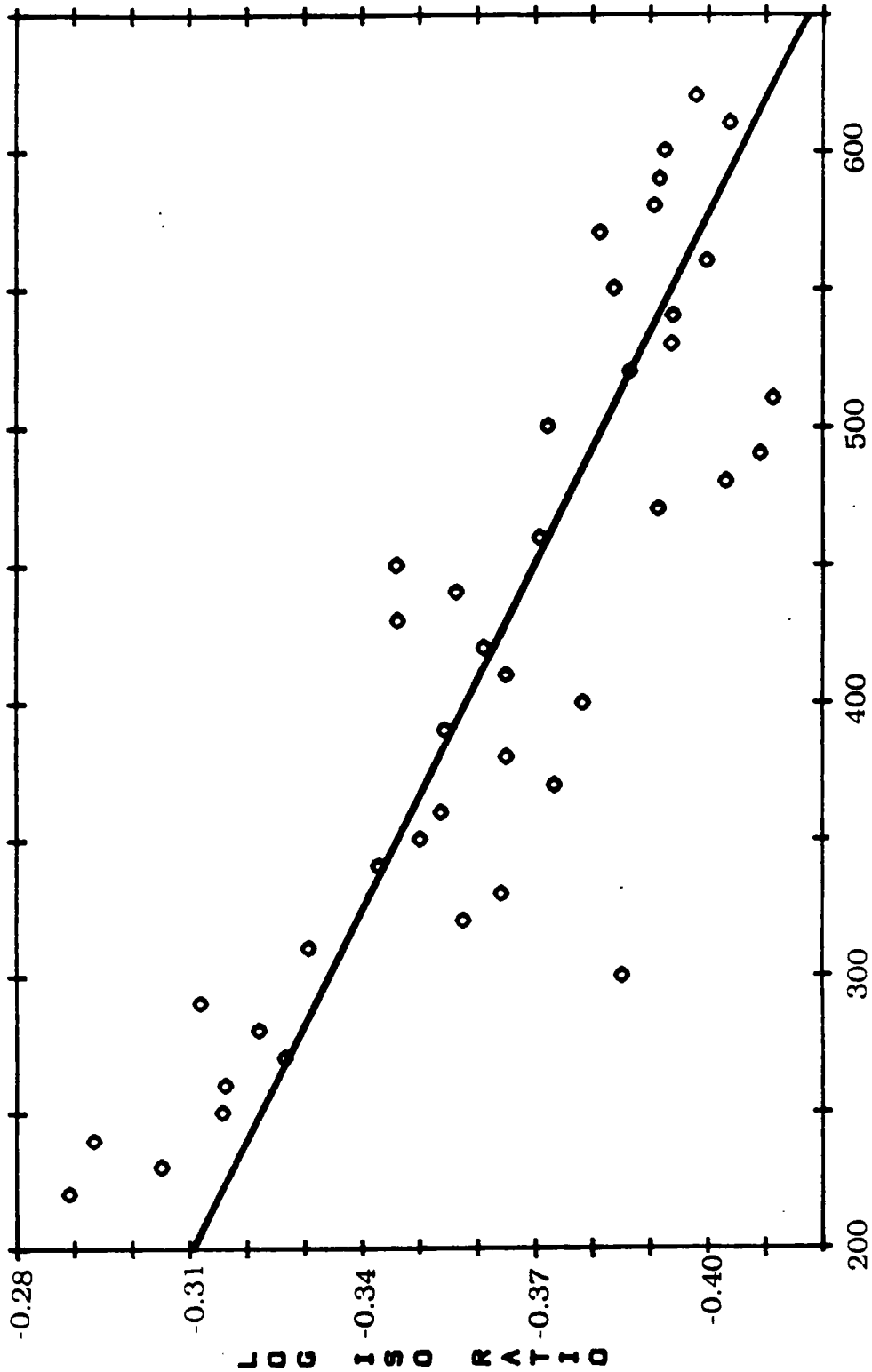

Figure 20: First Order Kinetic Plot for Isomerization at 160°C.

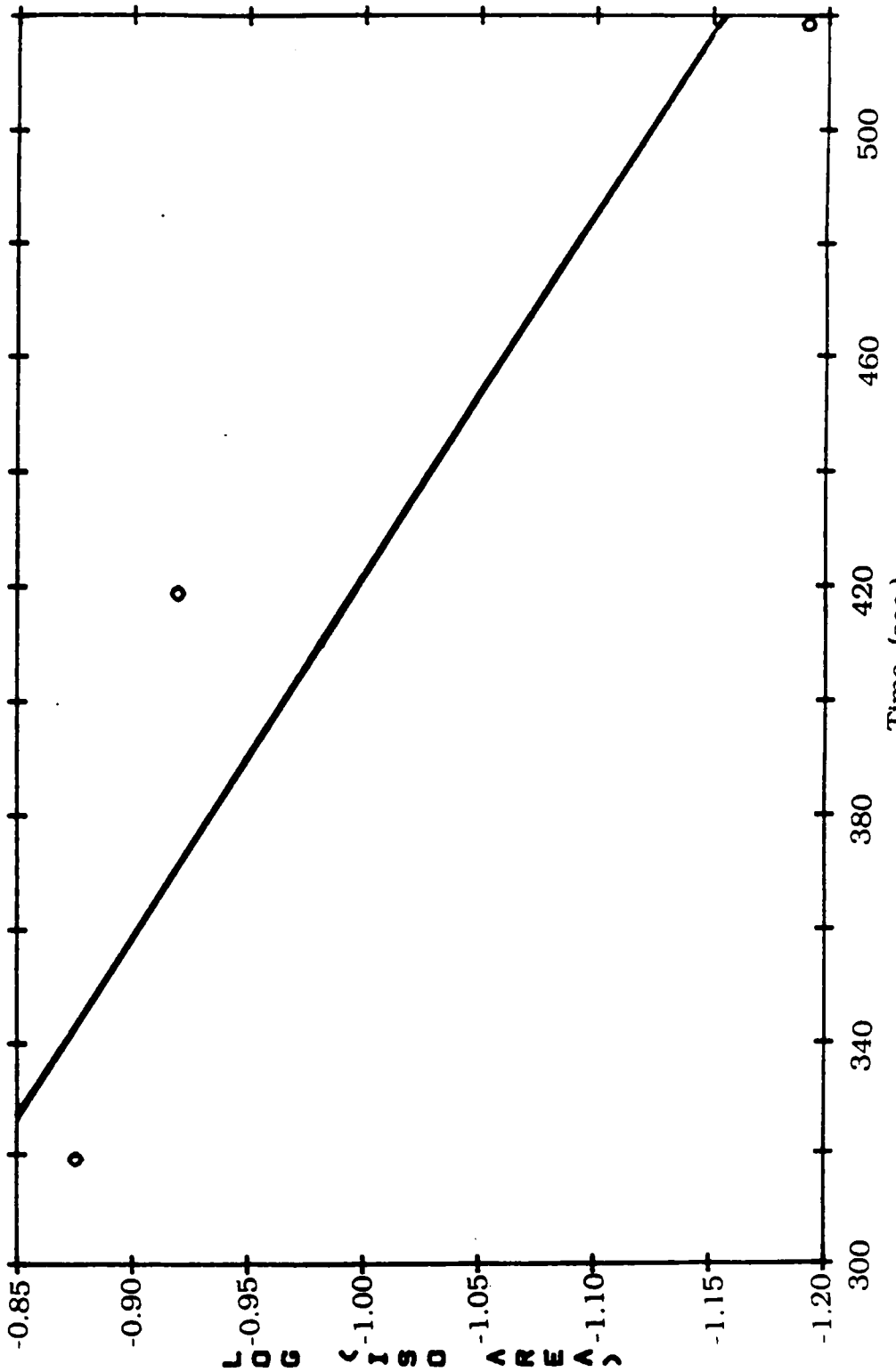

Figure 21: First Order Kinetic Plot for Isomerization at 200°C.

limited at this temperature just above the glass transition temperature of the oligomer. In the higher temperature experiment only 3 data points could be generated for the isoimide concentration due to the reaction being nearly complete before thermal equilibrium is reached at the sample. This data (Figure 21) is presented not for interpretation independently but only in the context of the other experiments. The apparent rate constants extracted from this analysis are shown in Table 14.

5.2.2.2 Energy Data from FT-IR Experiments

The Arrhenius plots for the crosslinking and isomerization reactions are shown in Figures 22 and 23, respectively. Although the straight lines are rather presumptuous based on only 3 data points the trend in the comparison of the activation energies for each reaction should still be valid. These activation energies are 34 kcal/mole for the crosslinking reaction and 22 kcal/mole for the isomerization reaction. Although these values do not agree quantitatively with those obtained from the DSC experiments the appropriate trend is still apparent and the values themselves are of a reasonable magnitude.

5.3 Summary

The data presented here suggest that both the reactions occurring in this system, crosslinking and isomerization, are first order processes. Further, it has been shown that the isomerization reaction proceeds more rapidly than crosslinking at each temperature studied. Both DSC and FT-IR were used to extract activation energies and, although not directly comparable, the trends are consistent among data obtained by each technique.

Table 14

Apparent Rate Constants from FT-IR Experiments

Temperature (K)	k (isomerization)(1/sec)	k (crosslinking)(1/sec)
433	3.3×10^{-3}	4.3×10^{-4}
456	1.6×10^{-3}	2.0×10^{-4}
573	2.3×10^{-4}	1.0×10^{-4}

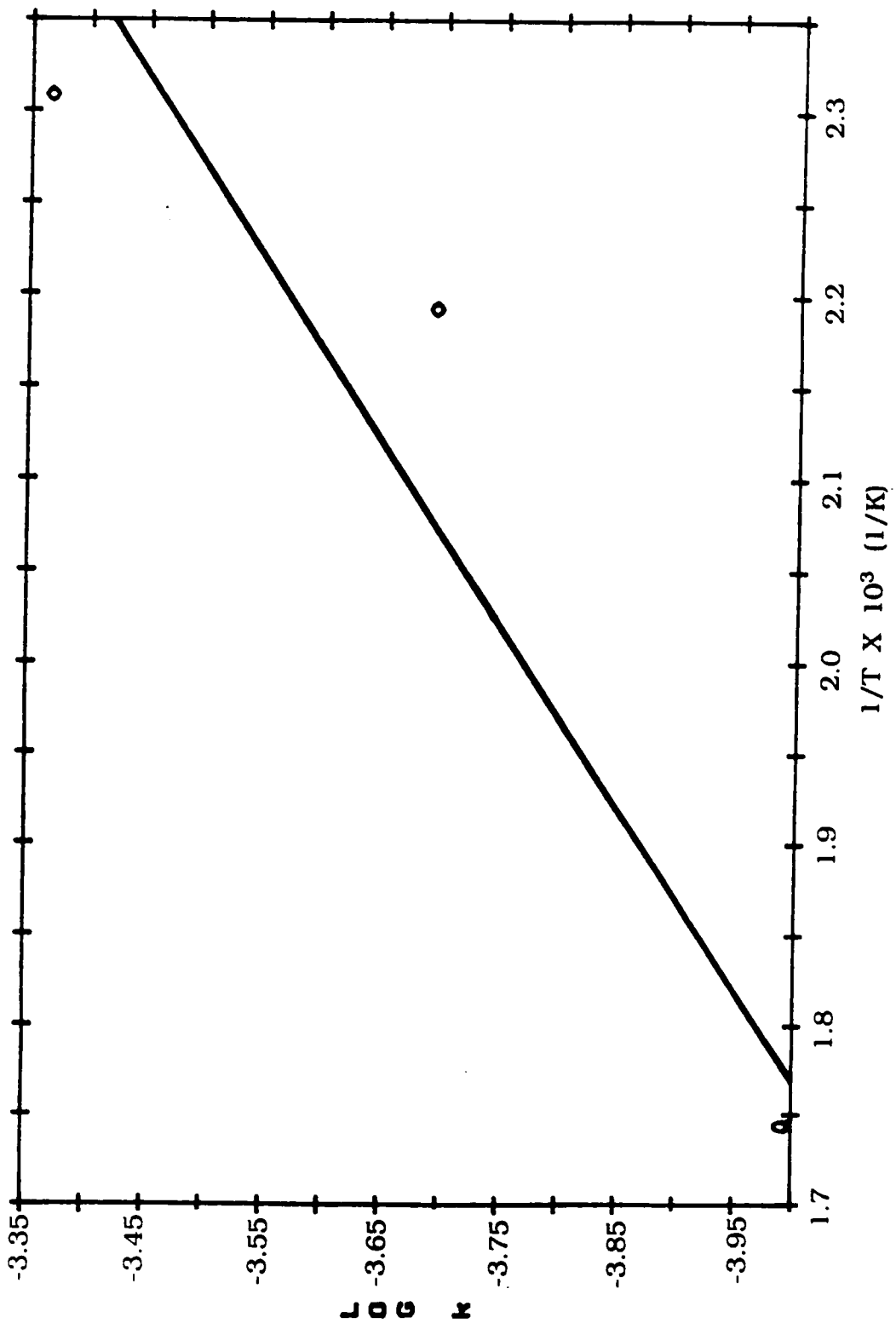

Figure 22: Activation Energy Plot for Crosslinking from FT-IR Data.

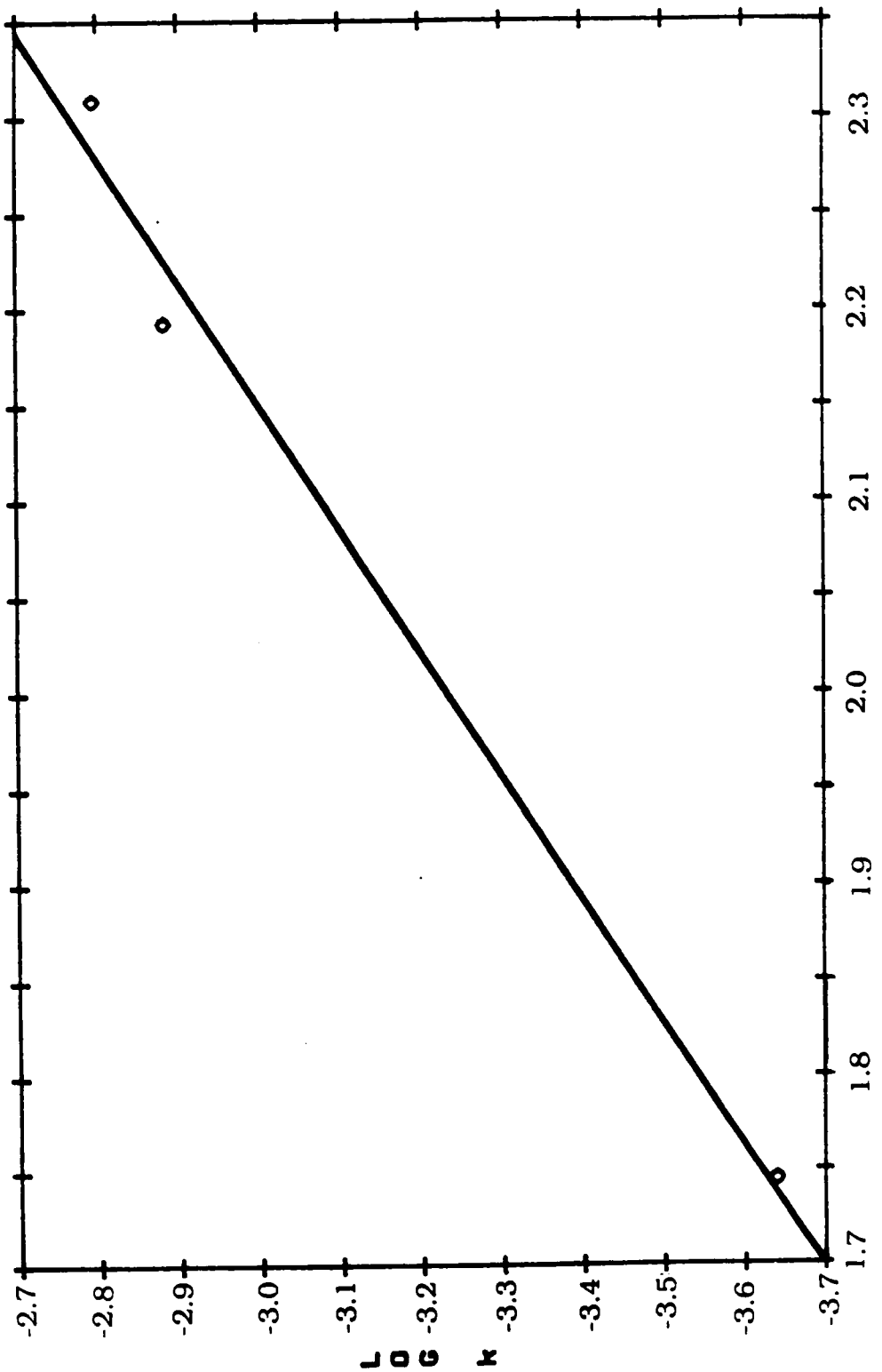

Figure 23: Activation Energy Plot for Isomerization from FT-IR Data.

6.0 Effect of Metal Particle Incorporation on Mechanical and Electrical properties of Acetylene Terminated Polyisoimide Prepolymers

6.1 Introduction

The improved processability that has been demonstrated (5) in addition-cured polyisoimide systems allows more utilization of the already excellent thermal and mechanical properties available in polyimide systems. Furthermore, the range of properties available in these materials may be extended significantly by the combination of heterogeneous fillers such as metal particles. These polymer/metal composites exhibit a unique combination of properties which extend the utility of polymeric materials. For example, in most polymer metal composite systems the heat distortion temperature and stiffness increase; while, the thermal expansion coefficient, tensile modulus and impact strength decrease (9). Another interesting effect is observed in the area of electrical conductivity. At a critical volume loading of metal filler the electrical conductivity of the composite increases dramatically (10). These observations have prompted this investigation of the chemistry and properties of an acetylene terminated polyisoimide prepolymer matrix (Figure 2) filled with an aluminum/nickel (1:1) alloy powder.

6.2 Results and Discussion

Previous work conducted in this study has focused on the thermal crosslinking and isomerization reactions occurring in polyisoimide prepolymer systems. Also investigated were the electrical properties of metal-filled polyisoimides at elevated temperatures when used for bonding aluminum conductor bars. During these studies it was observed

that qualitatively good adhesion was achieved with aluminum substrates. These observations prompted the investigation described herein which focused on the dynamic mechanical, adhesive and electrical properties of these systems.

As mentioned previously, FTIR spectrometry has been used in conjunction with DSC to establish the contributions of isomerization and crosslinking to the overall curing reaction of the neat polyisoimide. The presence of small, oxide coated metal particles in this matrix, however, may influence these reactions. Unfortunately, obtaining high quality FTIR spectra of this metal filled system was difficult. The data that have been obtained do not seem to indicate any influence of the metal powder on the reactions which occur during cure. This observation is further supported by the appearance of the DSC thermogram (Figure 24) comparing the neat polyisoimide (IP630) with a 25% (v/v) alloy-polyisoimide composite (MPC). In this study, the weight of metal was subtracted out so that the peak areas could be measured in energy per gram of polymer. The similarity of thermograms for the neat and filled polymer as well as the energies of reaction derived therefrom further suggest that the metal powder does not interact chemically with the polyisoimide during cure.

Although these data do not indicate any chemical interaction of the metal with the polymer, physical interactions occurring in these systems do give rise to modification of dynamic mechanical, electrical and adhesive properties (5,9,10,149). It is thought that these property modifications result from a combination of factors such as (1) large scale interactions of polymer chains with the metal particles, (2)

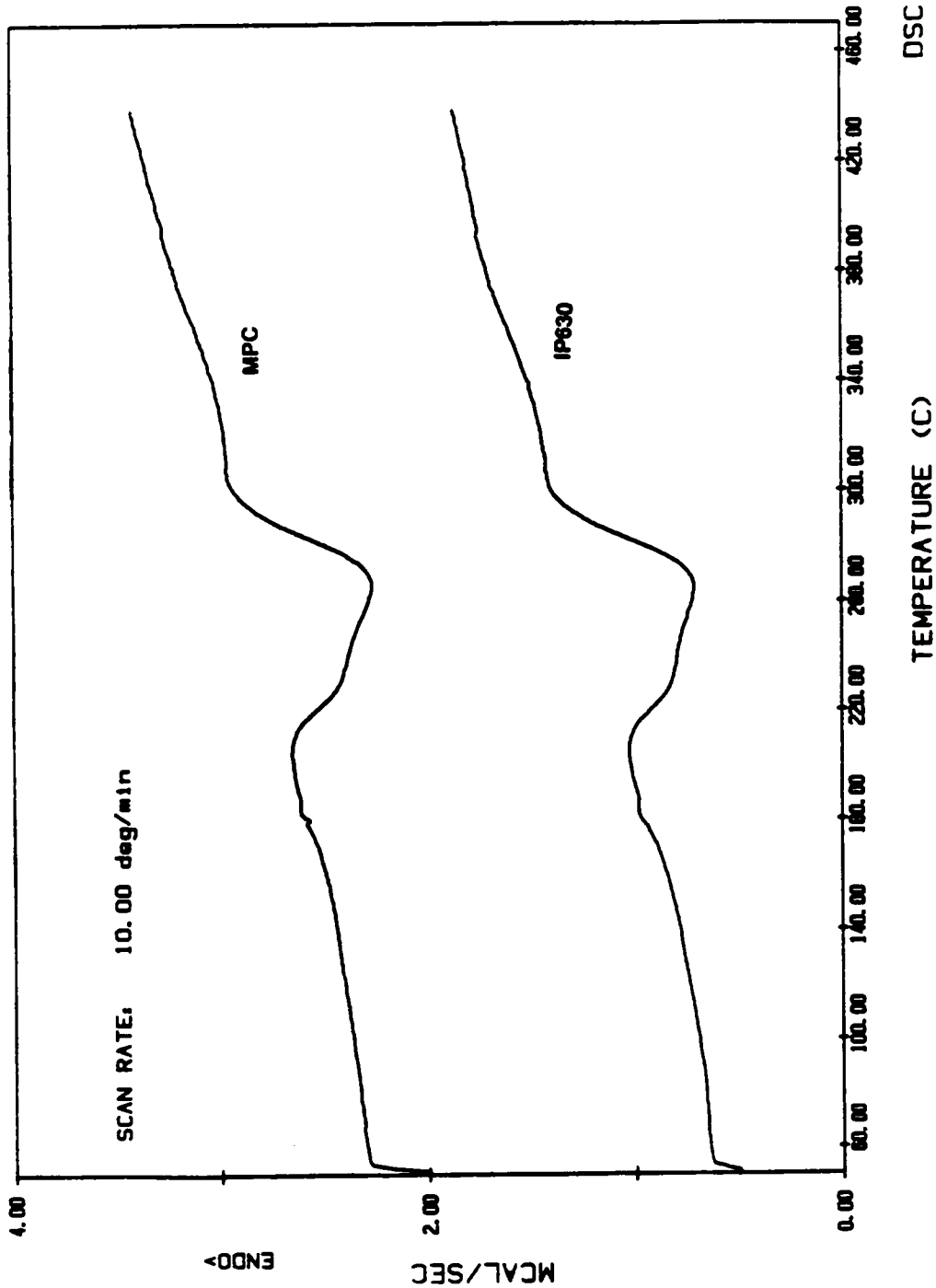

Figure 24: Comparison of DSC Thermograms for Neat Polyisoimide Oligomer and Metal/Polymer Composite.

interactions between the metal particles themselves and (3) interactions of both the polymer and metal powders with the surface of the adherends. In the following sections each of the modified properties will be treated individually.

6.2.1 Dynamic Mechanical Properties

Changes in both the damping and modulus-temperature behavior of these systems have been noted. Specifically, the mechanical behavior as a function of temperature was measured for both a neat, cured film of Thermid IP-630 isoimide prepolymer with a number average molecular weight of ~17,000 and a metal/polymer composite consisting of 5% (v/v) aluminum/nickel (1:1) alloy in a matrix of the same prepolymer. Both materials were cured at the same temperature and pressure. The tan δ relative damping spectra of these two materials are compared in Figures 25 and 26. Most apparent are the broadening of the main damping peak (i.e. glass transition) and also the appearance of a post T_g dispersion for the case of the metal/polymer composite. These two effects are presumably due to the greater dissipation of mechanical energy through frictional interfacial losses caused by the polymer segments moving across the surfaces of the metal particles. This reasoning would also explain the slightly larger magnitude of the tan δ peak for the case of the metal/polymer composite. Modulus temperature behavior is modified by the reinforcing effect of the filler particles in the polymer matrix. Also, The spectrum of relaxation times for the system is shifted due to the incorporation of the metal filler. This shift is manifested by smaller and smaller segments of the polymer backbone interacting with the particle surface. These effects also lead to a broadening of the

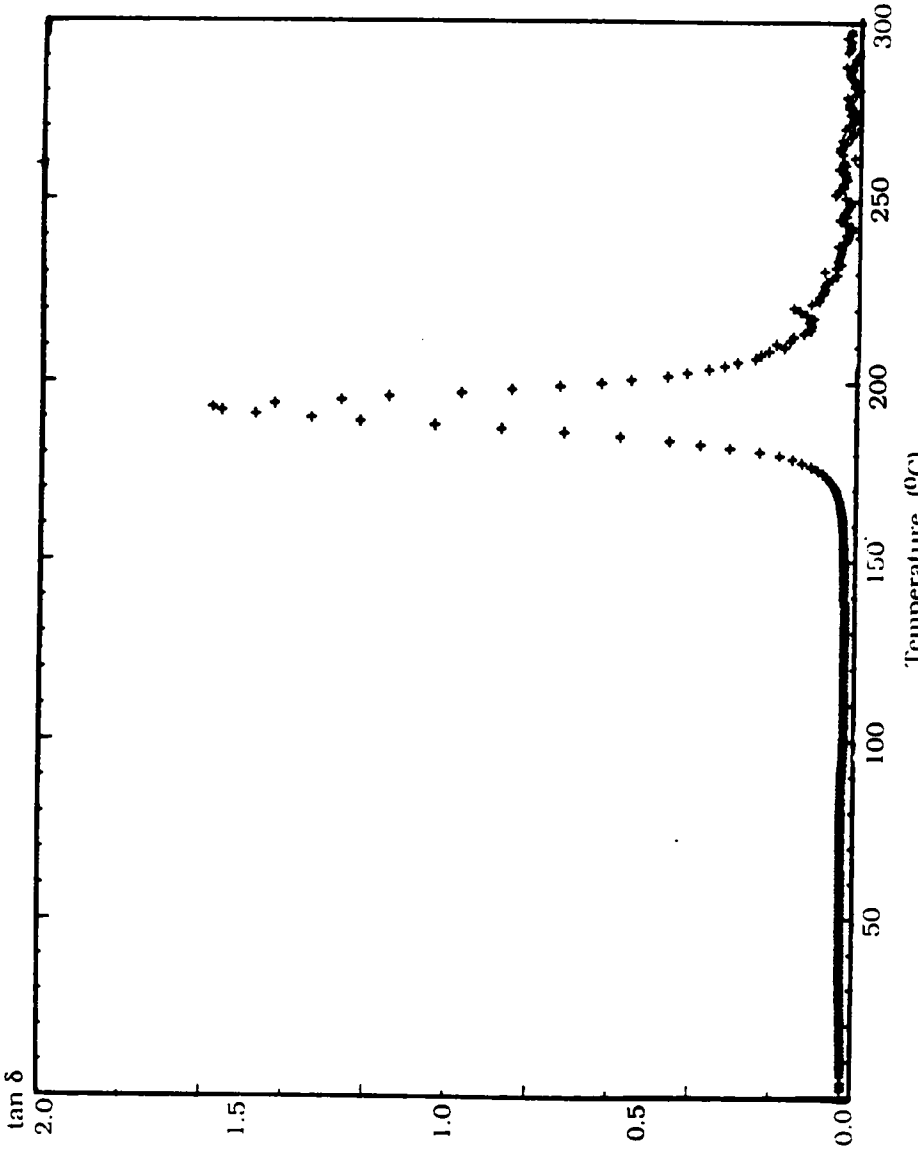

Figure 25: Tan δ Spectrum of Neat Polyisoimide Oligomer Cured at 220°C.

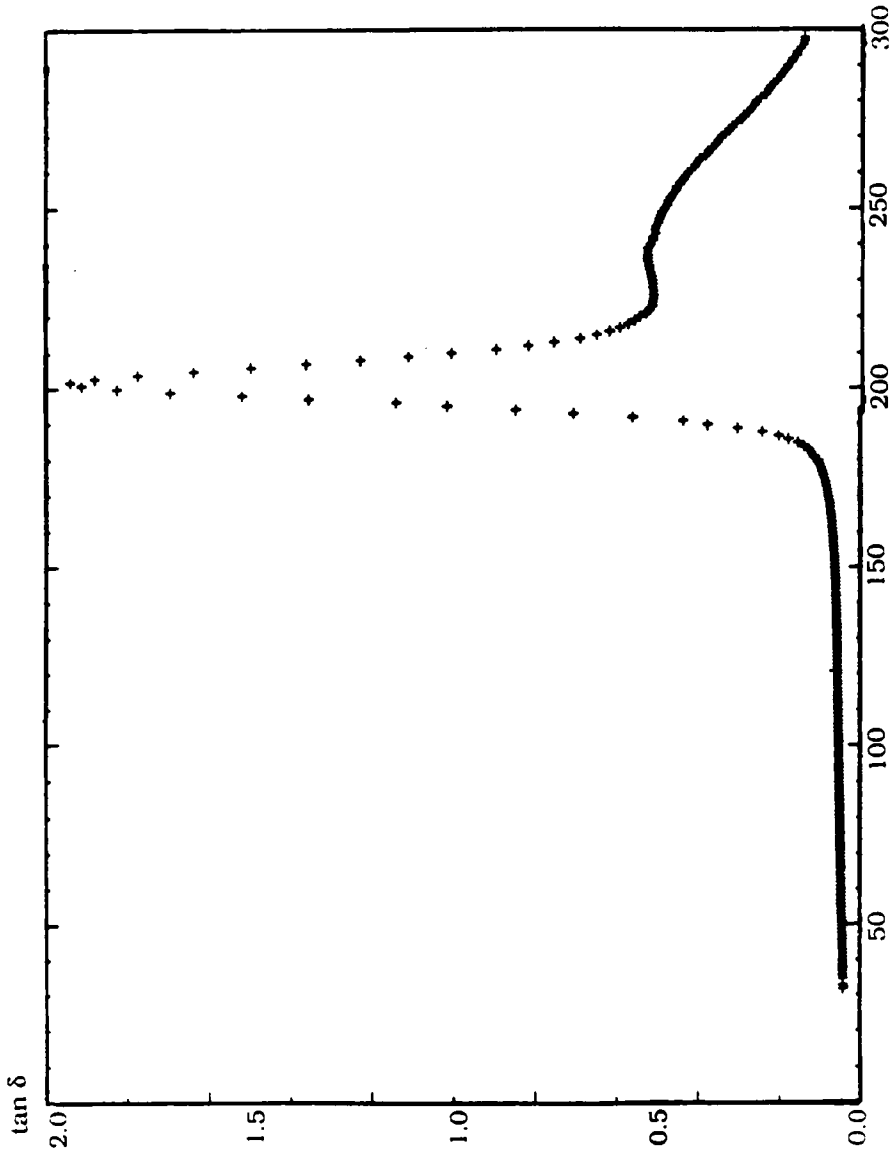

Figure 26: Tan δ Spectrum of 5/95 Metal/Polymer Composite Cured at 220°C.

tan δ spectrum in the post T_g flow region of the temperature scale. This interpretation is also consistent with the appearance of the tan δ vs temperature plots of the 20% and 50% (v/v) metal containing systems shown in Figures 27 and 28, respectively. In these spectra the definition of that post T_g dispersion is lost and the magnitude relative to the main tan δ peak increases. These differences at higher loading may be due to more polymer chains interacting with the metal particles as the volume of metal filler is increased. Also, the system is becoming more and more rigid as the volume of filler increases and more and more contact between particles may give rise to loss of definition of shape in the tan δ vs temperature plot.

Since the tan δ spectrum represents the ratio of the loss (E") to storage (E') modulus it is also instructive to examine these dynamic mechanical spectra as well. Although there are no distinct differences apparent in the shapes of the loss modulus curves for the neat and metal-loaded cases an examination of the storage modulus curves provides some explanation regarding differences in the tan δ plots. The reinforcing effects of the filler are expected to be more apparent in the storage modulus behavior (Figures 29 and 30). It must be noted, however, that the absolute values of the modulus data quoted here are not significant since absolute calibration was not performed. What can be used as a basis for comparison in this study is the difference in modulus values between the temperature limits which correspond to the breadth of the tan δ peak at one-half of its maximum value. This comparison shows that the metal/polymer composite storage modulus (E') decreases by a greater magnitude over this temperature range than does

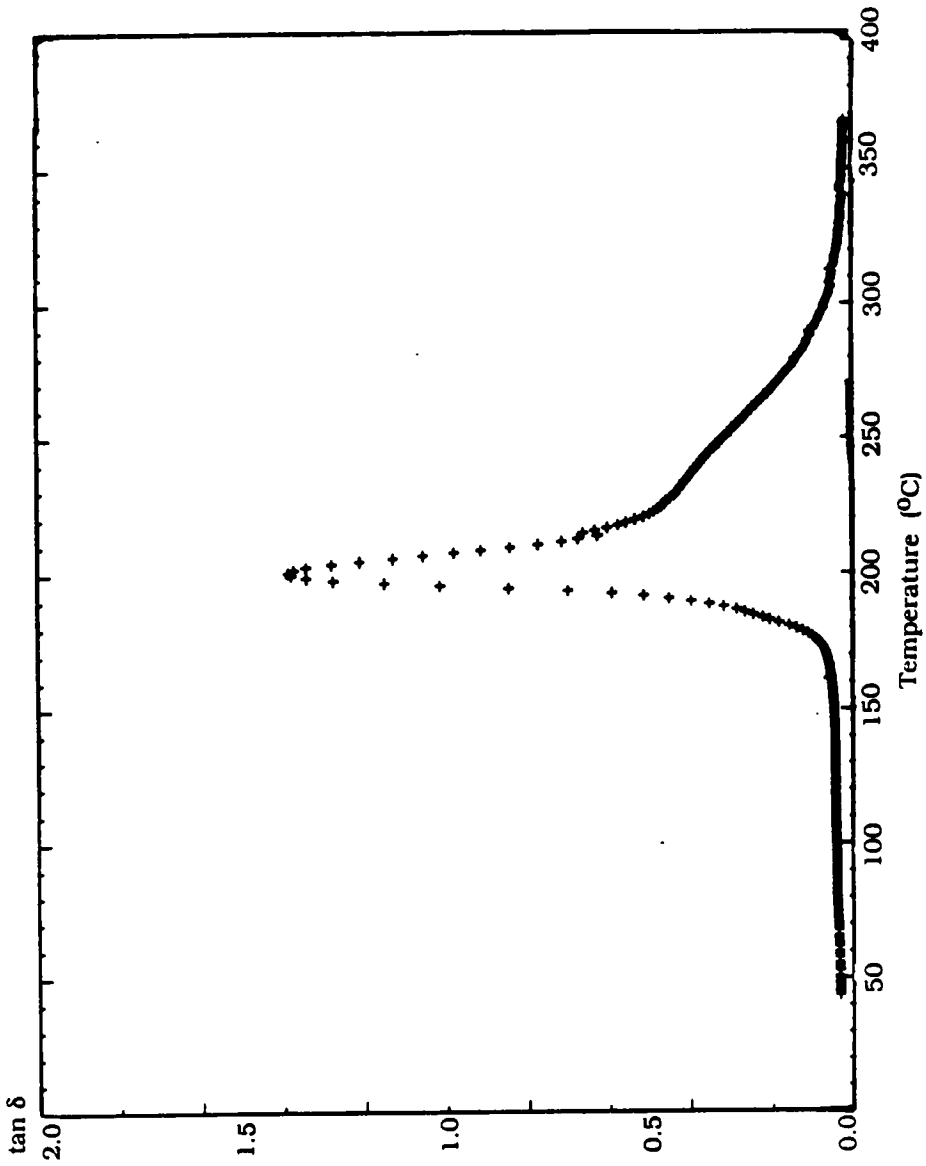

Figure 27: Tan δ Spectrum of 20/80 Metal/Polymer Composite Cured at 220°C.

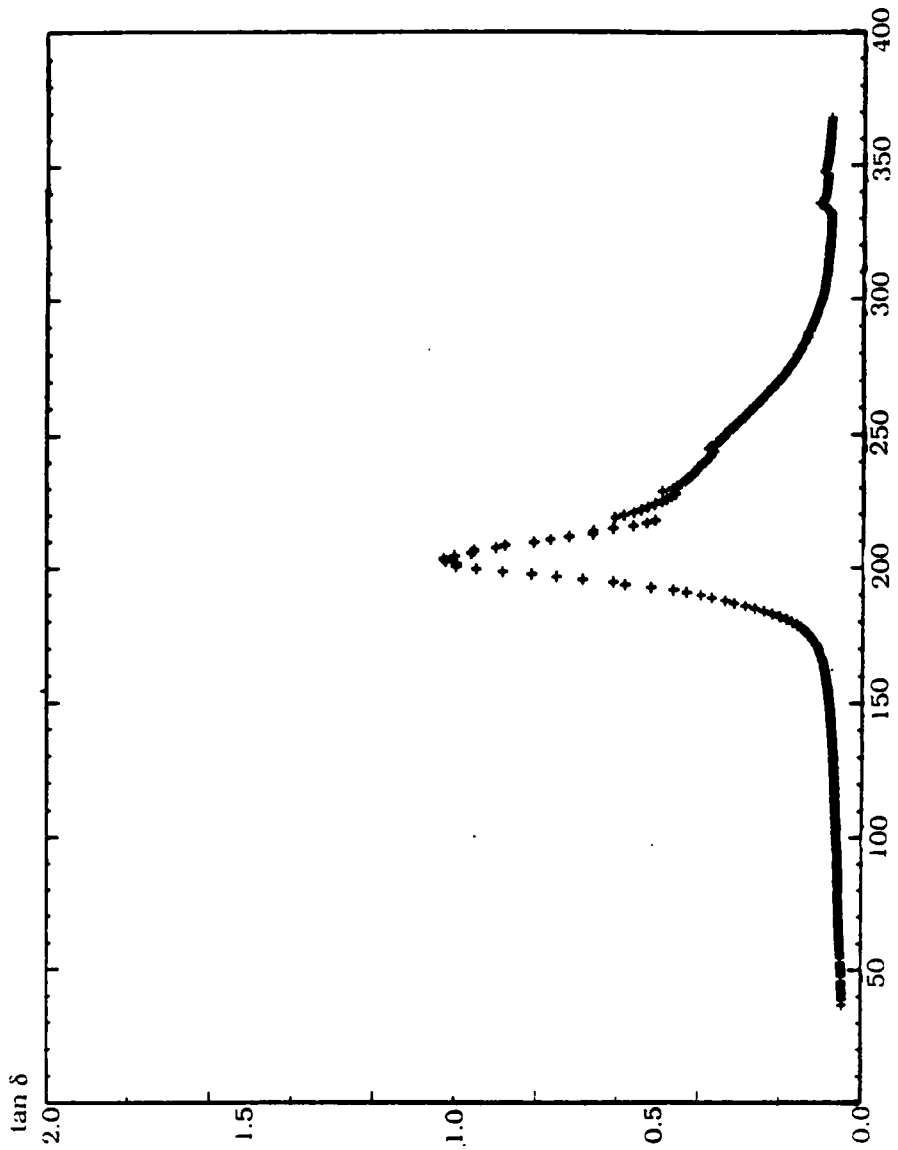

Figure 28: Tan δ Spectrum of 50/50 Metal/Polymer Composite Cured at 220°C.

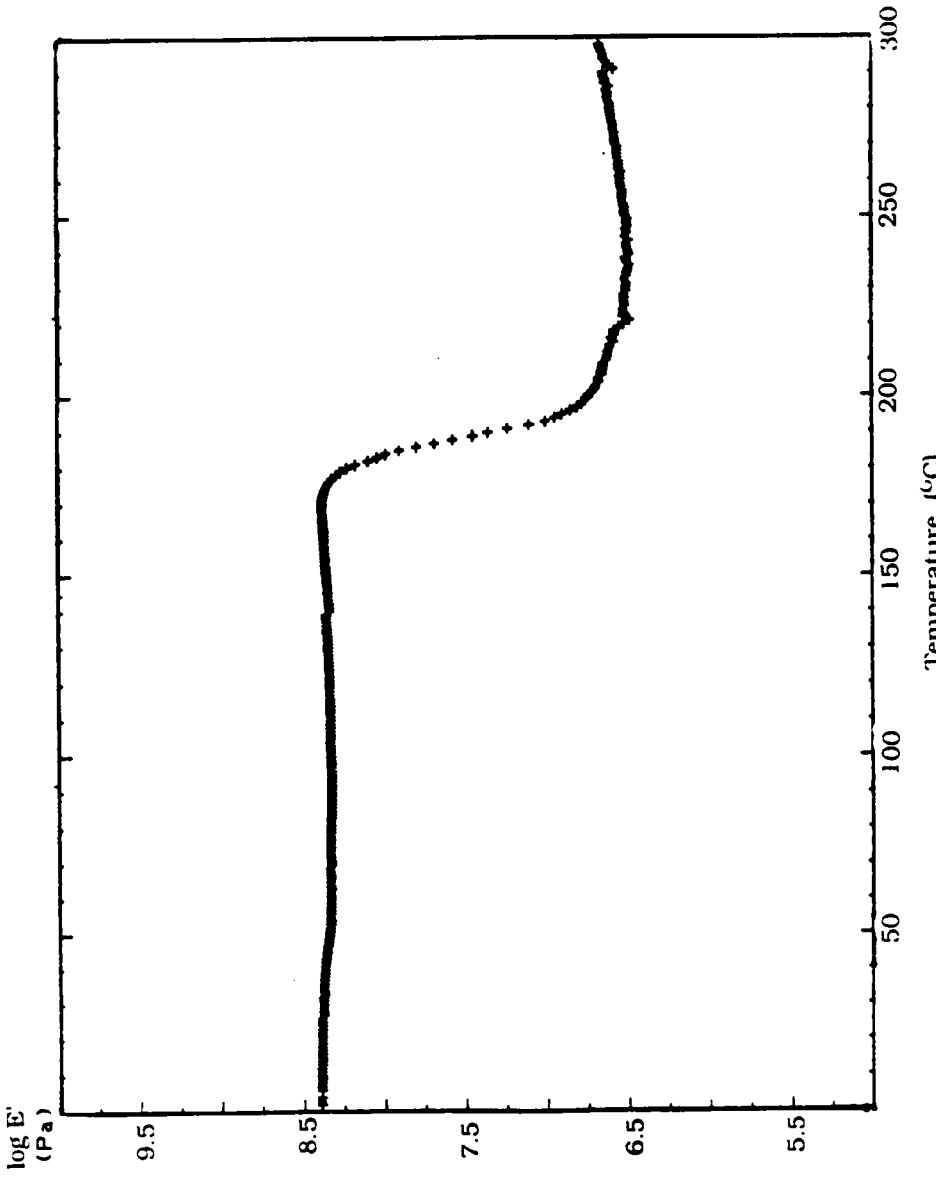

Figure 29: Storage Modulus Spectrum of IP-630 Polyisoimide Oligomer Cured at 220°C.

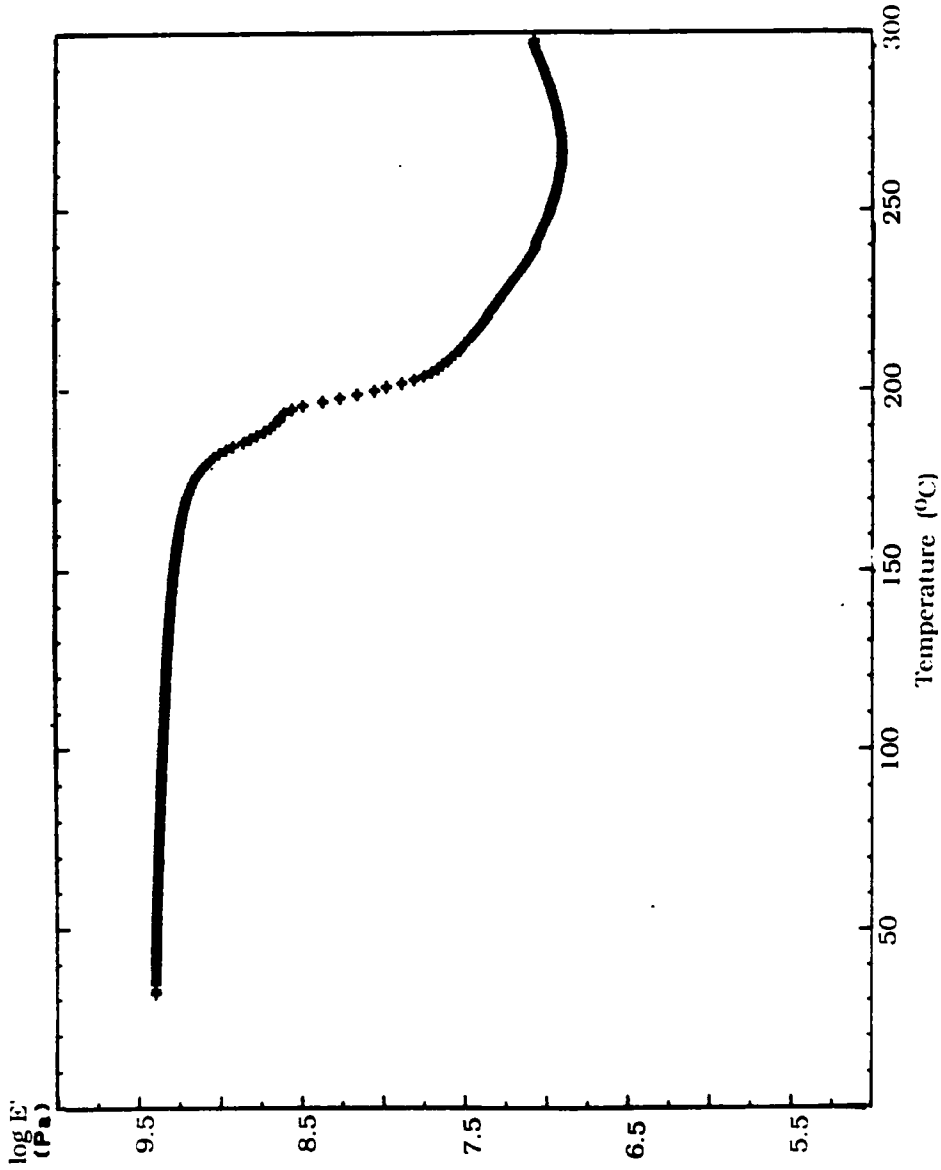

Figure 30: Storage Modulus Spectrum of 5/95 Metal/Polymer Composite Cured at 220°C.

the E' value for the neat polymer (1.15 log units for the MPC vs 0.97 log units units for the neat polymer). This observation can be explained on the basis of the reinforcing efficiency of the filler being diminished as the matrix proceeds from the vitrified to the rubbery state at the glass transition temperature. Data for the higher metal volume loading agrees with this interpretation. The storage modulus plots for the 20% and 50% (v/v) metal/polymer composites are shown in Figures 31 and 32, respectively. The storage modulus decrease is quite large in the glass transition region and the general shape shows a post T_g local minima which would give rise to the post T_g tan δ relaxation.

6.2.2 Thermomechanical Analysis

Investigation of the thermomechanical properties of these systems has also been instructive. First, the TMA plot for the neat cured prepolymer IP630 is shown in Figure 33. After softening of the polymer this plot shows two different slopes over the temperature range which the largest deformation takes place (190-250°C). These two slopes reflect the occurrence of two different processes during this experiment. Apparently, the penetration of the probe is influenced by the softening of the backbone initially but then retarded due to the crosslinked nature of the system. The positive slope after approximately 250°C further signifies the highly crosslinked nature of this material.

The other TMA plots in Figures 34 and 35 illustrate the thermomechanical behavior of the cured metal/polymer composite systems containing 5 and 20 volume percent metal respectively. In these cases a less distinct change in slope is observed since the materials are loaded

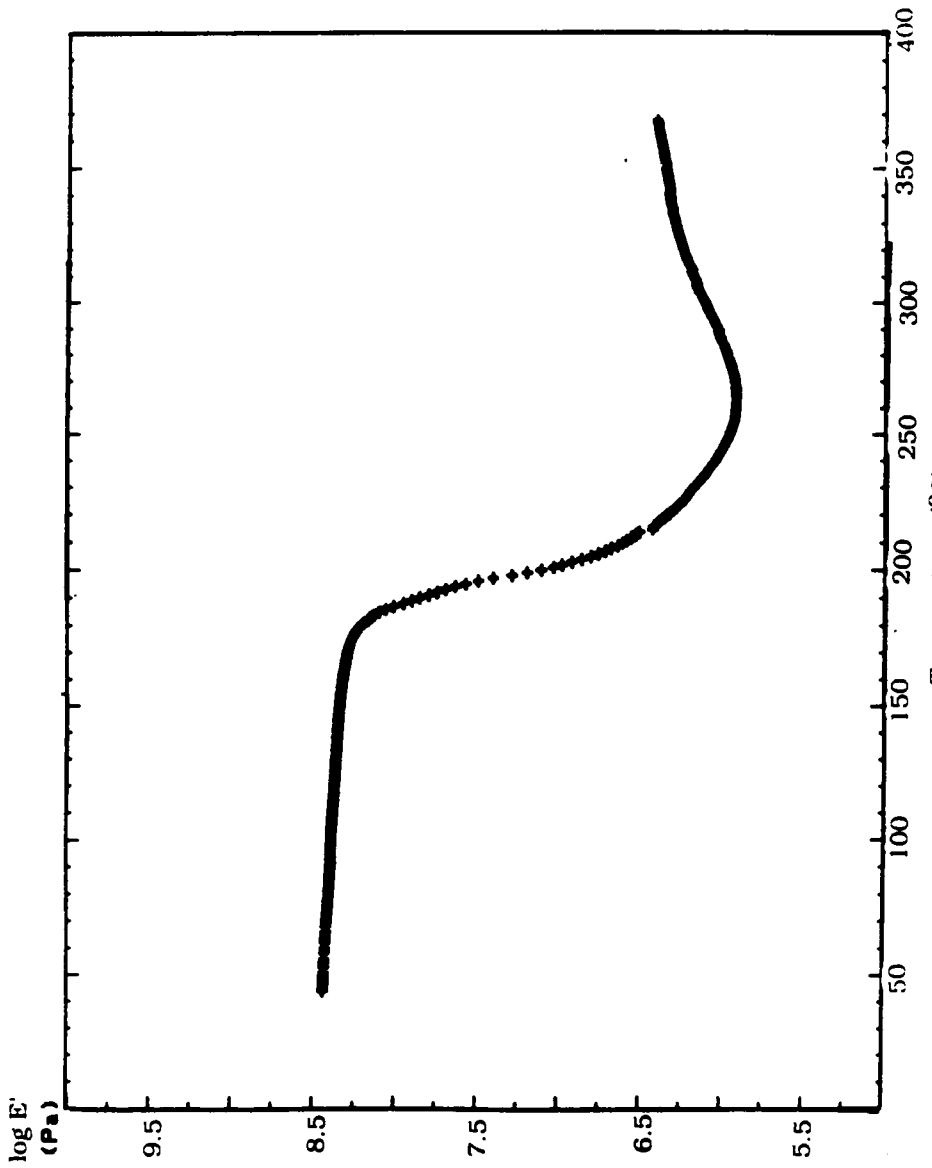

Figure 31: Storage Modulus Spectrum of 20/80 Metal/Polymer Composite Cured at 220°C.

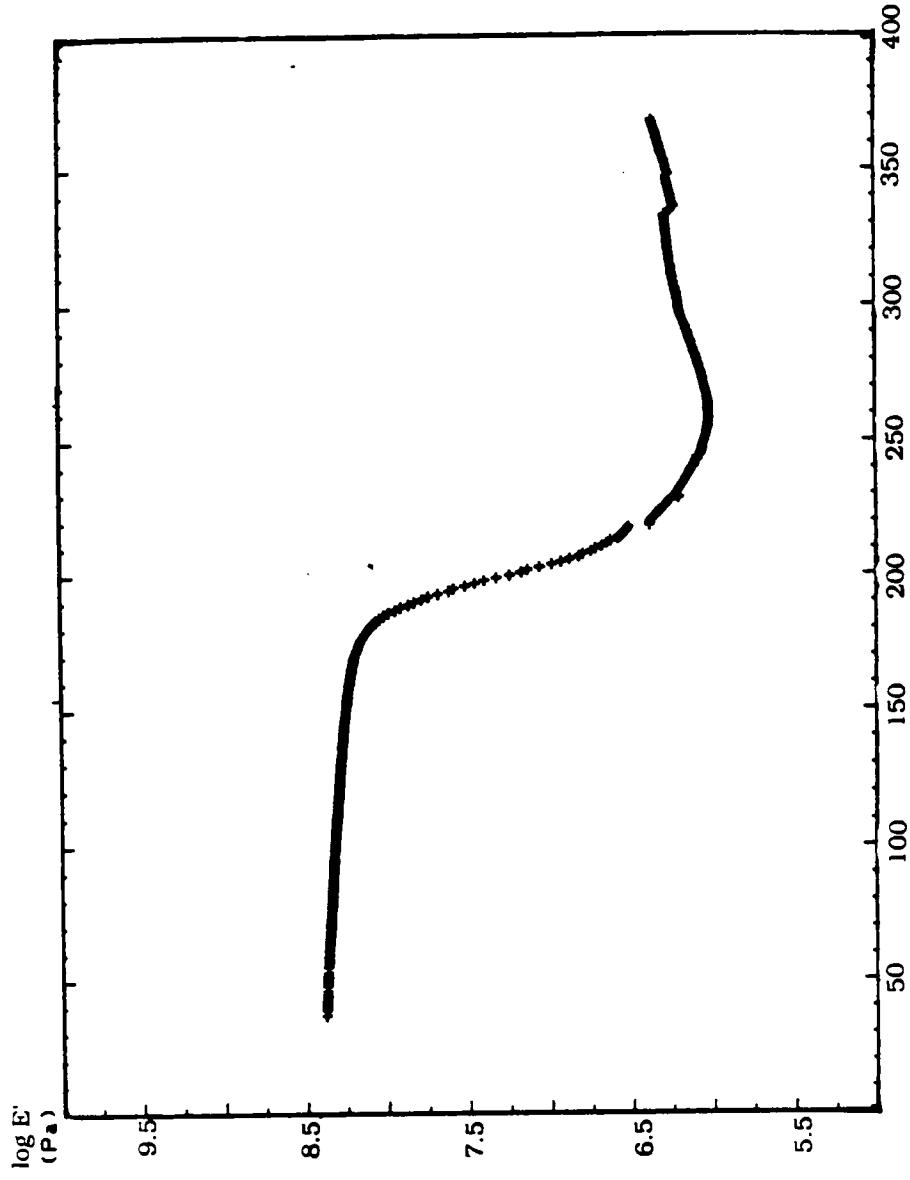

Figure 32: Storage Modulus Spectrum of 50/50 Metal/Polymer Composite Cured at 220°C.

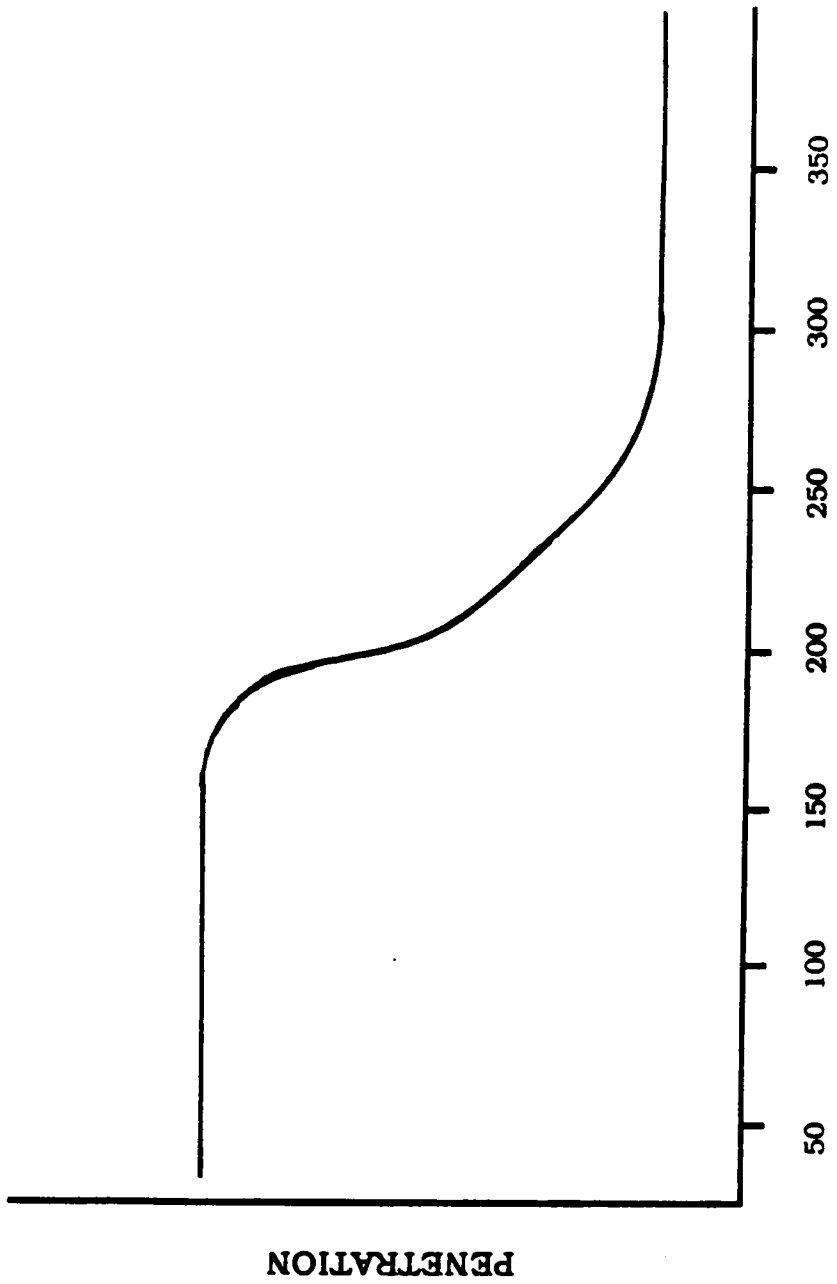

Figure 33: TMA of IP-600 Cured at 220°C.

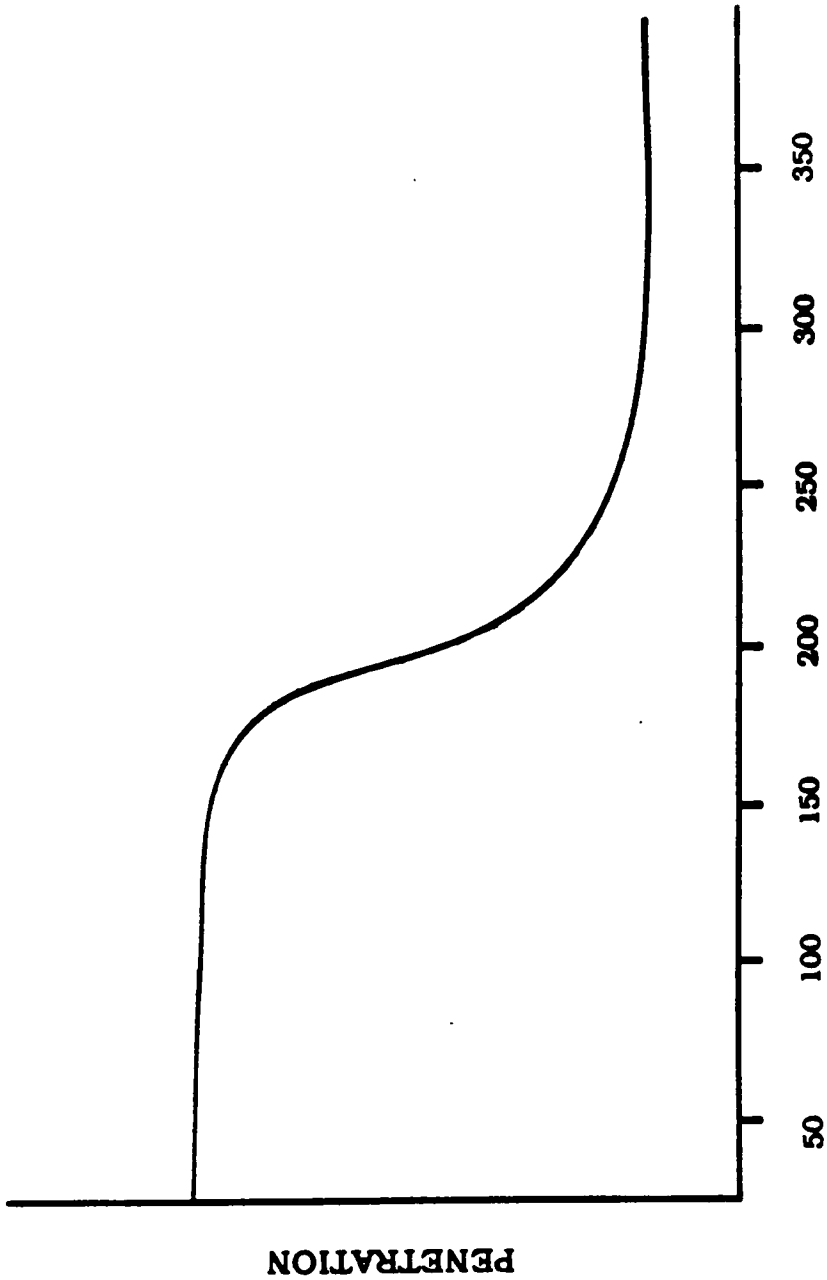

Figure 34: TMA of 5/95 Metal/Polymer Composite Cured at 220°C.

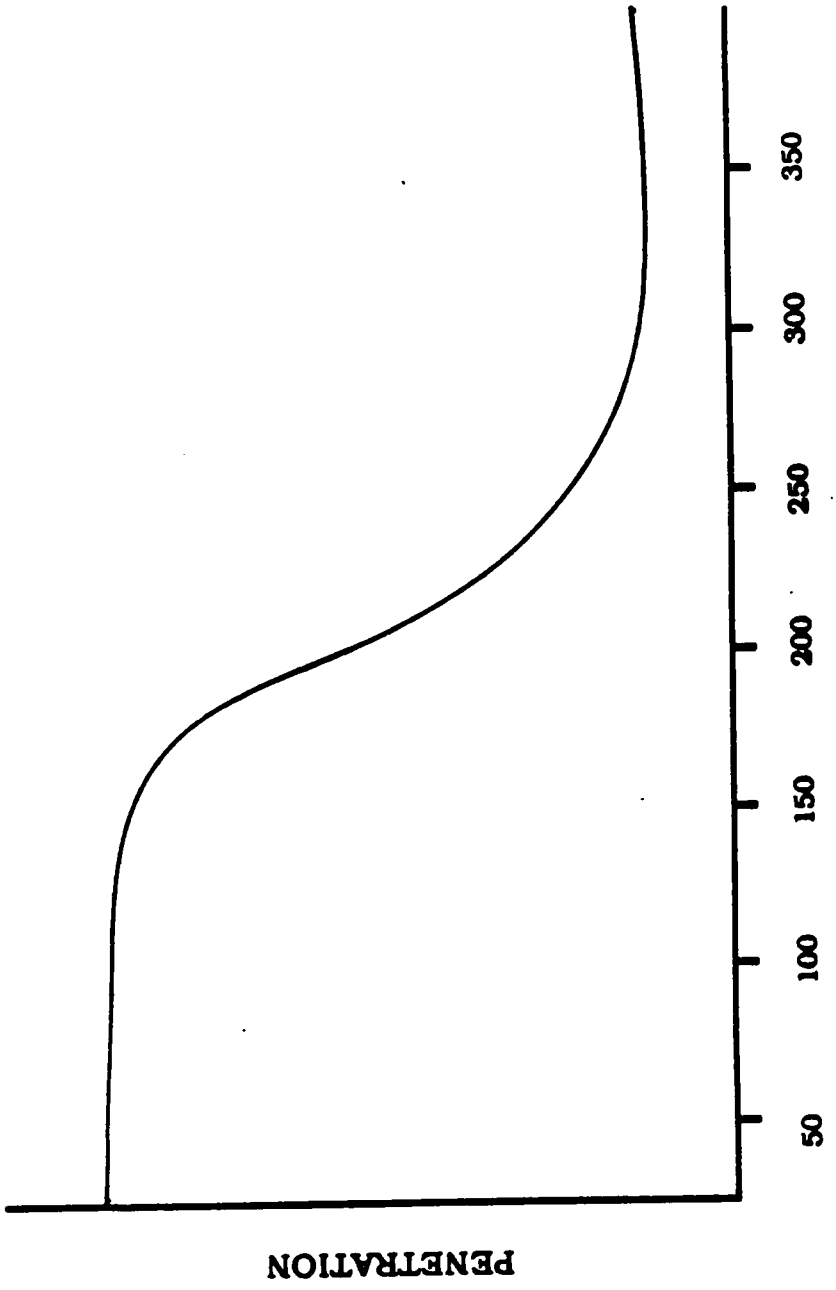

Figure 35: TMA of 20/80 Metal/Polymer composite Cured at 220°C.

with metal particles. The only apparent distinguishing feature of these data is the breadth of the glass transition region. It appears that as the loading of metal increases the breadth of the glass transition region also increases possibly due to the same influences giving rise to the tan δ behavior mentioned above.

6.2.3 Electrical Properties

The modification of electrical properties that occurs in MPC has been described in terms of percolation theory and is due to physical interaction among the metal particles themselves. At room temeprature the electrical properties of these composites are governed almost exclusively by the volume fraction, size, shape and distribution of the conductive metal particles in the composite. In the present case the data suggest that these materials behave as randomly dispersed composites (i.e. metal particles distributed in a random fashion) in contrast to a segregated composite. In the latter the filler particles are preferentially distributed at the interfaces defining the surfaces where the precursor polymer particles were sintered together during cure (9). Scanning electron microscopy has been used to characterize the shape and size of the particles in our composites; while, the densities of each component (metal and polymer) were used to calculate the volume loading. SEM analysis showed randomly shaped particles with no characteristic dimension. These particles were 20-70 μm in diameter and were assumed to approximate spheres. The percolation threshold for conductivity based upon our assumptions of particle shape and size is predicted to be above 30% (v/v) loading of metal particles.

The data obtained for two different molecular weight prepolymers (IP600, M_n ~1100; IP630, M_n ~17,000) in terms of both the actual lap shear joint resistance and also the calculated volume resistivity (ρ_v) are shown in Tables 15 and 16. At low loading levels the resistivity of the polymer dominates, and no current flow is measured through the sample. As the loading of metal is increased the resistivity begins to drop gradually until, at some critical loading level, the resistivity drops precipitously by ~3 orders of magnitude. This sudden drop marks the volume loading which is considered the percolation threshold for conduction.

These data suggest that in the case of the lower molecular weight material, IP600, the resistivity decreases at a lower volume percent loading than in the case of the higher molecular weight, IP630, material. This result may be due to several influences. First, since the IP600 has lower molecular weight, it would be expected to have a lower melt viscosity prior to gelation. This lower viscosity could lead to greater effective pressure on the bonds during cure. The greater effective pressure could be responsible for more metal-metal contact between the aluminum adherends and the metal particles present in the adhesive layer (106). Also, since these are acetylene terminated materials the lower molecular weight system would result in a more densely crosslinked network which would help to maintain contact during cool-down and subsequent vitrification of the material.

6.2.4 Adhesive Properties

Another aspect of these materials which has been investigated is the mechanical response, in terms of lap shear strength to aluminum, as

Table 15

Volume Percent Metal Loading vs Resistance for 0.5 in^2 Single Lap Shear Joints on Aluminum Employing IP-600 [a]

Percent Loading Metal/Polymer	Resistance	ρ_v ohm-cm
50/50	0.7 mΩ	3.7×10^{-2}
25/75	6.3 mΩ	0.73
20/80	6.2 mΩ	0.72
15/85	0.09 Ω	10.4
10/90	0.15 Ω	17.3
5/95	--	$> 1.2 \times 10^4$ [b]
0/100	--	$> 1.2 \times 10^4$ [b]

[a] Bond thicknesses ranged from 8-14 mils except for 50/50 case where bond thickness ranged from 21-27 mils.

[b] Less than 0.1 amp current flow @ 24 volt load.

Table 16

Volume Percent Metal Loading vs Resistance for 0.5 in^2 Single Lap Shear Joints on Aluminum Employing IP-630 [a]

Percent Loading Metal/Polymer	Resistance	ρ_v ohm-cm
50/50[b]	1.6 mΩ	9.0×10^{-1}
25/75	0.9 Ω	1.0×10^{2}
20/80	2.1 Ω	2.4×10^{2}
15/85	---	$>1.2 \times 10^{4}$[b]
10/90	---	$>1.2 \times 10^{4}$[b]
5/95	---	$>1.2 \times 10^{4}$[b]
0/100	---	$>1.2 \times 10^{4}$[b]

[a] Bond thicknesses ranged from 9-13 mils except for 50/50 case where bond thickness ranged from 21-24 mils.

[b] Less than 0.1 amp current flow @ 24 volt load.

a function of metal loading. Two different molecular weight prepolymers were employed. The lap shear data as a function of metal loading are shown in Tables 17 and 18 for the IP600 and IP630 materials, respectively. In both cases a maximum in lap shear strength occurs at a particular loading level. In the case of the lower molecular weight prepolymer, this maximum is observed at 15-20% (v/v) loading; while, in the higher molecular weight system the maximum occurs at 25% (v/v) loading. This maximum is presumably due primarily to changes in the compliance of the composite adhesive as a function of metal loading. Another factor which may contribute however, is the interfacial strength between the composite adhesive and the aluminum adherends. This contribution may be important since in all cases a mixed mode of failure is observed where both adhesive and cohesive debonding occur. It should also be noted that no optimization of bonding conditions was attempted. Conditions were chosen arbitrarily to insure comparability of samples. The potential strengths of these materials would thus be expected to be greater than those quoted here.

In all cases (but to varying degrees) deformation of the aluminum adherends occurs. The deformation that occurs is the bending of the bonded area of the adherends with respect to the line of force during the tensile test. This bending results in a dramatic increase in the peel forces at the edges of the bondline. Failure then appears to occur by propagation of a crack at the interface between the adhesive and adherend until the crack reaches the central region of the bond. The crack then propagates through the adhesive for a short distance, it then proceeds to the other interface and propagates to failure.

Table 17

Effect of Volume Percent Metal Loading on Lap Shear Strength Employing IP-6000 [a]

Sample Percent (v/v) Metal/Polymer	Lap Shear Strength MPa	(psi)
50/50	4.8 ± 0.7	(700 ± 100)
25/75	6.2 ± 0.5	(940 ± 80)
20/80	7.6 ± 0.3	(1100 ± 50)
15/85	7.7 ± 0.1	(1120 ± 20)
10/90	5.9 ± 0.2	(850 ± 30)
5/95	5.1 ± 0.4	(750 ± 60)
0/100	6.6 ± 0.4	(950 ± 60)

[a] Bonds were cured at 220°C for 1 hour under 3.5 MPa (500 psi) pressure, aluminum ahderends. Error limits were calculated from duplicate measurements on at least three samples.

Table 18

Effect of Volume Percent Metal Loading[a] on Lap Shear Strength Employing IP-630

Sample Percent Metal/Polymer	Lap Shear Strength MPa	(psi)
50/50	4.4 ± 1.0	600 ± 150
25/75	11.1 ± 0.3	1600 ± 40
20/80	9.0 ± 1.0	1300 ± 150
15/85	9.0 ± 0.8	1300 ± 110
10/90	10.0 ± 1.0	1450 ± 150
5/95	9.2 ± 0.6	1350 ± 80
0/100	9.9 ± 0.9	1430 ± 130

[a] Bonds were cured at 220°C for 1 hour under 3.2 MPa (500 psi) pressure, aluminum adherends. Error limits calculated from duplicate measurements on at least three samples.

Upon visual inspection of the bond, three regions are apparent (Figure 36). Region 1 is comprised of polymer with a lustrous coating of metal oxide. This region corresponds to region 3 of the opposite adherend; in this third region a clean oxide surface of the adherend is observed. Region 2 contains polymer on both adherends and is slightly narrower than either of the other regions. The XPS samples which are described next have been taken from region 1.

In order to better understand this failure process X-ray photoelectron spectroscopy (XPS) was used to examine the failure surfaces of several bonds. Table 19 shows the XPS data for two bonds prepared with IP630 prepolymer and either 5 or 25% (v/v) loading of metal. Also shown in this table are the lap shear strengths and the atomic concentrations of three elements which can be used to identify various components of the system. Nitrogen, which is present only in the polymer can provide a tag for the concentration of the polymer at the polymer-rich failure surface (Region 1, Figure 36). In both metal-loaded cases the surface is almost entirely polymer since the atomic concentration of nitrogen in the pure polyimide is calculated to be 4.7%. A significant amount of aluminum is also present due either to the filler particles or to the oxide surface of the adherend. Nickel is present only in the filler particles and would serve as a tag to determine what fraction of the surface is exposed filler particles. However, XPS analysis of the particles alone shows nickel at only 1.3 atomic % due to the large amount of aluminum and oxygen which comprise the majority of the particle surface. The carbon and oxygen signals were also monitored but were not used in the analysis because of the

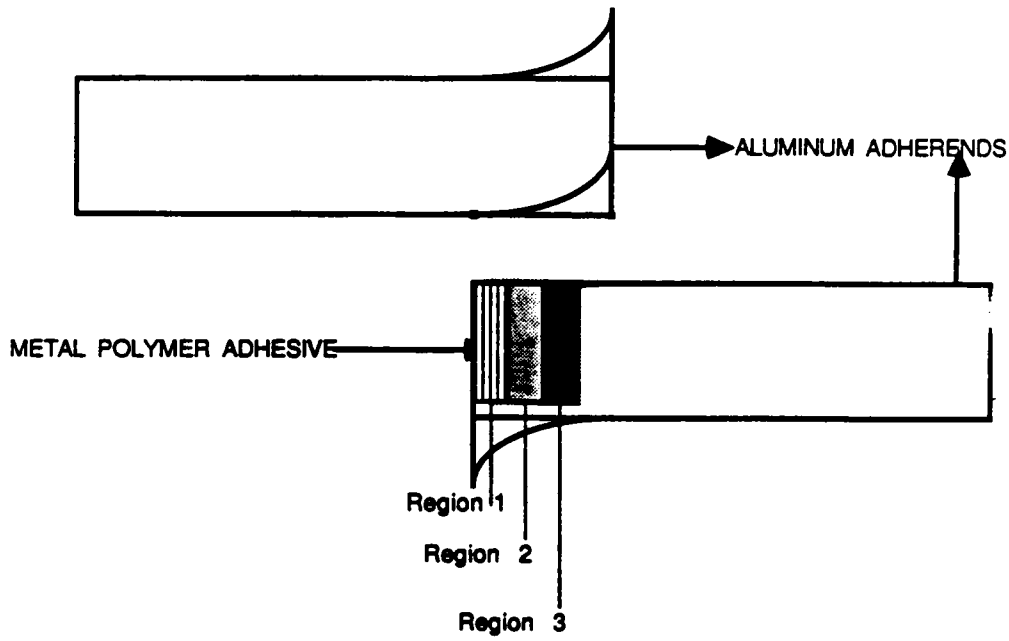

Figure 36: Schematic Representation of Failure Regions in Metal/Polymer Composite Adhesive Bonds.

Table 19

XPS Analysis of Polymer Failure Surface

Sample (V/V) Metal/Polymer (IP630)	Element	Atomic %	Lap Shear Strength (psi)
5/95	N	4.6	1350 ± 80
	Al	1.5	
	Ni	0.0	
25/75	N	3.7	1600 ± 40
	Al	4.3	
	Ni	0.2	

Broad oxygen peaks detected indicating both organic and oxide type oxygen.

varying chemical environments in which these elements are present. Both samples showed carbon at 35-40 atomic % on the surface. What does appear in these data is a trend to suggest that the stronger bond, consisting of 25% (v/v) metal filler, has more aluminum and less polymer on the fracture surface than the weaker bond with 5% (v/v) metal. The amount of aluminum in the stronger bond is almost three times that present in the weaker bond (4.3 at. % vs 1.5 at. %). Only a small amount of nickel is observed in the stronger bond (0.20 at. %) indicating that most of the additional aluminum present in this case is due to the aluminum oxide surface of the adherend rather than more exposed filler particles. The amount of nitrogen in the stronger bond is also decreased indicating less polymer at the failure surface. These data indicate that in the case of the 5% (v/v) loaded system the failure in this region is primarily at the interface between the polymer and the adherend; in contrast, the case of the 25% (v/v) bond failure occurs more within the aluminum oxide as evidenced by the greater aluminum signal in this case.

The surface pretreatment of the aluminum in this study was quite simplistic which undoubtedly affects the measured bond strenghts as well as the failure mechanisms. The abrasion of the aluminum surfaces with sandpaper is obviously not the optimal surface pretreatment in terms of bond strength or stability but it does have the advantage of simplicity. Also, since the study involved measurement of electrical properties of the matrix most other pretreatment procedures such as acid etch or anodization, which rely on forming uniform and rather thick oxide layers

on the aluminum, would have lead to less favorable conductivity through the bond.

6.3 Summary

The use of metallic fillers in acetylene terminated polyisoimide prepolymers is an effective way of modifying the electrical and mechanical properties of these materials. Good conductivity can be achieved in these composites without sacrificing adhesive behavior. In addition, post glass transition behavior is modified through the filler incorporation.

7.0 Poly(Imide Siloxane) Segmented Copolymer Structural Adhesives

7.1 Introduction

The potential widespread utilization of polyimides for structural adhesives and matrix resins has been significantly limited due to several problems concerning processing of these systems. Although polyimides generally possess excellent thermal and mechanical properties (6-8), they are predominantly insoluble and infusible, factors which severely limit their applicability. In structural adhesive applications polymers must flow to provide good wetting of adherend surfaces and good consolidation of the bond components (primed adherends and adhesive layer). In addition, the presence of residual volatiles present in the adhesive at the time of bond fabrication can lead to the creation of voids within the bond during the bonding process.

Conventional polyimides are formed by the bulk, thermal cyclodehydration of a poly(amic acid) precursor. This procedure, while allowing for preparation of some adhesive test samples, suffers from the presence of volatiles (residual solvent and water of dehydration). These problems would limit the types of applications for these materials. More recently, thermal solution imidization procedures have been explored which could help overcome these problems (150-151). These procedures keep the reacting species solvated at all times thereby eliminating the need for temperatures above the glass transition of the final polymer in order to obtain complete reaction. With careful cleanup, these procedures also result in volatile free polymer.

Summers et al (14,151) have used these procedures to synthesize fully imidized, soluble poly(imide-siloxane) segmented copolymers. The

incorporation of siloxane segments into a polyimide backbone, because of the flexibility of the siloxane and the dilution of imide functionality, can permit improvement of the solubility and processing characteristics while maintaining reasonably good thermal and mechanical properties. In addition, thermally stable siloxanes can impart a number of favorable properties to engineering polymers, including impact resistance, weatherability and surface modification (13,152). It has also been demonstrated that the incorporation of hydrophobic siloxane segments into polyimides favorably reduces the moisture uptake of these materials.

This chapter will describe the adhesive characterization of polyimides and poly(imide-siloxanes) prepared by both the bulk and solution thermal imidization processes. Special attention has been given to the hot/wet durability of these systems as measured by the stress durability test. This test was chosen since it allows discrimination between materials based on the "time-to-failure" under a given set of conditions. Additionally, it had the advantage of using standard single lap shear specimen geometry which was also used in determining ultimate room temperature strengths. The results of this testing were correlated with various polymer parameters such as synthesis method and siloxane content.

One generally desirable characteristic of these materials for applications such as matrix resins, coatings and electronic materials is that of good adhesive properties. Therefore, one of the goals of this study was to demonstrate that siloxane incorporation into polyimide backbone polymers would not detract significantly from the already

favorable adhesive properties of polyimides. In addition, certain characteristics have been observed which suggest that the siloxane block incorporation was an important advantage in resistance to moisture intrusion and subsequent bond failure (153-157). Comparison of the two synthesis methods mentioned above was also investigated with regard to possible influences on adhesive performance. Each of these characteristics will be treated separately below.

7.2 Results and Discussion

7.2.1 Room Temperature Adhesive Properties

Many tests exist for evaluation of the room temperature properties of structural adhesives. One of the most common uses the single lap shear geometry. Although this test has recognized problems, it provides an adequate test for rank ordering a similar series of polymers. Also, its simplicity allows for minimal sample requirements, an important criteria when dealing with research quantities of materials.

7.2.1.1 Effect of PDMS Incorporation on Lap Shear Strength

The effect of siloxane block incorporation on lap shear strength is shown in Table 20. All samples listed in this Table were prepared by the bulk thermal imidization method. In this case completion of imidization occurs during bonding. The data represent the averages of at least three samples. Errors are less than 10% between duplicate samples. All failures are cohesive. The data concerning the control polymer and 10% siloxane copolymer require further clarification since they deviate from the strength versus % (w/w) siloxane incorporation trend. These tests were repeated more than the others in an effort to improve reproducibility. Throughout this study both the bonding and

Table 20

Effect of Poly(dimethyl-siloxane) Incorporation on Room Temperature Lap Shear Strength

Wt.% Siloxane	PDMS M_n	Lap Shear Strength MPa (psi)
Control	---	20.6 (3000)*
5	950	16.5 (2400)
10	950	19.9 (2900)*
20	950	14.4 (2100)
40	950	12.4 (1800)

*Samples from the latest series.

All samples are bulk imidized.

Data represent averages of at least three samples. Errors are less than 10%.

synthesis techniques were constantly improving. In the latest series of samples there is no significant difference in room temperature adhesive properties between the control polymer and the 10% siloxane-containing copolymer.

As higher percentages of siloxane (>20% w/w) were incorporated the ultimate strengths diminished because the overall modulus of the adhesive was decreased significantly at those levels of incorporation. Also note that these samples were all thermally imidized and therefore would not have had as favorable flow properties as materials discussed later prepared by the solution technique.

7.2.1.2 Bulk Versus Solution Thermal Imidization

The comparison of the bulk with solution imidized materials in terms of room temperature adhesive properties is shown in Table 21. These samples were all prepared by the scrim cloth technique and had similar thermal histories prior to bonding. In the case of the control polymer there was virtually no difference in lap shear strength between bulk and solution preparations. However, in the case of the samples which contain 20% siloxane by weight there was a significant difference favoring the solution preparation. Since both of these samples had the same thermal treatment prior to bonding it was very unlikely that void content variations were responsible for this difference. All failures were cohesive. The difference appeared to have been due to the difference in flow characteristics of the two systems. In the case of the solution imidized polymer an intrinsic viscosity in NMP at 25°C of 0.65 dl/gm was measured. No comparable viscosity data exist for the bulk reaction system since this polymer is insoluble. Since the

Table 21

Bulk vs Solution Imidization Ultimate
Room Temperature Strength

Preparation (Composition)	Lap Shear Strength MPa (psi)
Bulk (Control)	20.6 (3000)
Solution (Control)	19.9 (2900)
Bulk (20%, 950 M_n)	14.4 (2100)
Solution (20%, 800 M_n)	27.6 (4000)

viscosity data indicate high molecular weight polymer in all cases the improvement in flow and adhesive characteristics was presumably due to an inherently more favorable physical structure or molecular weight distribution in the case of the solution imidized materials. This more favorable structure may have been due to less branching or chain defects in the case of the solution imidized systems or to a more favorable morphology eliminating ordering in the solution case.

7.2.1.3 Bonding Method

Samples of the control and 20% siloxane-containing samples were used to compare two methods of bond preparation. In this case all samples were bonded either with or without the presence of scrim cloth. Scrim cloth has traditionally been used as a carrier for the adhesive and also to help insure uniform bond thickness. In some cases however, its presence led to difficulty in analysis of failure surfaces. Evaluation of the presence of the scrim cloth was restricted to samples prepared by solution procedures, since conventional bulk imidized polymers did not flow enough during the thermoplastic bonding process for good bond consolidation. If bulk imidized samples were pretreated at lower temperatures to improve flow characteristics residual volatiles resulted in excessive void formation and extremely weak bonds. Consequently, no reproducible thermoplastic samples could be prepared with the bulk imidized samples because in many cases the samples failed immediately on removal from the bonding jig. In contrast, both solution imidized homo- and co-polymers formed good bonds without scrim cloth present. The data are shown in Table 22. In the case of the control polymer, the strength was slightly lower without (than with) scrim cloth

Table 22

Results of Thermoplastic vs Scrim Bonding *

Preparation (Composition)	Lap Shear Strength MPa (psi)
Without scrim (control)	15.8 (2300)
With scrim (control)	19.9 (2900)
Without scrim (20%, 800 Mn)	30.3 (4400)
With scrim (20%, 800 Mn)	27.5 (4000)

*All samples solution imidized.

present. However, this trend was reversed in the sample containing 20% (w/w) siloxane.

7.2.2 Stress Durability and Failure Analysis

One primary consideration in the testing of structural adhesives is that of environmental stress durability. Appropriate measurement of this property can provide another valuable criteria with which to evaluate and rank order adhesives. In this study the so called 3M durability test was used similar to ASTM D-2919. This test, shown schematically in Figure 10, Chapter 2, utilizes the same single lap shear coupon geometry that was used in the room temperature testing. The samples were placed into a fixture and a load applied by means of spring compression to the sample through holes drilled or punched in the coupons prior to bonding. The fixture was then attached to an electrical timer which measures the "time to failure". The entire fixture, excluding the spring and timer, was then exposed to the conditions of interest. In this case 80°C, 100% relative humidity and 8.3 MPa(1200 psi) load were used. These were quite severe environmental conditions and provide a very rigorous evaluation of these materials.

7.2.2.1 Effect of PDMS Incorporation on Durability

The effect of 10% (w/w) siloxane incorporation on the time to failure for a modified polyimide is shown in Table 23. In this case a significant improvement was observed with respect to moisture resistance for the siloxane containing system compared to the control polyimide. These data were obtained on samples which had been imidized in bulk and therefore are bonded using scrim cloth. Failure mode in this case was mixed. There appear to be approximately equal areas of both adhesive

Table 23

Effect of PDMS Incorporation on Durability

Composition	Time to Failure
Control	2.7 days
10% PDMS	9.7 days

Test Condition: 0.5 in^2 overlap single lap shear specimens (Ti 6-4, Pasa Jell 107 pre-treatment), 8.3 MPa (1200 psi) load, 80°C, 100% R.H.

PDMS Mn = 950 daltons

Bulk Imidization

and cohesive failure within the bond. It should be pointed out that the evaluation of these failure surfaces was complicated greatly by the presence of the scrim cloth within the bond. Later, data will be presented which more appropriately supports the generally accepted observation that the durability failure occurs by a predominately adhesive mechanism while room temperature failure occurs by a predominantly cohesive mechanism.

7.2.2.2 Effect of Synthesis Method on Durability

A comparison of the control and 10% (w/w) siloxane-containing polymer was also made based on the synthesis method. The data for the solution and bulk imidized samples are shown in Table 24. These data indicate that no significant difference in moisture resistance exists based on different synthesis methods. These observations were expected since there were no recognizable differences in the room temperature properties of these systems. Again, bond failures appeared to be a combination of adhesive and cohesive failure. It should be pointed out however, that this interpretation was based on visual and optical microscopic investigation and was complicated greatly by the presence of the scrim cloth within the bonds.

In the case of the siloxane modified polymer, the domains of siloxane are very small compared to the macroroughness of the adherend surface. At these siloxane molecular weights, M_n = 800-950 g/mole, one would predict poly(dimethyl-siloxane) phases of less than 100 Å in diameter. This diameter is in the range of the microroughness observed on the pretreated coupons. A scanning electron micrograph of this Pasa Jell 107 pretreated surface is shown in Figure 37. The marker is 0.5 μm

Table 24

Influence of Bulk vs Solution Imidization on Durability Properties

Preparation (composition)	Time to Failure *
Bulk (control)	2.7 days
Solution (control)	2.4 days
Bulk (10%, 950 Mn)	9.7 days
Solution (10%, 800 Mn)	8.9 days

All bonds contain scrim cloth.

*Test condition: 8.3 MPa (1200 psi) load, 80°C, 100% R.H.

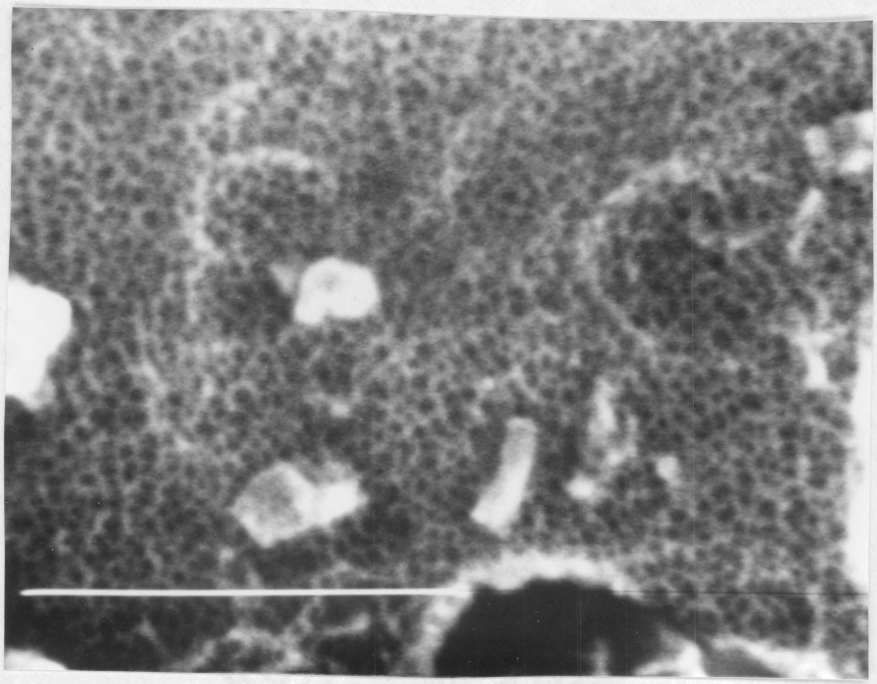

Figure 37: SEM Photomicrograph (100,000x) of Uncoated, Pasa-Jell 107 Pretreated Titanium (6-4) Surface.

and the magnification is 100,000X. The features observed are on the order of 100-250 angstroms in diameter. These features would be expected to be too small to interact physically with the adhesive.

On a more macroscopic scale, if the siloxane domains were very small compared to the macroroughness of the surface (1-2 μm) then their presence may reduce the uptake of moisture through the bulk polymer thereby improving durability. In this interpretation the primary adhesive bonding is accomplished by the polyimide segments while the siloxane simply serves to inhibit the penetration of moisture through the adhesive.

7.2.2.3 Effect of Bond Preparation on Durability

Another comparison in this study was based on the effect of scrim cloth on the stress durability "time to failure". In this case all samples were solution imidized since these materials exhibited superior flow properties. The data for the control polyimide and a 20% (w/w) siloxane-containing sample are shown in Table 25. No difference in time to failure was observed in the case of the control polyimide with and without scrim cloth. However, in the 20% (w/w) siloxane-containing case the sample with no scrim cloth lasted twice as long as the scrim containing sample. This effect may be due to the increase in interface areas for wicking* of water in the case of the scrim cloth containing sample. In this case a comparison of the failure surfaces was made between the 20% (w/w) siloxane-containing samples which failed under the durability conditions and under room temperature conditions.

---

*This "wicking" phenomenon may be due to the strong hydrogen bonding interaction of water with the polar glass surface.

Table 25

Durability Properties
Thermoplastic vs Scrim Bonding

Preparation (composition)	Time to Failure *
Without scrim (control)	3.2 days
With scrim (control)	2.7 days
Without scrim (20%, 800) Mn	12.1 days
With scrim (20%, 800) Mn	6.1 days

All samples were solution imidized.

*Test condition: 1200 psi load, 80°C, 100% R. H.

Interpretation was simplified greatly by examining bonds which do not contain scrim cloth. Low magnification (240X) scanning electron micrographs in Figure 38 show a room temperature failure surface of the polymer which indicates cohesive failure. No areas of metal oxide were exposed in this case and the surface appears rough. In the case of the durability test predominately adhesive failure was seen. The large smooth areas indicate interfacial type failure. It is proposed that the improvements in durability observed in the case of siloxane modified materials is due to the hydrophobic nature of the siloxane segments inhibiting the uptake of water at the critical interphase between the metal oxide and adhesive layers. Also, the enhancement in this property based on the absence of scrim cloth is presumably due to fewer paths for the wicking of moisture into the bond.

7.2.3 Sec butyl Aluminum Alkoxide Adhesion Promoter

The use of an adhesion promoter, Sec butyl aluminum alkoxide, has also been investigated in this system. This adhesion promoter was introduced into the system after pretreatment of the titanium coupons. This primer was applied to the dried coupons from a 10% (w/w) solution of the aluminum compound in NMP. The coupons were then additionally dried for 30 minutes at 160°C in vacuum to remove the solvent. After removal from the vacuum ovens, the coupons were allowed to cool for 10-15 minutes at which time they were coated with a solution of polymer to serve as a primer and treated as described in the experimental section for general sample preparation.

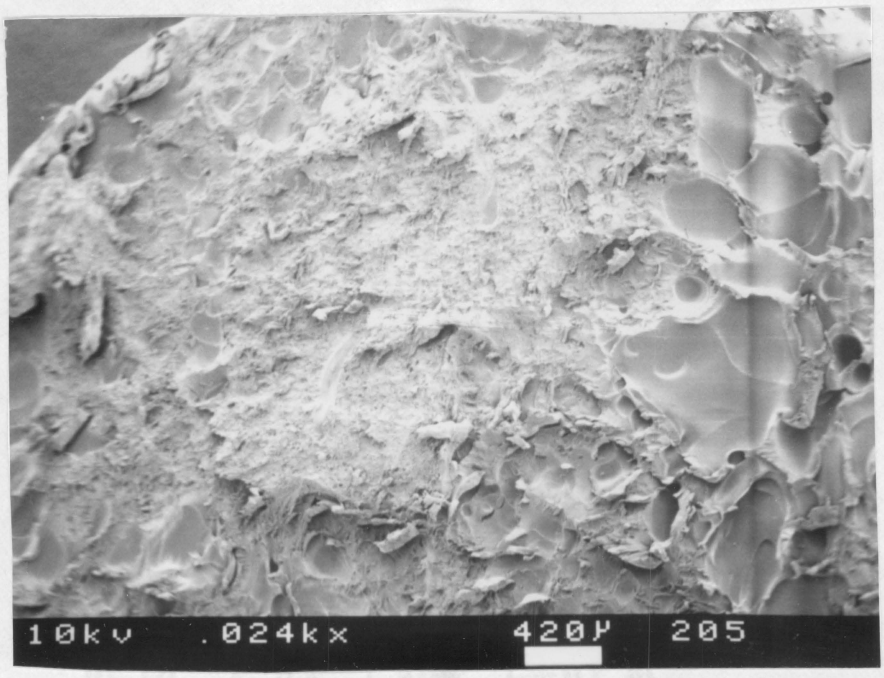

A) Room Temperature Failure

B) Durability Failure

Figure 38: SEM Photomicrographs (270x) of Failure Surfaces for Poly(imide-siloxanes) Containing 20% (w/w) PDMS.

7.2.3.1 Effect of Sec butyl Aluminum Alkoxide on Durability

Sec butyl aluminum alkoxide has been shown to be effective in enhancing the moisture resistance in adhesive bonds prepared using titanium adherends and epoxy adhesives (129,135-137). The utilization of this compound has been extended to the poly(imide-siloxane) segmented copolymer adhesive system. The data shown in Table 26 were obtained for polymers prepared by the solution thermal imidization technique. These were bonded both with and without the incorporation of sec butyl aluminum alkoxide adhesion promoter. Clearly, these data indicate that the presence of the aluminum compound does not detract from the ultimate strength measured at room temperature but it does improve the resistance of these systems to moisture**.

One possible explanation for the effectiveness of the aluminum alkoxide adhesion promoter is that it reacts chemically with water of hydration on the surface of the titanium dioxide thereby changing the surface energy in a way which allows more effective penetration of the polymeric adhesive into the features of the surface. Another mechanism may be the sealing by the aluminum compound, in a partially or fully hydrolyzed state, of features which would prevent or slow the lateral diffusion of water into the crucial interphase region where metal oxide and polymeric adhesive coexist. Understanding of this system may be clarified by resorting to an idealized model (Fig. 39). This model

---

**No bonds were prepared with the homopolymer, polyimide, because of the limited amount of this material available in the solution imidized form. It should be pointed out that all the bonds used in this study were prepared without scrim cloth. This factor also helped improve the overall durability of the bonds as described previously.

Table 26

Influence of Sec butyl Aluminum Alkoxide Primer on
Room Temperature Adhesive and Durability Properties *

Polymer	Primer	Lap Shear Strength MPa (psi)	Time to Failure (days)
10% (800)	$Al(sec\ BuO)_3$	17.2 (2500)	16.4
10% (950)	---	17.9 (2600)	8.9
20% (800)	---	27.5 (4000)	6.1
20% (800)	$Al(sec\ BuO)_3$	31.0 (4500)	20.5

*All samples solution imidized with scrim cloth.

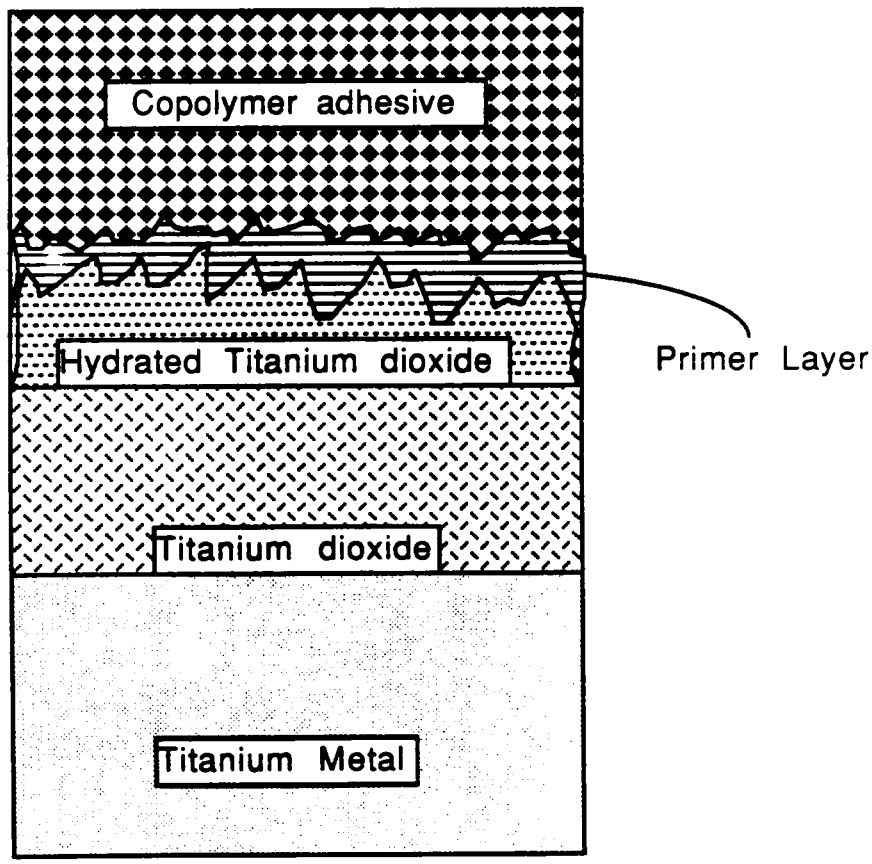

Figure 39: Idealized Model of Copolymer Adhesive on Titanium (6-4) Surface.

divides the system into four basic areas; 1) bulk metal, 2) titanium dioxide, 3) hydrated titanium dioxide and 4) copolymer adhesive. This simplistic model obviously ignores the microscopic aspects of the interphase region as well as any preferential bonding of either of the two segments comprising the adhesive. The basic idea which is expressed however, is that the copolymer diffusion into the features of the hydrated oxide layer maybe somewhat limited due to the presence of water adsorbed in these cracks etc. The effect may be predominantly hydrostatic in that water within the oxide prevents penetration of the polymer. The sec-butanol which is released during hydrolysis should not hydrogen bond as strongly with the surface as the water present before reaction with the alkoxide and therefore should be more easily removed during the drying steps. If this adsorbed water was reacted with metal alkoxide, however the polymer may be better able to penetrate into the features of the oxide due to less interference from adsorbed water either hydrostatically or through less favorable spreading of the polymer on a hydrated surface. It should be pointed out that this explanation is speculative based on limited experimental observations of this system. Obviously, more work needs to be done in this area to clarify the mechanism by which the enhancement of durability occurs.

The mechanism of failure in the stress durability samples is predominantly adhesive. That is, no matter what the actual time to failure of a particular sample; the locus of failure occurs primarily between the adhesive and the metal oxide. Therefore neither the incorporation of siloxane segments into the adhesive nor the use of aluminum alkoxides as adhesion promoters change the mechanism of failure

in a hot, wet environment. Both these strategies have been observed to prolong the time required for this failure to occur. It may be possible that the incorporation of the siloxane segments, known to be hydrophobic, into the polyimide copolymer adhesive slows the diffusion of water into the interphase where the intimate contact between adhesive and adherend takes place. If these primary adhesive bonds; dispersion, electrostatic, as well as any possible bonds excluding covalent are more slowly disrupted by the infusion of moisture then the bond should last longer under stress.

7.2.4 Surface Acidity

It has also been proposed that residual surface acidity may influence the effectiveness of the aluminum alkoxide adhesion promoter (127,133-135). A brief study was conducted where pretreated titanium coupons were prepared and exposed to excess rinsing in addition to normal rinsing with deionized water for various lengths of time. Indicator dyes were then applied to the surface of the dried coupon and allowed to dry. The dyes used, their pH transition and color change are shown in Table 27. The colors of the dry dyes are shown as a function of rinsing time in Table 28. It must be pointed out that the observation of these experiments was quite subjective in terms of judging residual color on a surface after a dye drop has receded by evaporation. However, the data do indicate that a shift to higher pH occurs at longer excess rinse times (>20 minutes). Additionally, FT-IR data in Appendix 2 may be useful in analyzing the surface acidity of

Table 27

Indicator Dyes, Transitions and
pH Ranges of Transitions

Dye	Transition	pH Range of Transition
Thymol Blue	Yellow ⟶ Blue	8 - 9.6
Bromophenol Blue	Yellow ⟶ Blue	3 - 4.6
Bromocresol Green	Yellow ⟶ Blue	3.8 - 5.4
Bromocresol Purple	Yellow ⟶ Blue	5.2 - 6.8
Orange I	Orange ⟶ Violet	7.6 - 8.9

Table 28

Response of Indicator Dyes as
a Function of Excess Rinse Time

Dye	Color After Excess Rinsing*		
	5 Minutes	10 Minutes	20 Minutes
Thymol Blue	Y	Y	Y
Bromophenol Blue	Y	Y	B
Bromocresol Green	Y	Y	B
Bromocresol Purple	Y	Y	B
Orange I	O	O	O

*Y = Yellow, B = Blue, O = Orange, V = Violet

these coupons after pretreatment. This change in surface acidity may affect the hydrolysis of the aluminum alkoxide thereby reducing its effectiveness as an adhesion promoter.

7.3 Summary

The data presented here indicate that the presence of siloxane segments in polyimide backbone polymers improve the resistance of adhesive bonds prepared with these materials to degradation by moisture in the stressed state. Additionally, no degradation in room temperature adhesive performance can be attributed to the presence of the siloxane. The data also show that solution thermal imidization synthesis methods result in polymers with comparable mechanical performance and superior fabrication properties than materials prepared by bulk thermal imidization. Finally, the effectiveness of sec butyl aluminum alkoxide in improving the stress durability of adhesive samples prepared with these polymers has been demonstrated.

8.0 Conclusions and Suggested Future Work

The results of the work presented here verify the observation that polymer properties can be effectively tailored to suit particular applications through a combination of chemical alteration of the polymer backbone architecture and the incorporation of fillers such as the metal particles employed in the present study. The specific conclusions for each of the areas studied will be presented in this chapter along with some suggestions for future studies in these areas.

Initially, it was shown that metal filled acetylene terminated polyisoimides were very effective in maintaining both thermal stability and good electrical conductivity when used in joining aluminum conductor bars. Future work in this area would be expected to focus on the optimization of application procedures and the scale up of the system.

The chemistry of the acetylene terminated polyisoimide has also been studied. Calorimetric and infrared kinetic analyses both support the assertion that both the crosslinking and isomerization reactions are first order and that the isomerization has a lower activation energy than the crosslinking. The potential future work in this area would focus on modeling the two reactions occurring in this system with other systems having similar mobility at these temperatures. Small molecule modeling is of little use since the thermally induced reactions of interest would occur in a much more mobile, less viscous environment in the case of small molecules than for the case of these oligomers. To study the acetylene crosslinking reaction it is suggested that one use acetylene terminated oligomers such as sulfones or quinoxalines which have similar glass transition temperatures to the isoimides, but which

have only one reaction (crosslinking) occurring. Perhaps it would even be possible to define a reduced kinetic rate constant which would be based on reduced temperature, $T-T_g$, rather than on the absolute temperature. This may allow for some of the chain mobility considerations to be normalized out of the analysis.

In the study of the isomerization reaction it is suggested that high molecular weight, linear polyisoimides be prepared. The isomerization reaction could then be studied without the added complication of the crosslinking. In addition, the increase in T_g due to the isomerization alone could be isolated. Generally, different techniques such as torsion braid analysis could be used to try to isolate the changes in mechanical properties due to each of the two reactions. Additionally, DMTA of sandwiches comprised of thin metal shims surrounding prepolymer film could also be investigated without damage to the instrument. Finally, and perhaps most importantly, the dielectric behavior of this system could be investigated. It is expected that both of these transformations, the isomerization and crosslinking reactions, will cause significant changes in the dielectric response of these materials. Perhaps this dielectric data could be utilized in conjunction with electromagnetic energy curing studies.

In the case of the metal/polymer composites it has been shown that the dynamic mechanical, electrical, and adhesive properties of these polymers can be modified by the incorporation of metallic fillers. In this area the future work would likely involve the extension to other filler morphologies or structures. Segregated composites based on these high temperature systems would certainly be of interest. Additionally,

other characterization techniques including fracture toughness, impact strength, transmission electron microscopy, and dielectric behavior would also be of considerable interest.

Finally, in the area of poly(imide-siloxane) adhesive properties it has been demonstrated that the incorporation of siloxane segments into polyimide backbone polymers significantly improves the moisture resistance of adhesive specimens prepared with these materials without adversely effecting the ambient condition properties. Two quite different synthetic procedures used to prepare the polymers gave comparable results although in some aspects the more novel solution thermal imidization preparation was more favorable than the more traditional bulk thermal imidization. Additionally, the presence of scrim cloth was found to have an adverse effect not only on analysis of bond failure surfaces but also on the resistance of stressed samples to moisture. The presence of aluminum alkoxide primers was found to be favorable in conjunction with the poly(imide-siloxane) copolymers in further improving the resistance of stressed, bonded samples to moisture intrusion and subsequent failure.

One study dealing with the adhesive properties of these poly(imide-siloxane) copolymers which is strongly suggested is that of a correlation of molecular weight, or flow properties, with adhesive performance. In this study a starting point would be the adhesive evaluation of a particular polymer structure and composition at a variety of molecular weights. This would allow the next step in a more sophisticated design of these adhesives to be pursued; that step being molecular weight control for optimized flow properties. Additionally,

variations in the polymer architecture through incorporation of novel monomeric components would also be of interest in order to potentially isolate the functionalities responsible for superior adhesive performance. These synthetic considerations should be combined with more diverse analytical techniques to better define the morphology, structure, and detailed composition of the system. Specifically, electron spectroscopy coupled with infrared and electron microscopy of various stages of the system prior to and after bonding should help to identify chemical and physical interactions at the interphase level of bond formation. The last area of analysis to be expanded would be that of adhesive testing. In this case the wedge test is suggested as a way to confirm the validity of the stress durability test discussed here. The stress durability test could be the more routine test with a few samples being run in both tests, stress durability and wedge, to support the trends. Additionally, elevated temperature testing of the samples would be suggested since much data indicates the use temperature of the siloxane modified materials will not be decreased greatly compared to the homo-polyimides.

Literature Cited

1. Hergenrother, P. M., "Heat Resistant Polymers," Encyclopedia of Polymer Science & Engineering, 2nd Ed. Wiley, 1, 5(1985).

2. Wittcoft, H. A., Chemtech, 17, 156(1987).

3. Hergenrother, P. M., in Encyclopedia of Polymer Science & Engineering, John Wiley & Sons, N.Y., 1, 61(1985).

4. Landis, A. L. and Naselow, A. B., Natl. SAMPE Tech. Conf. Ser. 14, 236(1982).

5. Landis, A. L., "Chemistry of Processible Acetylene Terminated Imides," Final Rept. for AFWAL Contract F33615-82-C-5016, August, 1983.

6. Burks, H. D. and St. Clair, T. L., in "Polyimides: Synthesis, Characterization and Applications," Mittal, K. L., Ed., 1, Pleuum, NY, 117(1984).

7. Young, P. R. and Wakelyn, N. T., "Proceedings from the Second International Conference on Polyimides," Ellenville, NY, 414(1985).

8. Critchley, J. P. and White, M. A., J. Polym. Sci., Polym. Chem. Ed., 10, 1809(1972).

9. Kusy, R. P., in "Metal Filled Polymers," Bhattacharya, C. S., Ed., Plastics Engineering, II, Marcel Dekker, N. Y., 13(1986).

10. Bigg, D. M. in "Metal Filled Polymers," Bhattacharya, C. S., Ed., Plastics Engineering, II, Marcel Dekker, N. Y., 169(1986).

11. Maudgal, S. and St. Clair, T. L., Int. J. Adhesion and Adhesives, 4, 87(1984).

12. Maudgal, S. and St. Clair, T. L., "Proceedings from the Second International Conference on Polyimides," Ellenville, NY, 47(1985).

13. Johnson, B. C., Yilgor, I. and McGrath, J. E., Polym. Prepr., 24(2), 54(1984); B. C. Johnson, Ph.D. Thesis, VPI and SU 1984; B. C. Johnson, J. D. Summers and J. E. McGrath, J. Poly. Sci, in press, 1987; J. E. McGrath, P. M. Sormani, C. S. Elsbernd and S. Kilic, Makromol. Chem., Macromol. Symp. 6, 67(1986).

14. Summers, J. D., Ph.D. Dissertation, VPI & SU, February 1988.

15. Bell, V. L., U. S. Patent 4,094,862, (to NASA) June 13, 1978.

16. St. Clair, A. K., St. Clair, J. L., and Smith, E. W., Polym. Prepr., 17, 359(1976).

17. Harris, F. W., Norris, S. O., Lanier, L. H., Reinhardt, B. A., Case, R. D., Varaprath, S., Pakaki, S. M., Torres, M. and Feld, W. A. in "Polyimides: Synthesis, Characterization and Applications," Mittal, K. L., Ed., 1, Plenum, NY, 3(1984).

18. Maudgal, S. and St. Clair, T. L. in "Proceedings from the Second International Conference on Polyimides," Ellenville, NY, 217(1985).

19. Summers, J. D., Arnold, C. A., Bott, R. H., Taylor, L. T., Ward, T. C. and McGrath, J. E., Polym. Prepr., 27, 403(1986).

20. Landis, A. L., Miller, L. J. and Bilow, N., U. S. Pat. 3,845,018 (October 29, 1974) (Hughes Aircraft Company).

21. Landis, A. L., Bilow, N., Boscham, R. H., Lawrence, B. E. and Aponyi, T. J., Polym. Prepr., 19, 23(1978).

22. Landis, A. L. and Naselow, A. B. in "Polyimides: Synthesis, Characterization and Applications," Mittal, K. L., Ed., 1, Plenum, NY, 39(1984).

23. Gay, F. P. and Berr, C. E., J. Polym. Sci., Part A-1, 6, 1935(1968).

24. Zurakowska-Orszagh, J., Chreptowlez, T., Orteszko, A., and Kaminski, J., Eur. Polym. J., 15, 409(1978).

25. Madigan, E. A., M.S. Thesis, VPI & SU, 1984.

26. Landis, A. L., Bilow, N., Boschan, R. H., Lawrence, R. F. and Aponyi, T. J., Polymn. Prepr., 15, 537(1974).

27. Hogewerff, S. and VanDorp, W. A., Recl. Trar. Chim. Pays-Bas, 12, 12(1893).

28. Roderick, W. R. and Bhatia, P. L., J. Org. Chem., 28, 2018(1963).

29. Cotter, R. J., Sauers, C. K. and Whelan, J. M., J. Org. Chem., 26, 10(1961).

30. Hedaya, E., Hinman, R. L. and Theodoropulos, S., J. Org. Chem., 31, 1317(1966).

31. Hoojewerff, S. and VanDorp, W. A., Recl. Trar. Chim Pays-Bas, 13, 93(1894); 14, 252(1895).

32. Tsou, K. C., Barrnett, R. J. and Seligman, A. M., J. Amer. Chem. Soc., 77, 4613(1955).

33. Sauers, C. K. and Cotter, R. J., U. S. Patent 2,995,577 (to Union Carbide) (1961).

34. Fletcher, T. L. and Pan, H. L., J. Org. Chem., 26, 2037(1961).

35. Roth, M., U. S. Patent 4,179,444 (1979).

36. McGrath, J. E., Ward, T. C., Schchori, E. and Wnuk, A. J., Polymer Eng. and Sci., 17, 647(1977).

37. Hergenrother, P. M. and Jensen, B. J., Org. Coat. App. Polym. Sci. Proc., 44, 914(1983).

38. Hedberg, F. L., Bush, D. L., Kane, J. J. and Unroe, M. K., Polym. Prepr., 21, 170(1980).

39. Lin, S. and Marvel, C. S., J. Polym. Sci., Polym. Chem. Ed., 22, 1939(1981).

40. Hergenrother, P. M., Polym. Prepr., 21, 81(1980).

41. Lind, A. C., Sandreczki, T. C. and Levy, R. L., "Characterization of Acetylene Terminated Resin Cure States," AFWAL/ML F33615-80-C-5170, August 1984.

42. Vollhardt, K. P. C., Acc. Chem. Res., 10, 1(1979).

43. Kuo, C. C. and Lee, C. Y. C., Org. Coat. Appl. Polym. Sci. Proc., 47, 114(1982).

44. Kuo, C. C. and Lee, C. Y. C., Polym. Prepr., 24, 7(1985).

45. Cotts, D. B., Bogler, G. and Rose, J. E., Org. Coat. Appl. Polym. Sci. Proc., 48, 919(1983).

46. Lee, C. Y. C., Goldfarb, T. J., Arnold, F. E. and Helminiak, T. E., Org. Coat. Appl. Polym. Sci. Proc., 48, 904(1983).

47. Reinhardt, B. A., Jones, W. B., Helminiak, J. E. and Arnold, F. E., Polym. Prepr., 22, 100(1981).

48. Stenzenberger, H. D., Herzos, M., Romer, W., Scheiblich, R. and Reeves, N. J., Brit. Polym. J., 15, 2(1983).

49. St. Clair, A. K. and St. Clair, T. L., Polym. Eng. and Sci., 22, 9(1982).

50. Kukertz, V. H., Makromol. Chem., 98, 101(1966).

51. Yerman, A. J., U. S. Patent 4,017,340 (to General Electric) (1977).

52. Berger, A., U. S. Patent 4,030,948 (to General Electric) (1977).

53. Hoback, J. T. and Holub, F. F., U. S. Patent 3,740,305 (to General Electric) (1973).

54. Lee, C. J., U. S. Patent 4,558,110 (to General Electric) (1985).

55. Maudgal, S. and St. Clair, T. L., "Proceedings from the Second International Conference on Polyimides," Ellenville, NY, 182(1985).

56. Maudgal, S. and St. Clair, T. L., 29th Natl. SAMPE Symp. Exhib., 29, 437(1984).

57. Berger, A. and Juliano, P., U. S. Patent 4,011,279 (to General Electric) (1977).

58. Mandgal, S. and St. Clair, T. L., SAMPE Q., 16, 6(1984).

59. St. Clair, A. K. and St. Clair, T. L., Int. J. Adhesion and Adhesives, 1, 249(1981).

60. Chowdhury, B., in "Polyimides: Synthesis, Characterization and Applications," Mittal, K. L., Ed., 1, Plenum, NY, 401(1984).

61. Yilgor, I., Riffle, J. S., Wilkes, G. L. and McGrath, J. E., Polym. Bull., 8, 535(1982).

62. St. Clair, A. K. and St. Clair, T. L., U. S. Patent 4,497,935 (to NASA) (1985).

63. Lee, C. Y. C., SAMPE J., 21, 34(1985).

64. Babu, G. N. in"Polyimides: Synthesis, Characterization and Applications," Mittal, K. L., Ed., 1, Plenum, NY, 51(1984).

65. Bargain, M., U. S. Patent 4,088,670 (1978).

66. Ryang, H. S., U. S. Patent 4,404,350 (to General Electric) (1983).

67. Berger, A., 30th Natl. SAMPE Symp., 30, 64(1985).

68. Lee, C. J., U. S. Patent 4,586,997 (to General Electric) (1986).

69. Berger, A., U. S. Patent 4,395,527 (to M & T Chemicals) (1983).

70. Edelman, R. in "Proceedings from the Second International Conference on Polyimides," Ellenville, NY, 182(1985).

71. Berger, A. in "Polyimides: Synthesis, Characterization and Applications," Mittal, K. L., Ed., 1, Plenum, NY, 67(1984).

72. Matzner, M. Noshay, A. and McGrath, J. E., Polym. Prepr., 14, 68(1973); Trans. Soc. Rheol., 21/22, 109(1977).

73. McGrath, J. E., Dwight, D. W., Riffle, J. S., Davidson, T. F., Webster, D. C. and Viswanathan, R., Polym. Prepr., 20, 528(1979).

74. Tang, S. H., Meinecke, E. A., Riffle, J. S. and McGrath, J. E., Rubber chem. Tech., 53, 1160(1980).

75. Yilgor, I., Riffle, J. S., Wilkes, G. L. and McGrath, J. E., Polym. Bull., 8, 535(1982).

76. Tyagi, D., Wilkes, G. L., Yilgor, I. and McGrath, J. E., Polym. Bull., 8, 543(1982).

77. Yilgor, I. Shaaban, A. K., Steckle, W. P., Tyagi, P., Wilkes, G. L. and McGrath, J. E., Polymer, 25, 1800(1984).

78. Tyagi, D., Yilgor, I., McGrath, J. E. and Wilkes, G. L., Polymer, 25, 1807(1984).

79. Tang, S. H., Meinecke, E. A., Riffle, J. S. and McGrath, J. E., Rubber Chem. Tech., 57, 184(1984).

80. Lee, C. Y., 30th Natl. SAMPE Symp., 30, 52(1985).

81. Schmitt, R. L., Gardella, J. A., Magill, J. H., Salvati, L. and Chin, R. L., Macromolecules, 18, 2675(1985).

82. Schmitt, R. L., Gardella, J. A. and Salvati, L., Macromolecules, 19, 648(1986).

83. Magila, T. L. and LeGrand, D. G., Polym. Eng. and Sci., 10, 349(1970).

84. Narkis, M. and Tobolsky, A. V., J. Makromol. Sci.-Phys., B4, 877(1970).

85. Gaines, G. L., J. Polym. Sci. Part C, 34, 115(1971).

86. Robeson, L. M., Noshay, A., Matzner, M. and Merriam, C. N., D. Angw. Makromol Chem., 29/30, 47(1973).

87. Juliano, P. C. and Mitchell, T. P., Polym. Prepr., 21, 72(1980).

88. Williams, E. A., Cargioli, J. D. and Hobbs, S. Y., Macromolecules, 10, 782(1977).

89. Grubbs, G. R., Kleppick, M. E. and Magill, J. H., J. Appl. Polym. Sci., 27, 601(1982).

90. Maung, W., Chua, K. M., Ng, T. H. and Williams, H. L., Polym. Eng. and Sci., 23, 439(1983).

91. Maung, W. and Williams, H. L., Polym. Eng. and Sci., 25, 113(1985).

92. Kajiyama, M., Nishikata, Y., Kakimoto, M. and Imai, Y., Polym. J. (Tokyo), 18, 735(1986).

93. Kakimoto, M., Kajiyama, M. and Imai, Y., Polym. J. (Tokyo), 18, 940(1986).

94. Auman, B. C., Percec, V., Schneider, H. A., Jishan, W. and Cantow, H. J., Polymer, 28, 119(1987).

95. Schneider, H. A., Jishan, W., Cantow, H. J., Auman, B. C. and Percec, V., Polymer, 28, 132(1987).

96. Kawakami, Y., Aoki, T. and Yamashita, Y., Polym. Bull., 17, 293(1987).

97. Ying, L. and Edelman, R., 31st Natl. SAMPE Symp., 31, 1131(1986).

98. Sacher, E., Klemberg-Sapieha, J. E., Schreiber, H. P. and Wertheimer, M. R., J. Appl. Polym. Sci: Appl. Polym. Symp., 38, 163(1984).

99. Davis, G. C., Heath, B. A. and Gildenblat, G. in "Polyimides: Synthesis, Characterization and Applications," Mittal, K. L., Ed., 2, Plenum, NY 847(1984).

100. Davis, G. C., ACS Symp. Ser., 242, 259(1984).

101. Iwama, A., Tasakag, K. and Kazuse, Y., U. S. Patent 4,618,534 (1986).

102. Seymour, J. in "Fillers and Reinforcements for Plastics," Deanin, R. D. and Schott, N. R., Eds., ACS Adv. in Chem. Ser., ACS, Washington, D.C., 134, 1(1973)

103. Lipatov, Y. S., "Physical Chemistry of Filled Polymers," Int. Polym. Sci. and Tech. Monograph #2, Rubber and Plast. Res. Assoc. of Great Britian, Shawbury, Eng. (1979).

104. Kusy, R. P. in "Metal Filled Polymers," Bhattacharya, S. K., Ed., Plast. Eng., II, Marcel Dekker, NY, Ch. 1(1986).

105. Jacopin, S. in "Fillers and Reinforcements for Plastics," Deanin, R. D. and Schott, N. R., Eds., ACS Adv. in Chem. Ser., 134, ACS, Washington, D. C., 114(1974).

106. Bhattacharyya, S. K., Polymer, 20, 1166(1979).

107. Paipetis, S. A., Papanicolaou, G. and Theocaris, P. S., Fibre Sci. and Tech., 8, 221(1975).

108. Theocaris, P. S. and Marketos, E., Fibre Sci. and Tech., 3, 21(1970).

109. Theocaris, P. S. and Paipetis, S. A., J. Strain. Analysis, 8, 286(1973).

110. Brassel, G. W. and Wischmann, K. B., J. Mat. Sci., 9, 307(1974).

111. Bhattacharyya, S. K. and Chaklader, A. C. D., Polym. Plast. Tech. Eng., 20, 35(1983).

112. Hansen, D. and Tomkiewicz, R., Polym. Eng. and Sci., 15, 353(1975).

113. Anerbach, A., Eichelberger, C. W. and Wojnarowski, R. J., J. Electrochem. Soc.: Electrochem. Sci. and Tech., 130, 1111(1983).

114. Miller, J. S., Inorg. Chem., 22, 3681(1983).

115. Korts-chot, M. T. and Woodhams, R. T., Polym. Comp., 6, 296(1985).

116. Bigg, D. M., Adv. in Polym. Tech., 4, 255(1984).

117. Bigg, D. M. and Stutz, P. E., Polym. Comp., 4, 40(1983).

118. Sherman, R. D., Middleman, L. M. and Jacobs, S. M., Polym. Eng. and Sci., 23, 36(1983).

119. Kusy, R. P. in "Metal Filled Polymers," Bhattacharyya, S. K., Ed., Plast. Eng., II, Marcel Dekker, NY, 27(1986).

120. Aharoni, S. M., J. Appl. Phys., 43, 2463(1972).

121. Pike, R. A., Novak, R. C. and DeCrescente, M. A., Proc. Ann. Conf. Reinf. Plast. Comp./Compos. Inst., Soc. Plast. Ind., 30(1975).

122. Bilow, N. Landis, A. L, Boschan, R. h. and Fasold, J. G., SAMPE J., 8(1982).

123. Blatz, P. S., Adh. Age, 21, 39(1978).

124. Burgman, H. A., Freeman, J. H., Frost, L. W., Bower, G. M.,Traynor, E. J., and Ruffing, C. R., J. Appl. Polym. Sci., 12, 805(1968).

125. Theocaris, P. S. in "Metal Filled Polymers," Bhattacharyya, S. K., Ed., Plast. Eng., II, Marcel Dekker, NY, 259(1986).

126. Zalucha, D. J. in "High Performance Adhesive Bonding," DeFrayne, G., Ed., Soc. Manuf. Eng., Dearborn, Michigan, 60(1983).

127. Filbey, J. A., Ph.D. Dissertation, VPI & SU, August 1987.

128. Minford, J. D. in "High Performance Adhesive Bonding," DeFrayne, G., Ed., Soc. Maruf. Eng., Dearborn, Michigan, 63(1983).

129. Kinloch, A. J. in "Durability of Structural Adhesives," Kinloch, A. J., Ed., Appl. Sci., NY, V(1983).

130. Brewis, D. M., Comyn, J. and Sharlash, R. J. A., Int. J. Adhesion and Adhesives, 2,(1982).

131. Brockman, W., Henneman, O. D. and Kollek, H., Int. J. Adhesion and Adhesives, 2, 33(1982).

132. Natan, M. and Venables, J. D., J. Adhesion, 15, 125(1983).

133. Pike, R. A. and Lann, P. P., ACS Div. Polym. Mat.: Sci. and Eng., 56, 299(1987).

134. Pike, R. A., Int. S. Adhesion and Adhesives, 6, 21(1986).

135. Pike, R. A., SAMPE J., 21, 1985.

136. Schneberger, G. L. in "High Performance Adhesive Bonding," DeFrayne, G., Ed., Soc. Manuf. Eng., Dearborn, Michigan, 14(1983).

137. Elliott, S. Y. in "Handbook of Adhesive Bonding," Cagle, C. V., Ed., McGraw-Hill, NY, 31-3(1982).

138. Cagle, C. V. in "Handbook of Adhesive Bonding," Cagle, C. V., Ed., McGraw-Hill, NY, 32-1(1982).

139. Minford, J. D. in "Durability of Structural Adhesives," Kinloch, A. J., Ed., Appl. Sci., NY, 135(1983).

140. Nock, J. A. in "Aluminum: Properties and Physical Mettalurgy," Hatch, J. E., Ed., American Society for Metals, Metals Park, Ohio, Chapter 9(1984).

141. Brown, S. R., Proc. Nat. SAMPE Symp. Exhib., 27, 363(1982).

142. Kinloch, A. J., in "Durability of Structural Adhesives," Kinloch, A. J., Ed., Applied Science, Essex, England, Chap. 1(1983).

143. Mason, J. G., Siriwardane, R. and Wightman, J. P., J. Adhesion, 11, 315(1981).

144. Eddy, L. T. R., Lucarelli, A. M., Helminiak, T., Jones, W., Picklesimer, L. F., An Evaluation of An Acetylene Terminated Sulfone Oligomer, Internal Report, A FWAL/MLBC, January 1983.

145. Koenig, J. L., Spectroscopic Characterization of the Cured State of An Acetylene-Terminated Resin, Final Report, AFWAL/ML Contract F33615-82-K-5038, August 1983.

146. Prime, R. B., Thermal Characterization of Polymeric Materials, Turi, E. A., Ed., Academic Press, NY, 1981, pp. 435-562.

147. Pickard, J. M., Jones, E. G., Goldfarb, I. J., Polym. Prepr., 20, 370(1979).

148. Pickard, J. M., Jones, E. G., Goldfarb, I. J., Macromolecules, 12, 895(1979).

149. T. S. Chow and R. C. Penwell, "Metal Filled Polymers" Plastics Engineering, II S. K. Bhattacharya ed., Marcel Dekker, New York, 13(1986), .

150. Takekoshi, T., Kochanowski, J. E., Manello, J. S. and Webber, M. J. J., Polym. Sci.: Polymer Symposium 74, 93(1986).

151. Summers, J. D., Arnold, C. A., Bott, R. H., Taylor, L. T., Ward, T. C., and McGrath, J. E., Proc. Intl. SAMPE Symp. Exhib. 32, 613(1987).

152. Sormani, P. M., Minton, R. J. and McGrath, J. E. in "Ring Opening Polymerization: Kinetics, Mechanisms, and Synthesis," McGrath, J. E. Ed., ACS Symposium Series No. 186, 147(1985).

153. Bott, R. H., Summers, J. D., Arnold, C. A., Taylor, L. T., Ward, T. C., and McGrath, J. E., J. Adhesion, 23, 67(1987).

154. Bott, R. H., Taylor, L. T., and Ward, T. C., ACS Division of Polymer Materials Science Engineering, 56, 665(1987).

155. Bott, R. H., Taylor, L. T. and Wefers, K., U. S. Patent applied for by ALCOA Corporation.

156. Bott, R. H., Taylor, L. T. and Ward, T. C., ACS Division Polymer Chemistry Polym. Prepr., 70, 72(1986).

157 Bott, R. H., Taylor, L. T. and Ward, T. C., in "Chemical Reactions on Polymers," Benham, J. L. and Kinstle, J. F., ed., ACS Symp. Ser. 364, 459(1988).

Appendix 1

Pasa Jell 107 Pretreatment Procedure

for Titanium (6-4) Lap Shear Coupons

1. Methanol wash Ti Coupons
2. "Sand blast" 2 inch length of surface to be bonded until uniformly dull surface occurs.
3. Methanol rinse Ti Coupons to remove excess abrasive.
4. Dip coupons in Pasa Jell 107 with up and down strokes covering about 1" length of coupon for about 1 minute.
5. Hang coupons in hood covered with "Pasa Jell" to etch for 10 minutes.
6. Re-dip coupons in "Pasa Jell" for 1 minute as in 4 above.
7. Hang coupons in hood covered with "Pasa Jell" to etch for another 10 minutes.
8. Wash coupons with hot tap water and remove excess "Pasa Jell" with acid brush then thoroughly rinse with flowing tap water.
9. Treat coupons suspended in ultrasonic tap water for 5 minutes.
10. Allow coupons to dry in hood for 5 minutes.
11. Treat coupons suspended in ultrasonic distilled water bath for 10 minutes.
12. Air dry coupons at room temperature for 10 minutes.
13. Heat coupons in oven at 70°C for 10 minutes.
14. Coat coupons with primer solution within 30 minutes after removal from oven.

Appendix 2

FT-IR Microscopy of Titanium 6-4 Pretreated Surfaces Prior to Bonding

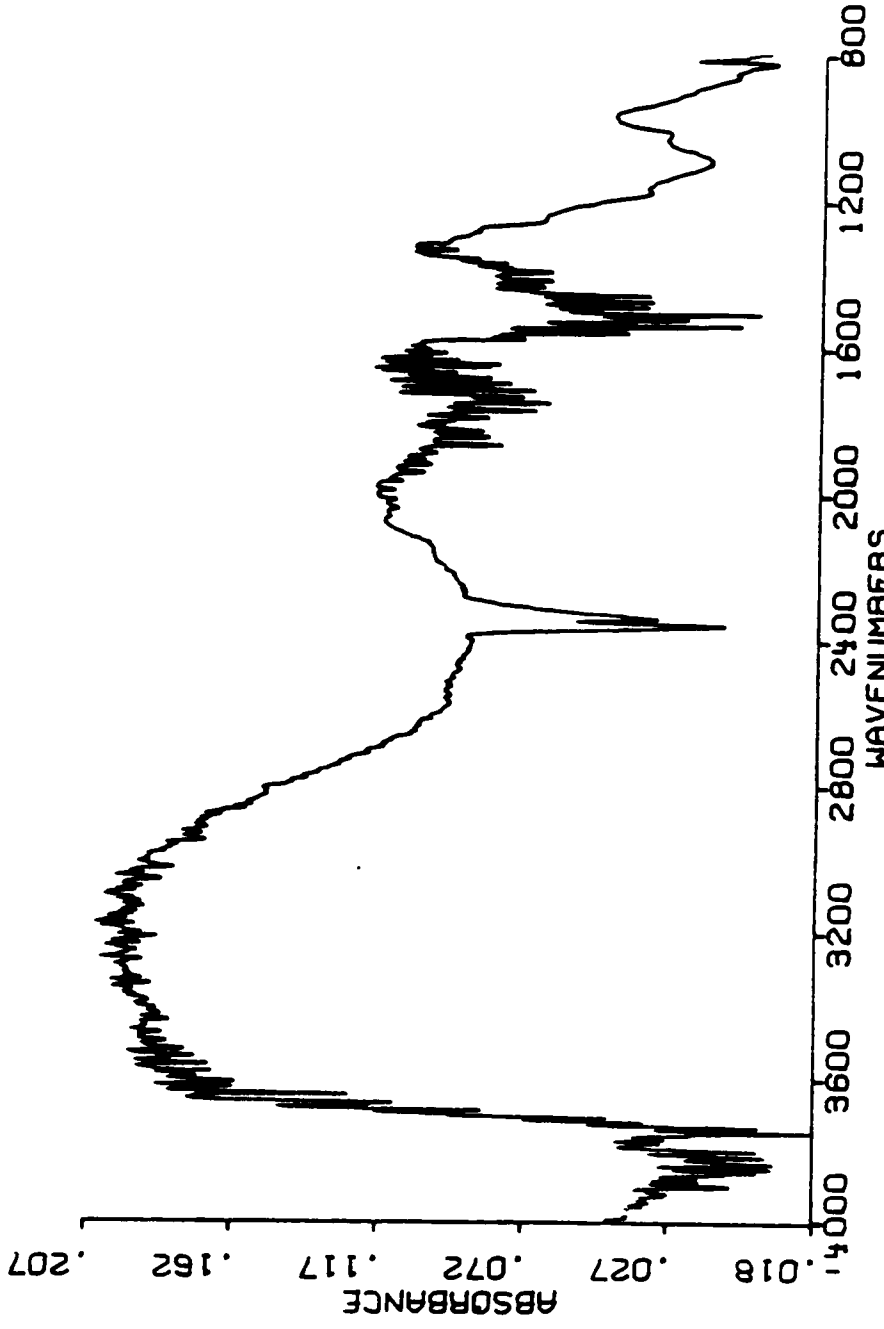

Figure A1: FT-IR Spectrum of Pasa Jell 107 Treated Titanium 6-4 Surface. Used as Background in Following Spectra.

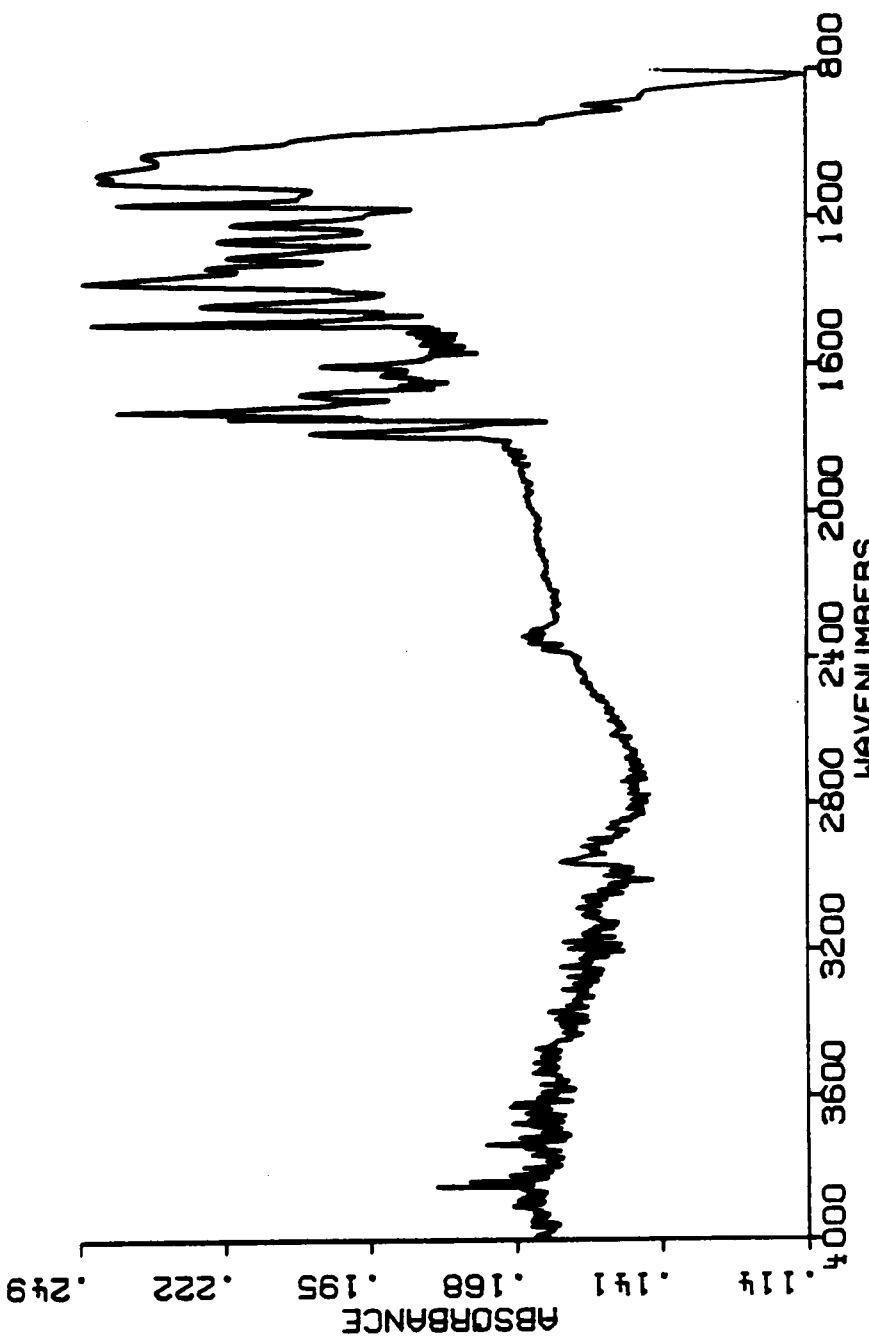

Figure A2: FT-IR Spectrum of Dried Poly(imide-siloxane) 20% w/w Siloxane on Pretreated Ti Surface Showing Characteristic Bands of Both Imide and Siloxane Functionalities.

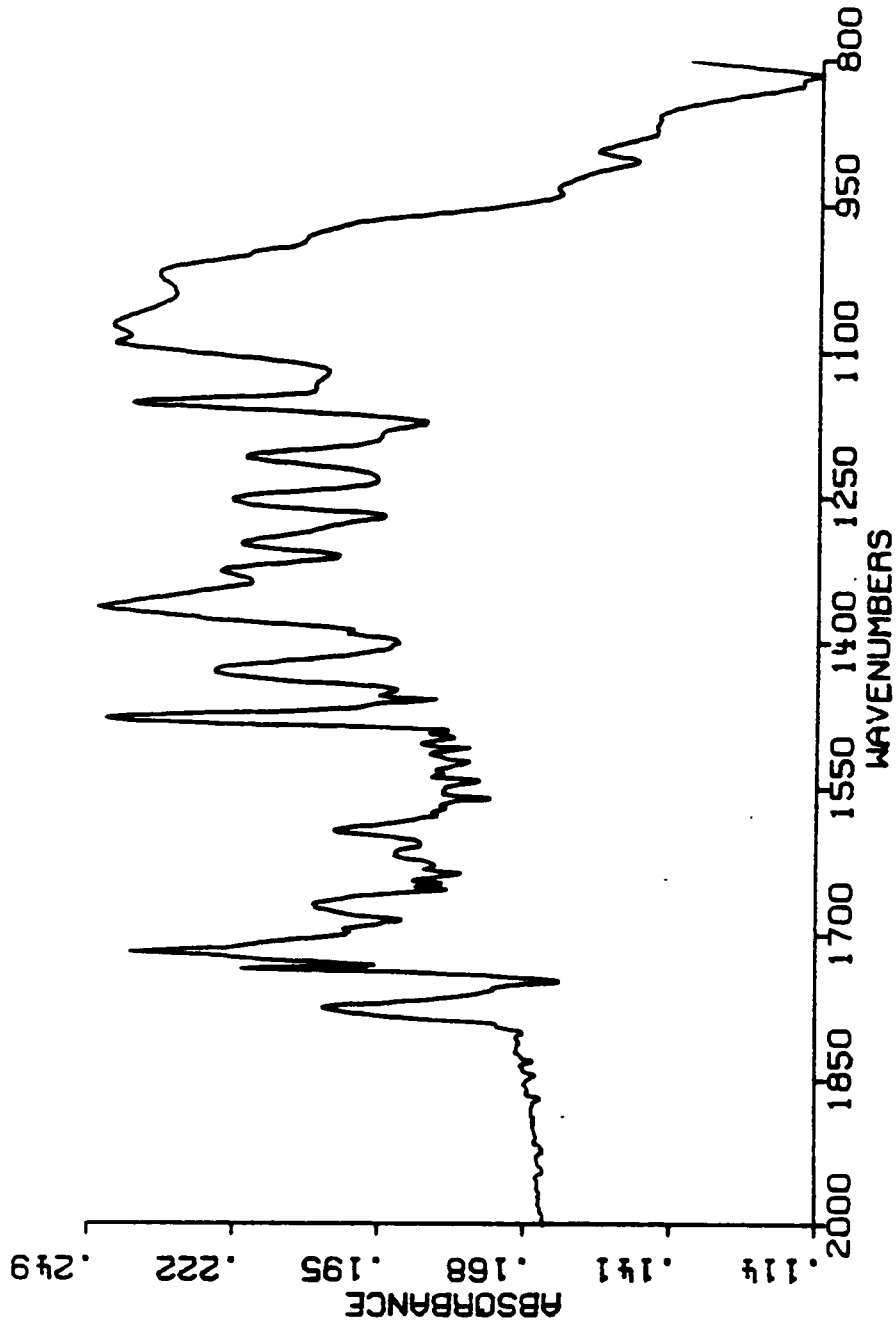

Figure A3: FT-IR Spectrum of "Fingerprint" Region of Figure A2.

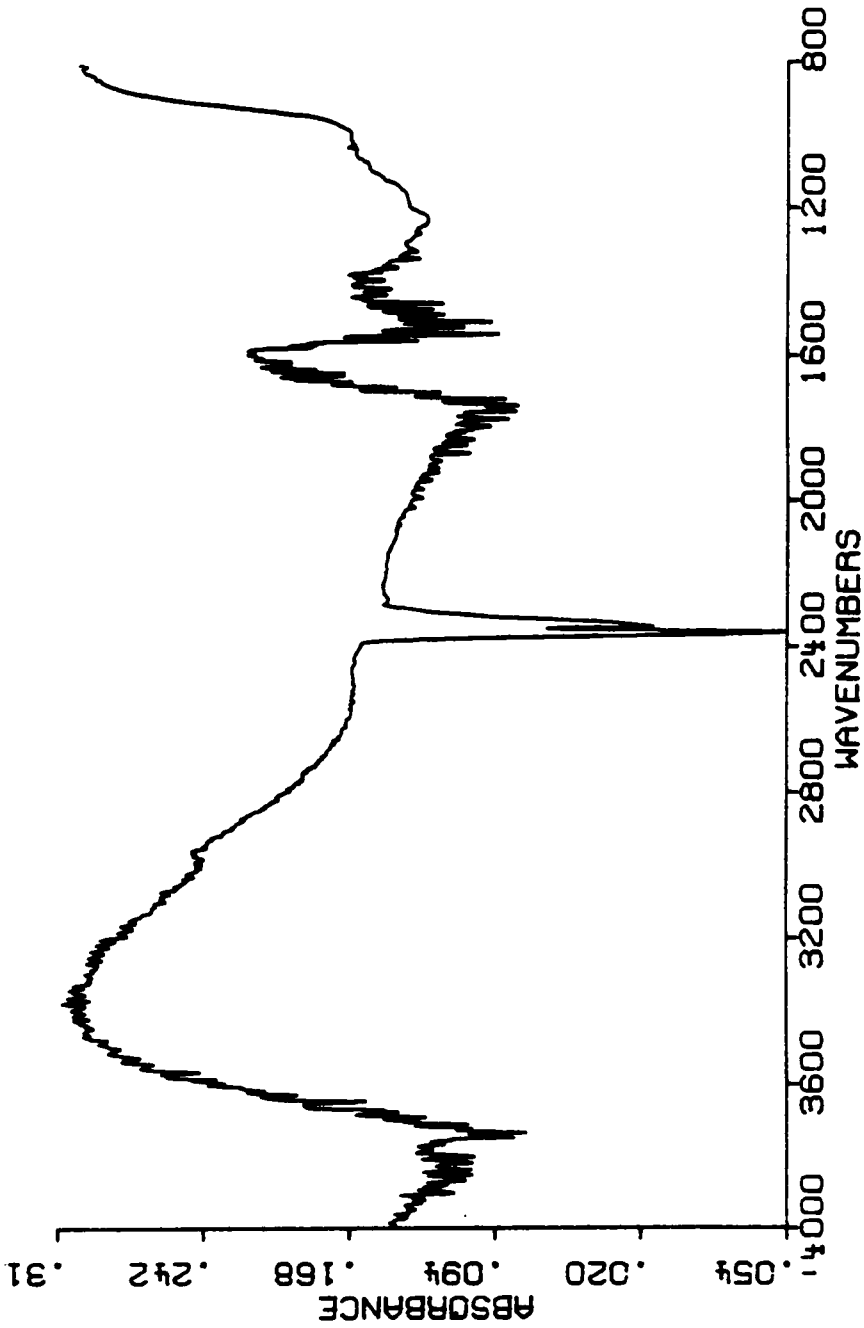

Figure A4: FT-IR Spectrum of Dried Film of Sec Butoxy Aluminum Alkoxide on Pretreated Ti Surface.

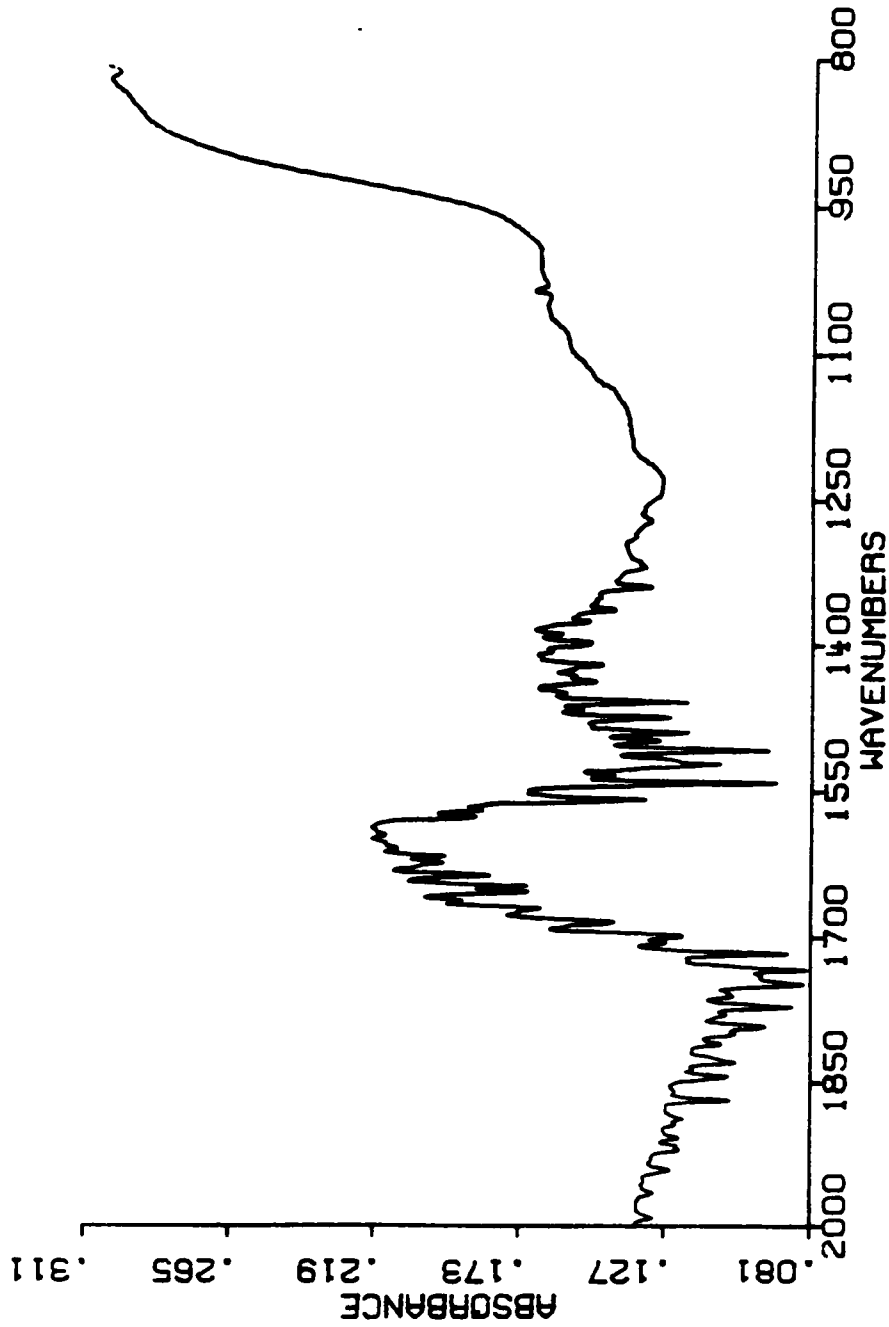

Figure A5: "Fingerprint" Region of Figure A4.

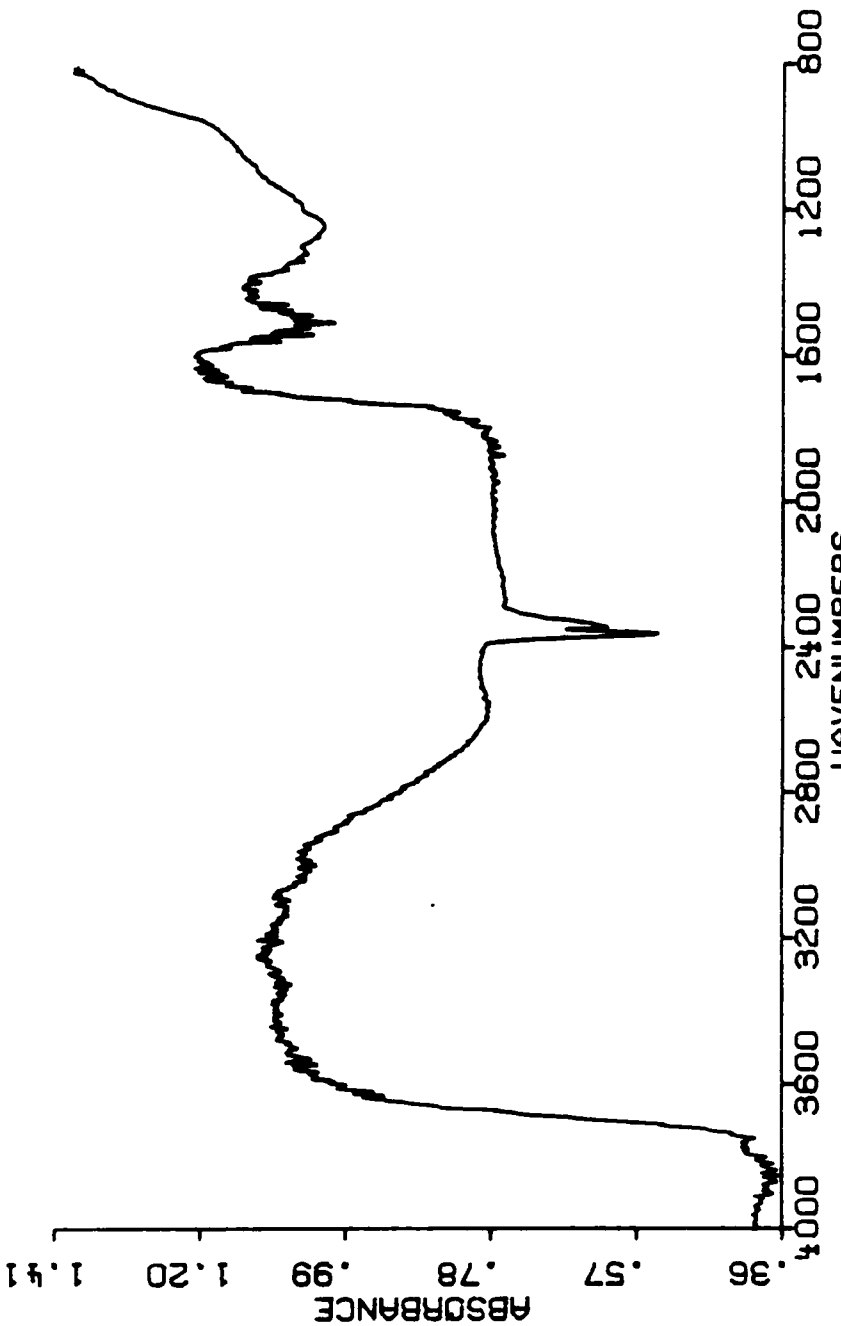

Figure A6: FT-IR Spectrum of Same Sample as A4, A5 but Apertured to Crystal on Surface.

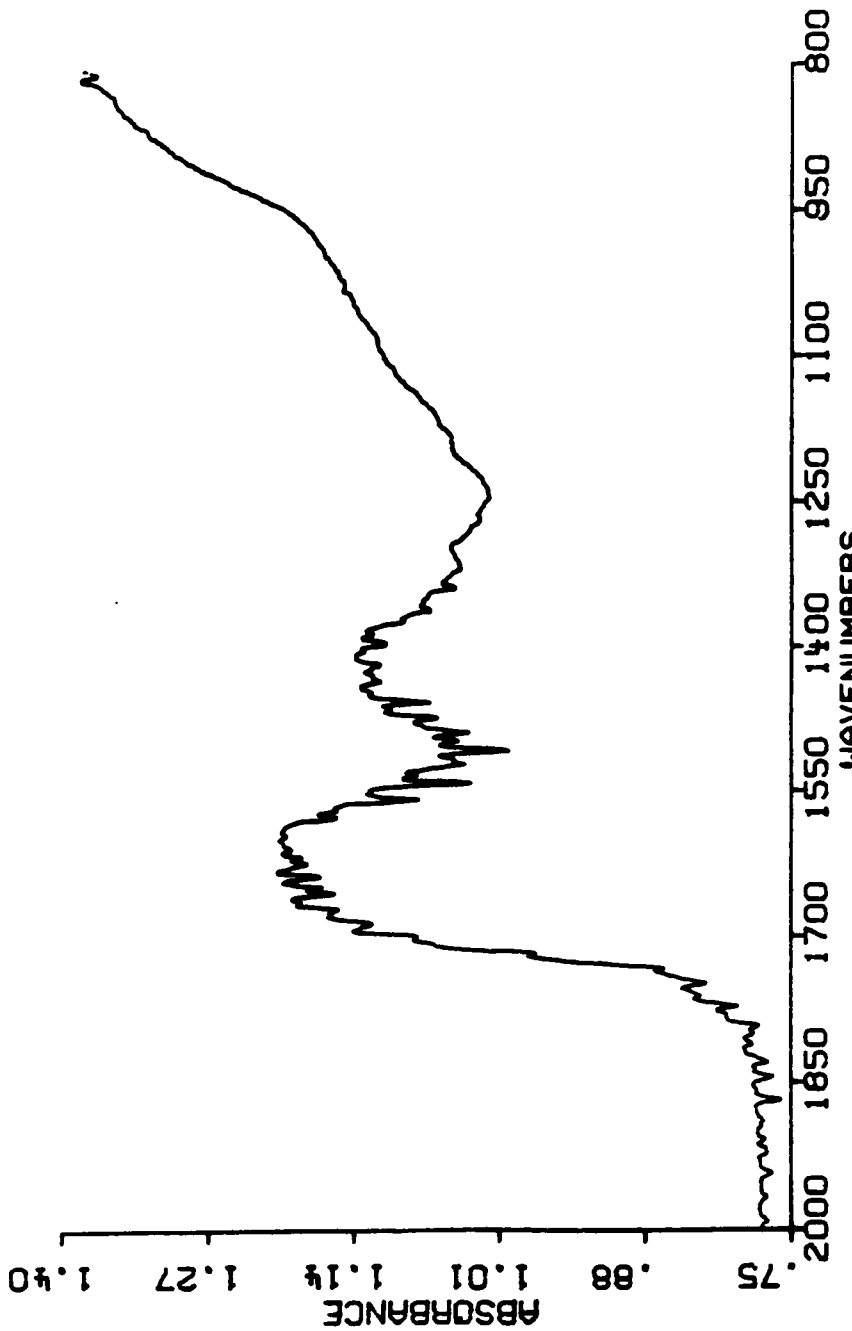

Figure A7: "Fingerprint" Region of Figure A6.

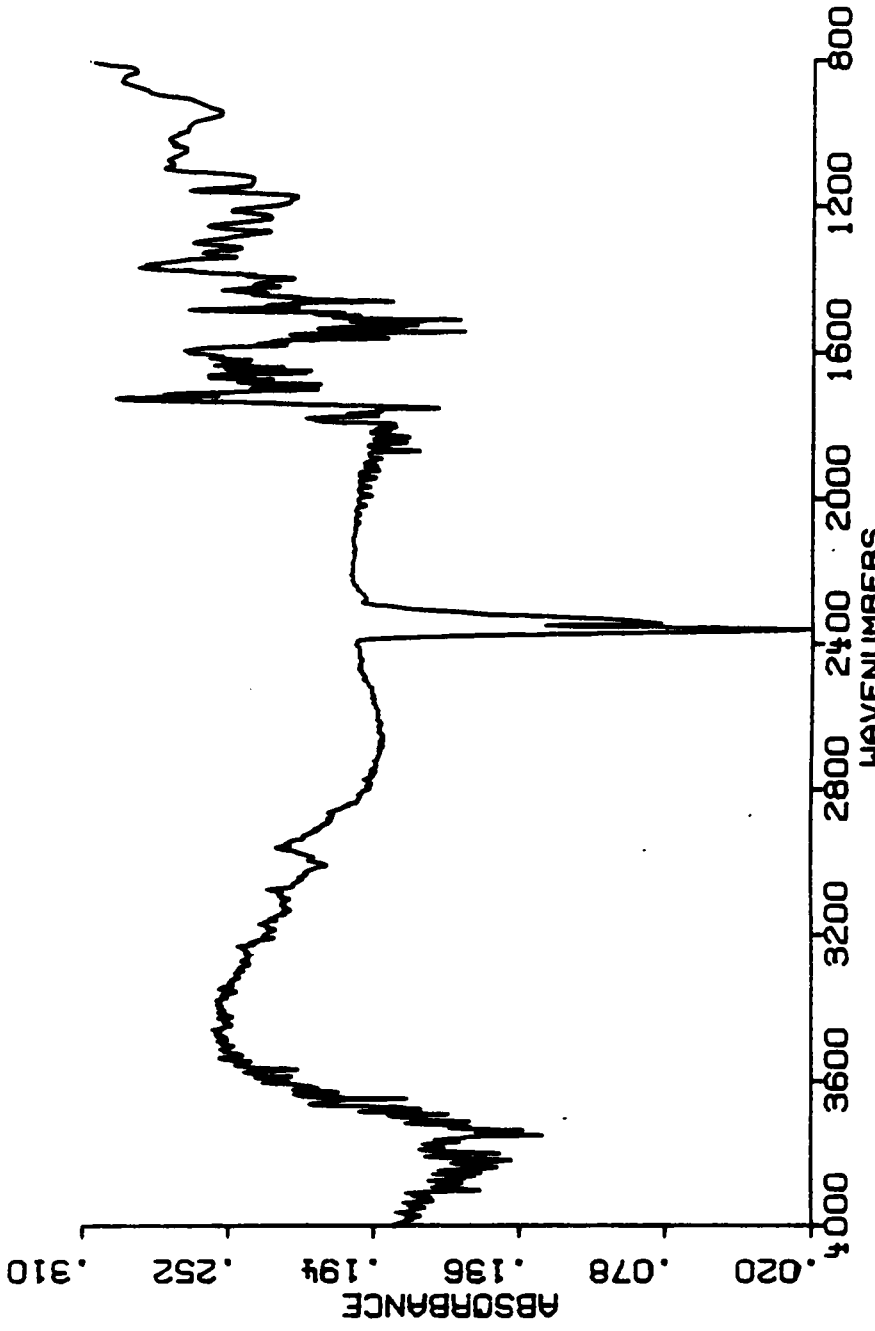

Figure A8: FT-IR Spectrum of Dried Sample Containing Both Poly(imide-siloxane) 20% (w/w) Siloxane and Sec Butyl Aluminum Alkoxide Showing Features of Both Components.

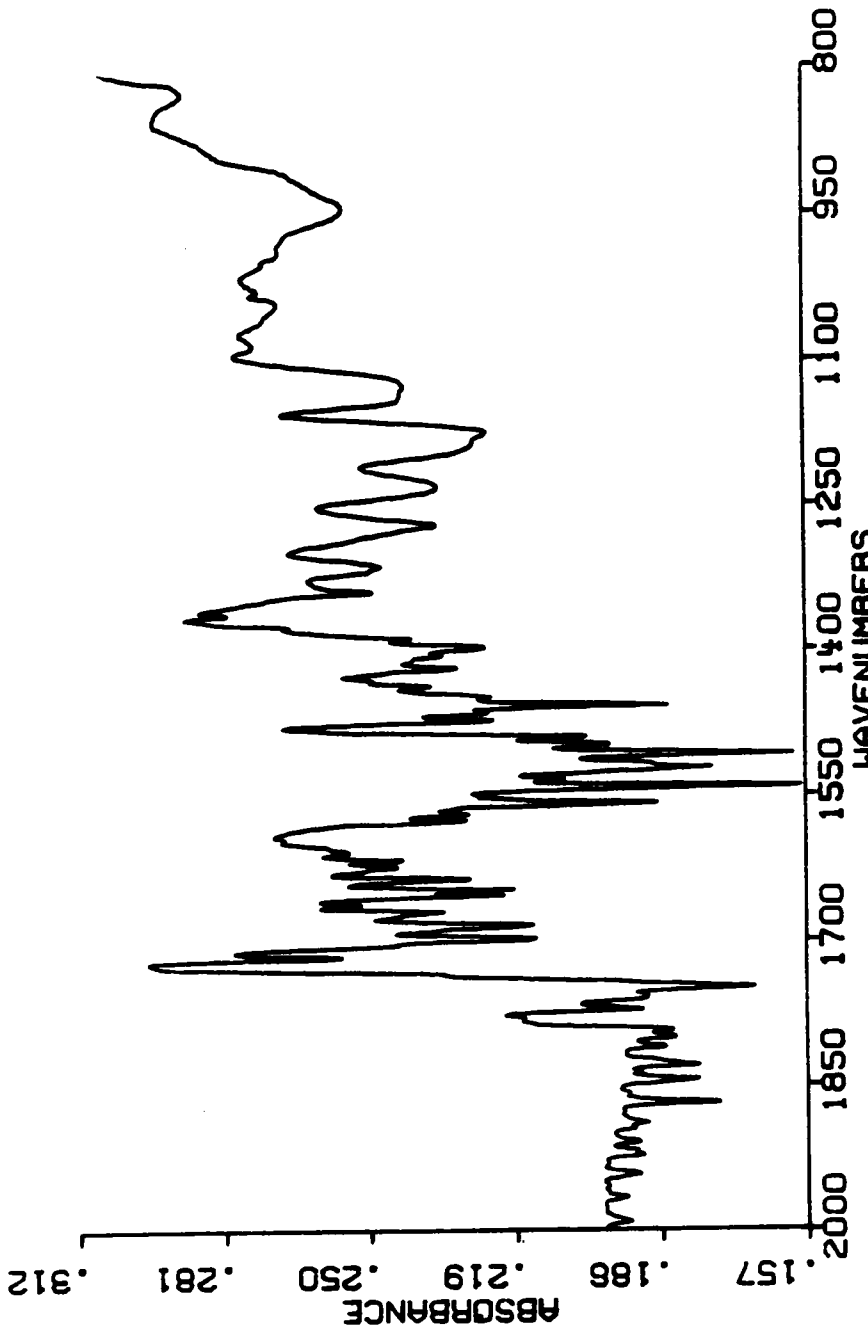

Figure A9: "Fingerprint" Region of Figure A8.

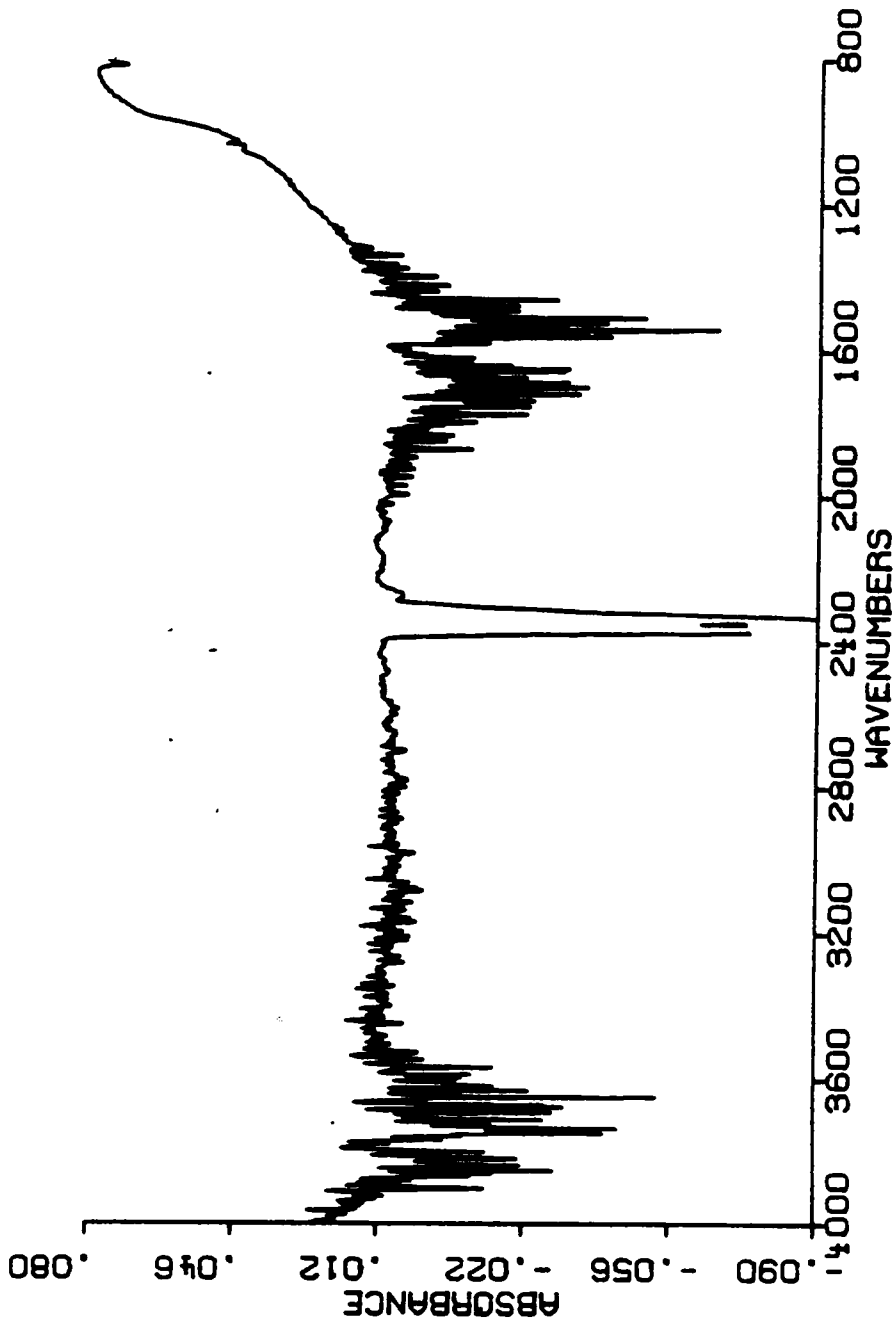

Figure A10: FT-IR Spectrum of Pretreated Ti Surface on Which a Drop of NMP was Dried. No Features Except for H_2O and CO_2 Present.

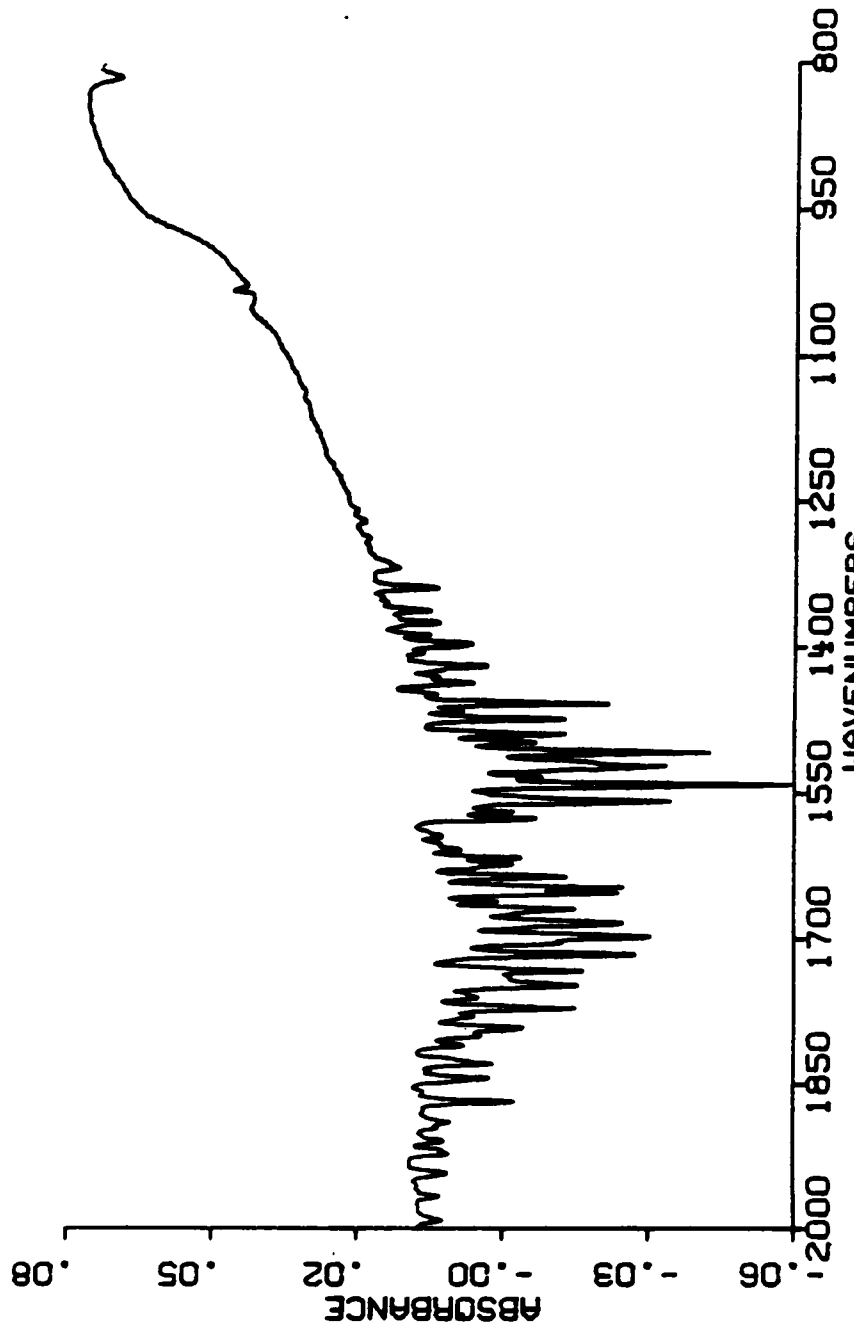

Figure All: "Fingerprint" Region of Figure A10.

The vita has been removed from the scanned document